Optimization of D-xylose and L-arabinose uptake in *Saccharomyces cerevisiae* by engineering the galactose permease Gal2

Dissertation
zur Erlangung des Doktorgrades
der Naturwissenschaften

vorgelegt beim Fachbereich Biowissenschaften
der Johann Wolfgang Goethe-Universität
in Frankfurt am Main

von
Sebastián Alfredo Tamayo Rojas
aus Providencia, Chile

Frankfurt am Main, 2022
(D 30)

vom Fachbereich Biowissenschaften
der Johann Wolfgang Goethe-Universität
als Dissertation angenommen

Dekan: Prof. Dr. Sven Klimpel

1. Gutachter: Prof. Dr. Eckhard Boles
2. Gutachter: Prof. Dr. Jörg Soppa

Datum der Disputation:

This thesis is based on the following publications:

Rojas, Sebastian A. Tamayo, Sina Schmidl, Eckhard Boles, and Mislav Oreb. 2021. “Glucose-induced internalization of the *S. cerevisiae* galactose permease Gal2 is dependent on phosphorylation and ubiquitination of its aminoterminal cytoplasmic tail.” *FEMS Yeast Research 21(3):1–10*. doi: 10.1093/femsyr/foab019.

Rojas, Sebastian A. Tamayo, Virginia Schadeweg, Ferdinand Kirchner, Eckhard Boles, and Mislav Oreb. 2021. “Identification of a glucose-insensitive variant of Gal2 from *Saccharomyces cerevisiae* exhibiting a high pentose transport capacity.” *Scientific Reports 11(1):24404*. doi: 10.1038/s41598-021-03822-7.

Rojas, Sebastian A. Tamayo, Eckhard Boles, and Mislav Oreb. 2022. “A yeast-based *in vivo* assay system for analyzing efflux of sugars mediated by glucose and xylose transporters.” *FEMS Yeast Research foac038*. doi: 10.1093/femsyr/foac038.

Contents

1 Summary 1

2 Introduction 4

2.1 Lignocellulosic biomass as a feedstock in industrial biotechnology 5

2.2 Xylose utilization in *S. cerevisiae* 6

2.3 Arabinose utilization in *S. cerevisiae* 7

2.4 Sugar transport: Prerequisite for fast metabolism 7

2.4.1 The sugar porter (SP) Family 8

2.4.2 The native sugar transporter spectrum of *S. cerevisiae* 10

2.5 Gene regulation of hexose transporters 10

2.5.1 Glucose induction pathway Snf3/Rgt2 10

2.5.2 Glucose repression pathway Snf1/Mig1 11

2.5.3 cAMP-PKA pathway 12

2.5.4 Gene regulation of the galactose permease Gal2 12

2.6 Hexose transporters catabolite degradation 13

2.6.1 Nitrogen signaling for transporters turnover 15

2.6.2 Glucose signaling for transporters turnover 15

2.6.3 Gene regulation of Rsp5 adaptors 16

2.6.4 Degradation of cargoes via multivesicular body (MVB) pathway 18

2.7 Cell response in the presence of xylose and arabinose 19

2.7.1 Strategies to circumvent the lack of sensing of xylose and arabinose 19

2.8 Steric inhibition of xylose and arabinose transport by glucose 23

2.9 Relevance of the galactose permease Gal2 in the uptake of non-physiological substrates in *S. cerevisiae* 24

3 Aim of the thesis 26

4 General discussion 27

4.1 Identification of Gal2 lysine residues involved in ubiquitination 27

4.2 Identification of serine residues involved in phosphorylation signal for Gal2 degradation 29

4.3 ARTs Rod1 and Bul1 involvement in Gal2 internalization 31

4.4 Increase the stability of Gal2 by direct disruption of ubiquitination sites or phosphorylation sites, perspectives 31

4.5 Identification of glucose-insensitive Gal2 variants 33

4.5.1 Relationship between the co-consumption of glucose/xylose and an improved pentose permeability 33

4.6 Intracellular glucose inhibition in xylose uptake 36

4.7 Conclusions and future perspectives 40

5 References 41

6 Publications 58

6.1 Glucose-induced internalization of the *S. cerevisiae* galactose permease Gal2 is dependent on phosphorylation and ubiquitination of its aminoterminal cytoplasmic tail 58

6.2 Identification of a glucose-insensitive variant of Gal2 from *Saccharomyces cerevisiae* exhibiting a high pentose transport capacity 78

6.3 A yeast-based *in vivo* assay system for analyzing efflux of sugars mediated by glucose and xylose transporters 93

7 Deutsche Zusammenfassung 101

8 Acknowledgments 106

9 Curriculum vitae 107

1 Summary

A promising strategy to reduce the dependency from fossil fuels is to use the yeast *Saccharomyces cerevisiae* to bioconvert renewable non-food feedstocks or waste streams, like lignocellulosic biomass, into bioethanol and other valuable molecule blocks. Lignocellulosic feedstocks contain glucose and significant fractions of the pentoses xylose and arabinose in varying proportions depending on the biomass type. *S. cerevisiae* is an efficient glucose consumer, but it cannot metabolize xylose and arabinose naturally. Therefore, extensive research using recombinant DNA techniques has been conducted to introduce and improve the biochemical pathways necessary to utilize these non-physiological substrates. However, any functional pathway capable of metabolizing D-xylose and L-arabinose in *S. cerevisiae* requires the transport of these sugars across the plasma membrane. The endogenous sugar transport system of *S. cerevisiae* can conduct a limited uptake of D-xylose and L-arabinose; this uptake enables only basal growth when the enzymatic pathways are provided. For this reason, the uptake of D-xylose and L-arabinose has been recognized as a limiting step for the efficient utilization of these non-physiological substrates.

Gal2, a member of the major facilitator superfamily, is one of the most studied hexose transporters in *S. cerevisiae*. Although its expression is repressed in the presence of glucose, it also transports this sugar with high affinity when constitutively expressed. Recent efforts to engineer yeast strains for the utilization of plant biomass have unraveled the ability of Gal2 to transport non-physiological substrates like xylose and arabinose, among others. Improving Gal2 kinetic and substrate specificity, particularly for pentoses, has become a crucial target in strain engineering. The main goal of this study is to improve the utilization of xylose and arabinose by increasing the cell permeability of these non-physiological substrates through the engineering of the galactose permease Gal2.

GAL2 gene expression depends on galactose, which acts as an inducer; nevertheless, even in the presence of galactose, glucose act as a strict repressor; consequently, *GAL2* gene is usually placed under the control of a constitutive promoter. However, the presence of glucose additionally triggers the Gal2 degradation, which is mediated by the covalent attachment of the small 76 amino acid protein ubiquitin (Ub) to the targeted transporter; in a multi-step process called ubiquitination.

Ubiquitination of hexose permeases involves the activation of the Ub molecule by the E1 Ub-activating enzyme using ATP; then, the activated Ub is transferred to a specific Ub-conjugating enzyme E2, which donates the Ub indirectly through a specific HECT E3

enzyme (Rsp5) to a lysine residue of the substrate, with the aid of an adaptor protein which recognizes the target (Rsp5-adaptor). Ubiquitinated permeases are sent by membrane invagination to early endosomes, where they encounter ESCRTs (endosomal sorting complex required for transport). The targeted permeases are sorted in intralumenal vesicles (ILV) inside of the endosome, which after several cycles, turns into a multivesicular body (MVB) that subsequently fuses with the vacuole to expose the protein content of the ILVs to lumenal hydrolases for degradation.

Gal2 contains 30 lysine residues that may accept the ubiquitin molecule, which targets its degradation. It is known that mono-ubiquitination by Rsp5 on multiple lysine residues is necessary to internalize Gal2 (Horak & Wolf, 2001). However, the authors did not identify the specific lysine residues involved in the ubiquitination processes. This study screened several Gal2 variants where lysine residues were mutated or removed from the protein sequence to discover which lysine residues are likely involved in ubiquitination and consequent turnover of the transporter. The results of the screening showed that mutation of the N-terminal lysine residues 27, 37, and 44 to arginine ($Gal2_{3KR}$) produced a functional transporter that, when fused with GFP ($Gal2_{3KR\_GFP}$), showed an exclusive localization at the plasma membrane in cells growing in galactose or glucose as a sole carbon source (Tamayo Rojas et al., 2021b).

This study furthermore evaluated upstream signals caused by phosphorylation which triggers ubiquitination and consequent turnover of the targeted protein; using similar screening approaches to assess the stabilization of Gal2 by lysine residue modifications, it was possible to identify that N-terminal serine residues 32, 35, 39, 48, 53, and 55 are likely involved in the internalization of Gal2, since a Gal2 construct where all these serines were mutated to alanine residues and tagged with GFP ($Gal2_{6SA\_GFP}$) exhibited practically complete localization at the plasma membrane in cells growing in galactose or glucose as a sole carbon source (Tamayo Rojas et al., 2021b).

This work aimed to identify Rsp5 adaptors involved in recognizing Gal2 permease. Our findings revealed that Rsp5 adaptors Bul1 and Rod1 are presumably involved in the ubiquitination of Gal2, as their individual deletion led to a stabilization of Gal2 at the plasma membrane in cells growing in glucose as a sole carbon source; however, the stabilization was not as robust as the variant $Gal2_{3KR}$ or $Gal2_{6SA}$. For this reason, it was presumed that multiple Rsp5 adaptors might be involved in the internalization of Gal2 (Tamayo Rojas et al., 2021b).

Uptake impairments of xylose or arabinose by steric inhibition of glucose result in a

decreased uptake of these pentoses in co-fermentations of these sugars. In this study, by using error-prone PCR (epPCR) and a screening system based on a recombinant strain AFY10X which lacks all hexose transporters and hexo-/glucokinases and is genetically engineered to use pentoses as a carbon source (Farwick et al., 2014), two mutations in Gal2 (N376Y/M435I) were found, that together incorporate two desirable properties for fermentation of lignocellulosic hydrolysates: the ability to transport pentoses in the presence of glucose and an improved capacity for xylose and arabinose transport (Tamayo Rojas et al., 2021a). In addition, insertion of serine to alanine mutations at the residues 32, 35, 39, 48, 53, and 55 yielded a transporter ($Gal2^{6SA\_N376Y\_M435I}$) with the abovementioned features plus the increase in stability at the plasma membrane, being one of the most advanced pentose transporters. The overexpression of this transporter in a recombinant industrial diploid strain, capable of consuming xylose, reduced the overall fermentation time of the total xylose consumption by approximately 20h, corresponding to 40% of the total fermentation course of a glucose/xylose mixture fermentation; however, the strain was only able to consume glucose and xylose sequentially, proving that the xylose uptake is not the sole determinant of the co-consumption of both sugars (Tamayo Rojas et al., 2021a).

Gal2 asparagine's 376 substitution by tyrosine ($Gal2^{N376Y}$) or phenylalanine ($Gal2^{N376F}$) resulted in a transporter variant that completely abolished the uptake of glucose in comparison to the wild type (Farwick et al., 2014); therefore, in these variants, the uptake of xylose is not competitively inhibited by glucose, during co-fermentation. However, it is unknown if these Gal2 variants are still inhibited by intracellular glucose and if the decrease in the glucose affinity is symmetrical or asymmetrical regarding the glucose flux direction. To answer this question, an assay platform was developed that allows for qualitative and quantitative assessment of the glucose efflux mediated by facilitative hexose and pentose transporters. The assay uses the previously mentioned strain AFY10. This strain, when fed with the disaccharide maltose, which is intracellularly hydrolyzed by maltases into two glucose moieties, glucose achieves growth-inhibitory levels inside the cells since it cannot be further metabolized. When a permease mediating glucose efflux is expressed in this system, the inhibitory effect is relieved proportionally to the capacity of the introduced transporter (Tamayo Rojas et al., 2022). Feeding the system with maltose and xylose accompanied with the expression of the $Gal2^{N376F}$ variant and xylose isomerase (XylA from *Clostridium phytofermentans*), it could be shown that intracellular glucose did not inhibit the uptake of xylose; that is to say, it was proved that this Gal2 variant exhibit a symmetric insensitivity for glucose from both sides of the plasma membrane in comparison to the wild type which is internally and externally inhibited by glucose (Tamayo Rojas et al., 2022).

2 Introduction

Nowadays, there is a dependency on fossil fuels, like crude oil, coal, and natural gas. They have a crucial role in the energy sector as well as in bulk and fine chemicals synthesis. Fossil fuel availability is restricted to a limited number of deposits worldwide; consequently, their supply is limited due to its depletions and economic and geopolitical reasons. Furthermore, its use contributes to climate change due to the high greenhouse gas emissions released into the atmosphere as it is burned. To overcome these problems, it is necessary to exploit alternative sources of energy and chemical manufacturing using biotechnological processes that are environmentally friendly and only require feedstocks from renewable sources, which are widely available.

A promising strategy to reduce the dependency on fossil fuels is to use microorganisms to bioconvert renewable feedstocks or waste streams into valuable molecule blocks. The yeast *Saccharomyces cerevisiae* (typically referred to as "yeast") is one of the most relevant microorganisms in biotechnology, among the bacteria *Escherichia coli*, *Corynebacterium glutamicum*, *Bacillus subtilis*, and the filamentous fungi *Aspergillus niger* and *Aspergillus oryzae* (Hong & Nielsen, 2012). The advantage of yeast over other microorganisms is its strong fermentative capacity and high robustness to toxic inhibitors, low pH, and osmotic and mechanical stress (Weber et al., 2010). It is also classified as GRAS (generally regarded as safe) by the U.S. Food and Drug Administration (FDA).

The most preferred substrate for *S. cerevisiae* is glucose, and the primary fermentation product is ethanol, which forms part of alcoholic beverages. In addition, purified ethanol is used as a solvent, preservative additive, and disinfectant; it is also extensively used as a renewable biofuel.

New recombinant DNA tools allow engineering yeast strains by modifying their metabolic pathways, enzymes properties, and regulatory proteins to produce a new range of biotech products, like pharmaceuticals, food ingredients, fine chemicals, biofuels, and bulk chemicals (Hong & Nielsen, 2012; Generoso et al., 2015; Wess et al., 2019; Baumann et al., 2020). Furthermore, recombinant DNA tools allow to exploit non-physiological substrates in yeast, present in large quantities in lignocellulosic biomass feedstocks (Wiedemann & Boles, 2008; Brat et al., 2009).

2.1 Lignocellulosic biomass as a feedstock in industrial biotechnology

Sugars and starch hydrolysates comprise the feedstock of around 90% of the produced bioethanol today (Kumar et al., 2008). The use of these feedstock constitutes an ethical concern since these products can be used as potential food and feed; In addition, the use of food as feedstock to produce biofuels has economic and ecological drawbacks; this conflict led to a pursuit of non-food feedstock sources to produce bioethanol and other biotech products (Limayem & Ricke, 2012). An alternative feedstock for biotechnical conversion is lignocellulosic biomass from agricultural and forest residues, which do not compete with food and animal feed production. Lignocellulosic biomass is a renewable and abundant resource, generally formed of three main components, the polysaccharides cellulose, and hemicellulose, who together comprise around 70% of the total biomass; Both components are tightly linked with the aromatic polymer lignin, which represents 20% to 30% of the total biomass (Limayem & Ricke, 2012). Covalent and hydrogen bonds between cellulose and hemicellulose with lignin turn the structure highly robust and recalcitrant (Zoghlami & Paës, 2019).

It is necessary to break down lignocellulosic materials to release the fermentable substrates that will provide the carbon and energy source to the microorganism. Usually, its breakdown is performed with a pre-treatment that can be mechanical or thermochemical to disrupt the material and rearrange the lignin distribution, increasing the substrate porosity, allowing an effective subsequent enzymatic hydrolysis treatment that targets the cellulose and hemicellulose portions (Limayem & Ricke, 2012).

Cellulose consists of a long chain of glucose monomers; therefore, its hydrolysis release only D-glucose; in contrast, the hydrolysis of the hemicellulose, which is and heteropolymer, releases the pentoses D-xylose and L-arabinose as well as the hexoses D-glucose, D-galactose, and D-mannose, it also may contain sugar acids like D-glucuronic, D-galacturonic, and methylgalacturonic acids, depending on the source of the feedstock (Zabed et al., 2016).

Lignocellulosic feedstocks contain significant fractions of the pentoses xylose and arabinose in varying proportions depending on the biomass type. For example, common agricultural and agro-industrial residues like corn fiber contain 21.6% of xylose and 11.4% of arabinose, brewery's spent grain contains 15% of xylose and 8% of arabinose, and wheat bran contains 16% and 9% of xylose and arabinose, respectively (Gírio et al., 2010).

S. cerevisiae is an efficient glucose consumer, but it cannot metabolize xylose and arabinose naturally. Therefore, extensive research using recombinant DNA techniques has been carried out to exploit these non-physiological substrates.

2.2 Xylose utilization in *S. cerevisiae*

There are two established degradative pathways for xylose in nature (Figure 1A, and 1B). The first pathway involves D-xylose reduction to form D-xylitol and a subsequent oxidation to produce D-xylulose, using the enzymes xylose reductase (XR) and xylitol dehydrogenase (XDH), which require NADPH and NAD^+ as cofactors, respectively (Figure 1A). The second pathway, commonly found in bacteria, involves the direct isomerization of D-xylose to D-xylulose through the enzyme xylose isomerase (XylA) and does not require an oxidative-reductive cofactor (Toivari et al., 2004; Brat et al., 2009) (Figure 1B). D-xylulose is then phosphorylated to D-xylulose-5-phosphate by xylulokinase (XK) and subsequently metabolized in the non-oxidative branch of the pentose phosphate pathway (noxPPP) (Figure 1E). From the noxPPP, the intermediates fructose-6-phosphate and glyceraldehyde 3-phosphate (GAP) are funneled into the glycolysis pathway to generate pyruvate, which under fermentative conditions, is converted to ethanol (Figure 1F).

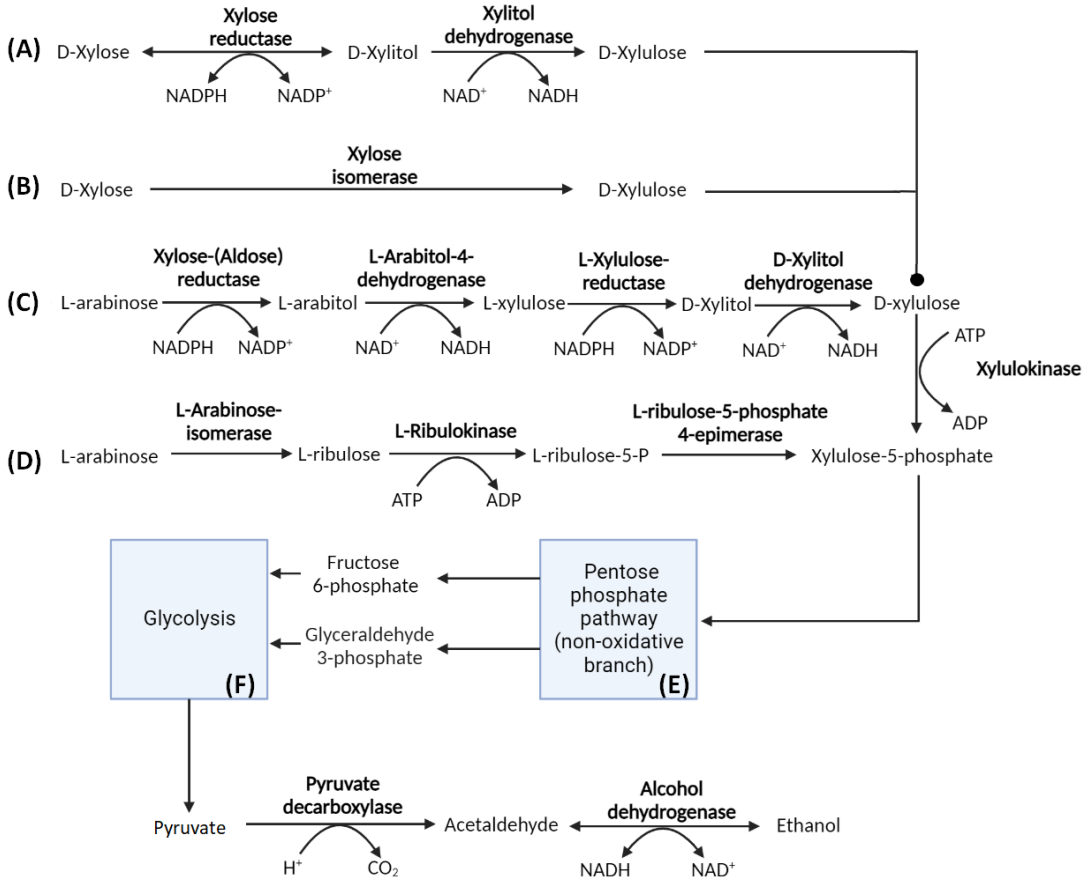

Figure 1: Established degradative pathways for xylose and arabinose. For more details see chapters 2.2 and 2.3.

Although *S. cerevisiae* contains the enzymes required to convert D-xylose to D-xylulose, the conversion rate is insufficient to allow growth in a medium containing D-xylose as the sole carbon source. Overexpression of the endogenous XR (*GRE3*) and XDH (*XYL2*) enables *S. cerevisiae* to grow on xylose as the sole carbon source (Träff et al., 2002; Toivari et al., 2004). However, the conversion of D-xylose to D-xylulose with D-xylitol as an intermediate leads to an accumulation of NADH under anaerobic conditions, creating a cofactor imbalance that obstructs the further conversion of D-xylitol to D-xylulose, as consequence D-xylitol is accumulated (Pitkänen et al., 2003; Jin et al., 2004). On the other hand, the direct conversion of D-xylose to D-xylulose with XylA has the advantage that no redox reactions are required; XylA from *Clostridium phytofermentans* (used in this study) was the first bacterial XylA found to be functional in *S. cerevisiae* (Brat et al., 2009).

2.3 Arabinose utilization in *S. cerevisiae*

The degradation of arabinose has two established pathways in nature (Figure 1C, and D), which end up with xylulose-5-phosphate formation in a similar way to the xylose degradation pathways. One of them, commonly found in eukaryotic cells, involves the conversion of L-arabinose to D-xylulose via four enzymatic steps consisting of two reducing and two oxidizing reactions, which require NADPH and NAD^+ as cofactors, respectively (Becker & Boles, 2003) (Figure 1C). The heterologous expression of the genes coding these enzymes in *S. cerevisiae* led to poor growth in arabinose and a lack of ethanol production attributed to cofactor imbalances (Richard et al., 2002). In contrast, the second pathway commonly found in bacteria has the advantage that no redox reactions are required and consequently does not cause a cofactor imbalance. In this pathway, L-arabinose conversion to xylulose-5-phosphate is performed in three steps using an isomerase, a kinase, and an epimerase enzyme (Figure 1D). This study uses L-arabinose isomerase from *Bacillus subtilis*, L-ribulokinase, and L-ribulose-5-P 4-epimerase from *Escherichia coli* for the conversion of L-arabinose to xylulose-5-phosphate, which is further converted to ethanol under fermentative conditions (Becker & Boles, 2003; Wiedemann & Boles, 2008).

2.4 Sugar transport: Prerequisite for fast metabolism

Any functional pathway capable of metabolizing D-xylose and L-arabinose in *S. cerevisiae* requires the transport of these sugars across the plasma membrane. The endogenous sugar transport system of *S. cerevisiae* can conduct a limited uptake of D-xylose and L-arabinose; this uptake enables only basal growth when the enzymatic pathways are

provided; for this reason, the uptake of D-xylose and L-arabinose has been recognized as a limiting step for the efficient utilization of these non-physiological substrates, especially at low concentration of them (Richard et al., 2002; Gárdonyi et al., 2003; Runquist et al., 2010; Tanino et al., 2012; Farwick et al., 2014). Heterologous expression of xylose transporters from other species in *S. cerevisiae* is usually inefficient as they may encounter problems during their secretion to the plasma membrane; in addition, overexpressed heterologous transporters may undergo cellular degradation, ending up in vacuoles (Shin et al., 2015). A more promising solution is to utilize the endogenous sugar transport system of *S. cerevisiae* and determine suitable components that can be enhanced to improve their ability to transport xylose and arabinose.

2.4.1 The sugar porter (SP) Family

In *S. cerevisiae*, the uptake of sugars across the plasma membrane is mediated by the sugar porter (SP) family, which belongs to the major facilitator superfamily (MFS), the largest and most diverse superfamily of secondary carriers found across all kingdoms of life (Drew et al., 2021). The sugar porter family consists of a wide variety of membrane transport proteins that may be grouped in different phylogenetic clusters according to the substrate or range of substrates transported. Some phylogenetic clusters include hexose transporters, alpha-glucoside symporters, and glucose sensors (Saier, 2000; Palma et al., 2009).

Yeast hexoses transporters, like many members of the MFS, share 12 putative transmembrane domains (TM), organized in two bundles of 6 TM, connected by a long and flexible intracellular loop that may contain structural elements. Each bundle of 6 TM consists of a pair of inverted 3 TM (Figure 2), which support the idea that three TM repeats represent a fundamental structural unit for MFS proteins (Yan, 2013; Drew et al., 2021).

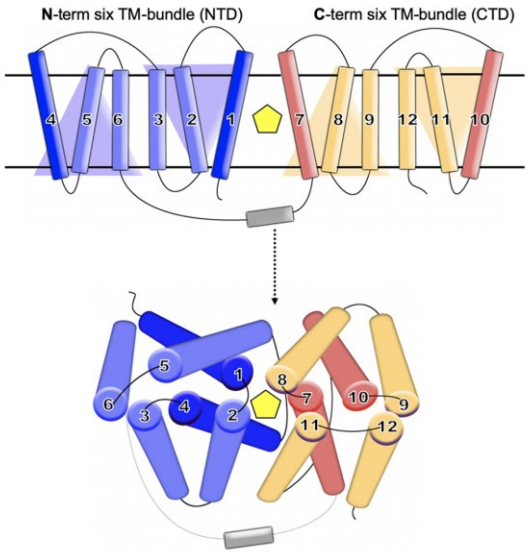

Figure 2: Schematic illustration of the canonical MFS transporter topology. Canonical MFS topology comprises 12 transmembrane domains (TM), comprising two structurally similar six-helix bundles. The N-terminal bundle (TM1−6; light blue/ blue) and the C-terminal bundle (TMs 7−12; light orange/red) are connected by a cytosolic loop, which can occasionally contain structural elements (gray). Each of the bundles is made up of 3-TM structural-inverted repeats. The first TM in each of the 3-TM repeats (TM1, TM4, TM7, and TM10) constitutes the central cavity in the transporter, which usually undergo local changes to bind and release the substrate (yellow pentagon) during alternating access. The figure was taken from Drew et al. 2021.

Hexose transporters are believed to operate with the so-called "rocker-switch alternating access mechanism" to upload and release the substrate across the membrane. This mechanism consists of a nearly symmetrical movement of the two 6 TM bundles around the centrally located substrate, which is alternatively exposed to only one side of the membrane at a time. The different conformational changes of the transporter result in the outward-facing, occluded, and inward-facing states; these changes are required to complete a complete transport cycle (Figure 3) (Drew et al., 2021).

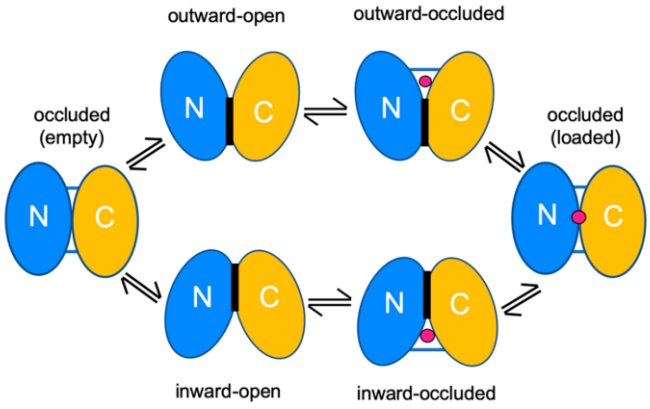

Figure 3: Schematic representation of MFS transporter cycle. Six major conformations of an MFS transporter cycle: outward-open, outward-occluded with bound substrate (pink sphere), occluded with substrate, inward-occluded with substrate, inward-open and occluded with no substrate. The figure was taken from Drew et al. 2021.

2.4.2 The native sugar transporter spectrum of *S. cerevisiae*

There are 17 functional hexose transporters in *S. cerevisiae*, encoded by *HXT1* to *HXT17* and *GAL2* genes (except *HXT12*, a pseudogene). A large number of hexose transporters in *S. cerevisiae* allows it to adapt to its environment, where the sugar concentration may vary over a fermentation time. However, under physiological conditions, the most crucial hexose transporters appear to be Hxt1 to 4 and Hxt6 to 7. The *GAL2* expression occurs only under galactose conditions. *HXT5* and *HXT8* to *17* (except *HXT12*) were reported to be marginally expressed under physiological conditions (Reifenberger et al., 1995; Diderich et al., 1999). One of the main characteristics of yeast hexose transporters is their affinity for glucose, which can be divided into high (Hxt6, Hxt7, and Gal2; K_m = 1 to 2), moderate (Hxt2, Hxt4, and Hxt5; K_m = 2 to 10 mM), to low affinity (Hxt1, and Hxt3; K_m = 30 to 100 mM) (Boles & Hollenberg, 1997; Diderich et al., 2001; Farwick et al., 2014; Shin et al., 2015).

2.5 Gene regulation of hexose transporters

There is a correlation between sugar availability in the medium and the hexose transporters' transcription. Low-affinity transporters are expressed in cells growing in glucose-rich media; meanwhile, moderate and high affinity transporters are expressed in cells growing in media with limiting glucose concentrations (Diderich et al., 1999; Özcan & Johnston, 1999).

Three major sugar signaling pathways are involved in regulating the glucose transporters and glycolytic gene expression: the glucose induction pathway Snf3/Rgt2, the glucose repression pathway Snf1/Mig1, and the cAMP/PKA pathway, which is involved in both previous pathways. However, the transcriptional regulation pathways of the hexose transporters are not yet fully elucidated; nevertheless, they give us an insight into how different transcriptional pathways ensure the expression of the central low, moderate, and high glucose affinity, as well as hexose transporters variants like Gal2, under scenarios of different sugars availability (Platt & Reece, 1998; Özcan & Johnston, 1999; Jouandot et al., 2011; Hsu et al., 2015).

2.5.1 Glucose induction pathway Snf3/Rgt2

Expression of the transporter genes *HXT1* to *4*, *6* to *7*, and the major hexokinase *HXK2* is induced at low glucose concentration by the inactivation of the transcriptional repressor Rgt1. The derepression involves the plasma membrane glucose sensors Snf3 and Rgt2,

which in response to extracellular glucose, generate a signal that activates the yeast casein kinase Yck1 and its paralog Yck2, which phosphorylates the corepressors Mth1 and Std1, who are required to form a repressive complex with Rgt1. The phosphorylation by the kinases Yck1/Yck2, targets the corepressors Mth1 and Std1 to ubiquitination by the SCFGrr1 ubiquitin ligase complex. Ubiquitinated Mth1 and Std1 corepressors are subsequently targeted for degradation by the 26S proteasome (for more details about ubiquitin signaling, see chapter 2.6). Without the corepressors Mth1/Std1, Rgt1 cannot form the transcription repressor complex with Ssn6 and Tup1 to target the promoter regions of the genes mentioned above. However, at high glucose concentrations, Rgt1 is hyperphosphorylated by the cAMP-dependent protein kinase (PKA), turning it into a transcriptional activator of the low-affinity glucose transporter *HXT1* gene (Ozcan et al., 1996; Özcan & Johnston, 1999; Jouandot et al., 2011). Rgt2 is also responsible for the gene repression of the transcription factor Mig2; Mig2 cooperates redundantly and synergistically with Mig1. Mig1 is a repressor transcription factor in the glucose-induced gene repression pathway Snf1/Mig1 (Kaniak et al., 2004).

2.5.2 Glucose repression pathway Snf1/Mig1

Transcriptional repression at high glucose concentrations of the genes which codify Hxt2, Hxt4, Hxt6, Hxt7, and Gal2 (indirectly via Gal4) is mediated by the deactivation of Snf1 kinase complex and the presence of the repressor transcription factor Mig1 in the nucleus. Contrariwise, at a low glucose concentration, close to its depletion, Snf1 is active and responsible for the phosphorylation of Mig1 and Hxk2; the phosphorylation of these proteins prevents them from entering the nucleus to form the transcription repressor complex with Ssn6 and Tup1 in the promoter regions of the abovementioned genes. The activation or deactivation of Snf1 depends on its phosphorylation state. Snf1 is activated under low glucose concentration by the kinases Sak1, Tos3, and Elm1 and deactivated under high glucose concentration by the phosphatases Glc7 with its regulatory subunit Reg1 (together, PP1 phosphatase) (Hong et al., 2003; Nath et al., 2003; Sutherland et al., 2003). Snf1 is also involved in the catabolite inactivation of the transporters Hxt2, Hxt4, Hxt6, and Hxt7. However, this subject is described in detail in chapter 2.6. Snf1 kinase is also involved in regulating protein, carbohydrate, and lipid biosynthesis as well as cell growth and proliferation when the cell's energy levels are compromised, as the ratios of AMP/ATP or ADP/ATP increase (Hardie, 2007).

Mig1 represses gene expression from low to high glucose concentrations; contrariwise, Rgt1 represses gene expression from low to depleted glucose concentrations; superimposition of these repressors ensures the proper expression of the high-affinity

transporters Hxt7 and Hxt6 as well as moderate glucose transporters of Hxt2, Hxt4 at low glucose concentrations (Özcan & Johnston, 1999; Kaniak et al., 2004; Westholm et al., 2008).

2.5.3 cAMP-PKA pathway

The cAMP-dependent protein kinase (PKA) regulates numerous cellular processes at transcriptional and translational levels, including cell growth, response to stress, carbon storage, and differentiation (Smith et al., 1998; Wu et al., 2020). *S. cerevisiae* contains three partially redundant forms of the PKA catalytic subunits, named Tpk1, Tpk2, and Tpk3, and one form of the regulatory subunit, called Bcy1 (Budhwar et al., 2010). Extracellular glucose or sucrose activates PKA via the plasma membrane G protein-coupled receptor, Gpr1, which in the presence of these sugars promotes the transition of the G Protein Alpha subunit Gpa2 from an inactive form (bound with GDP) to an active form (bound with GTP). GTP-Gpa2 form activates the adenylate cyclase Cyr1, which catalyzes cAMP synthesis from ATP. cAMP binds the regulatory subunit Bcy1 of PKA, exposing the active site of Tpk1, 2, and 3, resulting in PKA activation (Gancedo, 2008; Wu et al., 2020). cAMP-PKA pathway is also activated by intracellular glucose, fructose, mannose, and their phosphorylated metabolites, which increase the activity of the guanine nucleotide exchange factors Cdc25 and its paralog Sdc25; these enzymes stimulate the exchange of GDP for GTP in the G-protein Ras1 and its homolog Ras2. Active GTP-Ras1/2 forms, similarly to Gpa2, increase Cyr1 activity and, consequently, PKA activity (Gancedo, 2008; Wu et al., 2020).

PKA is involved in the phosphorylation of many substrates, including the glycolytic enzymes 6-phosphofructo-2-kinases PfK26 and PfK27, as well as pyruvate kinases Pyk1 and Pyk2 (Portela et al., 2002, 2006). PKA indirectly controls the activity of Snf1 by the activation of PP1 phosphatase (Glc7-Reg1) and the partial deactivation of the kinase Sak1 (see chapter 2.5.2) (Barrett et al., 2012; Castermans et al., 2012). As previously mentioned in chapter 2.5.1, PKA hyperphosphorylates Rgt1, turning it from a transcriptional repressor into a transcriptional activator of *HXT1*.

2.5.4 Gene regulation of the galactose permease Gal2

The galactose permease *GAL2* gene expression depends on intracellular galactose. The induction is mediated by Gal3 protein, which acts as a galactose sensor. The protein Gal3 is structurally similar to its paralog galactokinase Gal1, which phosphorylates alpha-D-galactose to alpha-D-galactose-1-phosphate in the first step of galactose catabolism; the difference between Gal1 and Gal3 is that Gal3 does not have kinase

activity. Gal3 binds galactose and ATP, allowing the formation of the protein complex with the negative regulator Gal80, which interacts directly with the domain of Gal4, a transcriptional activator required to express *GAL* genes. The tripartite protein complex enables the inhibition of Gal80 and subsequent activation of Gal4, required for the transcription of *GAL2*, among other *GAL* genes (Platt & Reece, 1998).

2.6 Hexose transporters catabolite degradation

Internalization of hexose transporters, like many other yeast nutrient-permeases, is an additional regulatory step that complements their gene expression. Together they allow the cell to respond to substrate availability, overall nutrient supply conditions, and stress. The degradation of yeast nutrient-permeases is mediated by the covalent attachment of the small 76 amino acid protein ubiquitin (Ub) to the targeted transporter; in a multi-step process called ubiquitination (Figure 4) (briefly mentioned in chapter 2.5.1), where ubiquitin serves as a signal for promoting the internalization of the targeted transporter.

The multi-step ubiquitination process is an evolutionarily conserved process that involves the activation of the Ub molecule by the E1 Ub-activating enzyme using ATP; then, the activated Ub is transferred to a specific Ub-conjugating enzyme E2, which can donate the Ub directly to a lysine residue of the protein substrates through the formation of the complex with an Ub–ligase E3 of the RING family (Figure 4C) or indirectly through specific HECT E3 enzymes (Figure 4B). Target proteins can be ubiquitinated on a single lysine residue or multiple lysine residues; alternatively, Ub can be ligated to other Ub, creating Ub chains where each Ub is linked to one of the seven lysine residues of the prior Ub (Figure 4D, and 4E) (Rotin & Kumar, 2009; Lauwers et al., 2010). The role of mono, multi, or poly-ubiquitination in the internalization of the transporters is not entirely understood; nevertheless, there is strong evidence that mono-ubiquitination is enough to trigger the transporter internalization, multi ubiquitination accelerates the internalization process, and polyubiquitination may be required in later steps of endocytosis (Lucero et al., 2000; Horak & Wolf, 2001; Blondel et al., 2004; Lauwers et al., 2009).

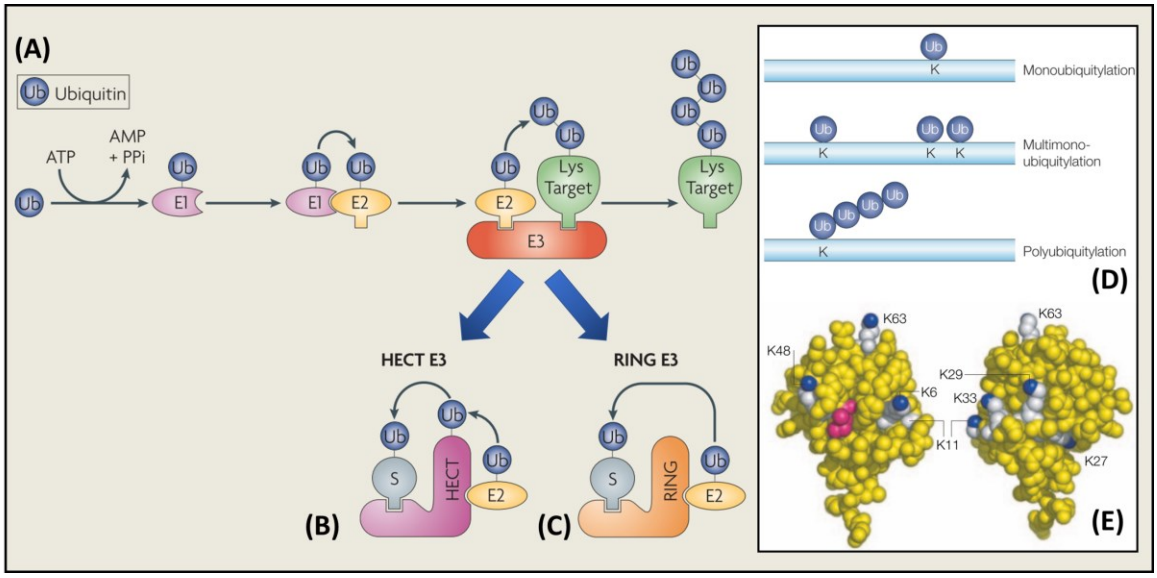

Figure 4: Ubiquitination cascade, with two types of E3 ubiquitin–protein ligases, ubiquitin molecule and ubiquitin modifications. (A) Multistep conjugation process of the ubiquitin molecule to a protein substrate, (B, C) two main groups of ubiquitin protein ligases E3, HECT and the RING, (D) mono ubiquitination, (multi)mono ubiquitination and polyubiquitination, (E) seven lysine residues of the ubiquitin molecule, lysine residues are depicted in white and the ε-amino-group nitrogen in blue, in red Ile44 ubiquitin-binding domain. The figures A, B, C were taken and modified from Rotin and Kumar 2009; the figures D, E were taken from Hicke, Schubert, and Hill 2005.

Yeast genome encodes a single E1, eleven E2s, and 54 E3s (Hicke et al., 2005). However, the Ub transfer in the last step of ubiquitination of the yeast nutrient-permeases is only mediated by Rsp5, a NEDD4 family E3 ubiquitin ligase. The architecture of Rsp5 features an N-terminal C2 domain, which binds to phospholipids and mediates intracellular targeting to the plasma membrane, endosomes, and multivesicular bodies (MVBs), three WW domains, where each domain contains two conserved tryptophan (W) residues, spaced by 21 amino acids apart within the conserved sequence domain, which are required to bind with PY motifs (PPxY, LPxY) for protein−protein interaction and finally a C-terminal HECT ligase domain. This architecture signature is conserved in the NEDD4 family members (Rotin & Kumar, 2009; Lauwers et al., 2010).

Several *S. cerevisiae* permeases under Rsp5 control do not contain any PY motif. Therefore, Rsp5 binds via its WW domains to the PY motif of accessory proteins, which act as specific Rsp5 adaptors to achieve the ubiquitination of the target permease. Many Rsp5 adaptor proteins have been identified in the past years, including the arrestin-related trafficking adaptors (ARTs) protein family comprised of Art1 to Art10 (Nikko & Pelham, 2009), Bul1 and its paralog Bul2 and homolog Bul3 (Yashiroda et al., 1996, 1998; Novoselova et al., 2012), Ear1 and its homolog Ssh4 (Stimpson et al., 2006) (Stimpson et al., 2006), Tre1 and its paralog Tre2 (Stimpson et al., 2006) and Bsd2 (Hettema et al., 2004). Rsp5 adaptors play a crucial role in the selective recognition of the nutrient

permeases, bringing the ubiquitin ligase Rsp5 into the proximity to achieve ubiquitination. However, it is still unclear how Rsp5 adaptors recognize targeted proteins, considering that nutrient permeases in several cases are phosphorylated prior to ubiquitination, in which phosphorylation is a requirement for the correct recognition by Art adaptors (Marchal et al., 1998; Kelm et al., 2004; Nikko et al., 2008).

In many cases, the endocytic activity of Rsp5 adaptors is modulated by their phosphorylation/dephosphorylation status. Phosphorylation of Rsp5 adaptors generally impairs their endocytic trafficking function, while dephosphorylation facilitates or improves Rsp5 adaptor-mediated endocytosis. In *S. cerevisiae*, multiple kinases like Snf1 (see chapter 2.5.2), Npr1, Pho85, Ypk1, the protein kinase A (PKA), Yck1, and its paralog Yck2 are capable of directly phosphorylating Rsp5 adaptors (Shinoda & Kikuchi, 2007; O'Donnell et al., 2010; Muir et al., 2014; Herrador et al., 2015; Hovsepian et al., 2017), and many more kinases have been shown to have catalytic activity towards Rsp5 adaptors in high-throughput in vitro kinase assays (O'Donnell & Schmidt, 2019).

2.6.1 Nitrogen signaling for transporters turnover

A nitrogen-dependent regulation of Rsp5 adaptors involves the kinase Npr1. The nitrogen permease reactivator kinase Npr1 phosphorylates Rsp5 adaptors involved in amino acid permeases internalization, including Ldb19 (Art1), causing its inactivation. Ldb19 is involved in the internalization of the arginine permease Can1. Furthermore, the highly conserved multiprotein kinase complex, which senses cellular and environmental signals, including nutrient availability, energy levels, and growth signals, TORC1, negatively regulates Npr1 by phosphorylation. This regulatory loop acts in response to amino acid availability to ensure proper levels of them inside the cell (O'Donnell et al., 2010; MacGurn et al., 2011).

2.6.2 Glucose signaling for transporters turnover

The alpha arrestin Rod1 is involved in the degradation of nutrient permeases, including the monocarboxylate/proton symporter Jen1, the high-affinity glucose transporter Hxt6 and probably due to its high homology (99%), the high-affinity glucose transporter Hxt7. Under low glucose conditions, the Snf1 kinase phosphorylates Rod1 and drastically decreases its endocytic activity. Rod1, under phosphorylation, binds with the 14-3-3 proteins Bmh1 and Bmh2; they act as negative regulators impeding their own ubiquitination by Rsp5, which is a modification required to activate Rod1 mediated trafficking like many other ARTs. On the other hand, under high glucose availability, the PP1 phosphatase

(phosphatase Glc7 with the regulatory subunit Reg1) dephosphorylates Rod1 and blocks Snf1 activity through the dephosphorylation of its threonine 210. These synergistic effects result in the activation of Rod1, and subsequent ubiquitination of Hxt6 by Rsp5 (Becuwe et al., 2012; Llopis-Torregrosa et al., 2016). In vitro assays have identified other Rsp5 adaptors as substrates of Snf1, like Rog3, Aly2, and Bul2; Nevertheless, the interaction between Snf1, Rog3, Aly2, and Bul2 Rsp5 adaptors and the target nutrient permeases is not yet fully elucidated; however, many Rs5p adaptors target similar nutrient permeases in a duplicated or synergistic manner; for this reason, they probably share common regulatory steps involving the above-described steps under similar scenarios (O'Donnell & Schmidt, 2019).

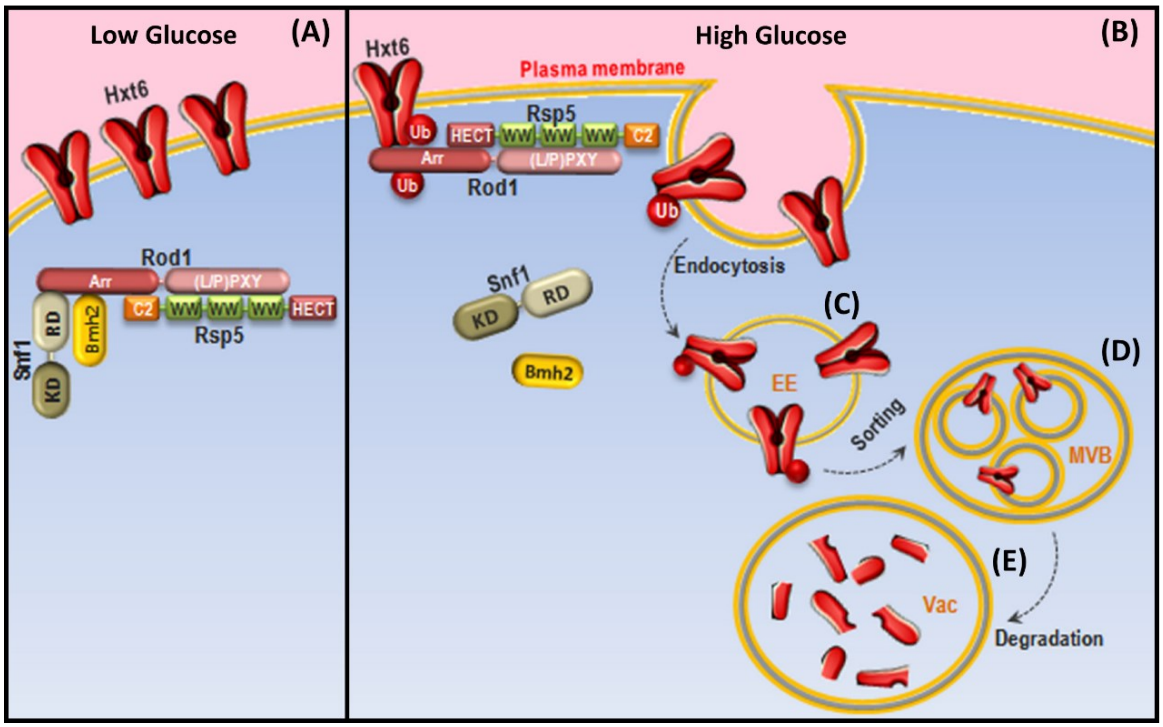

Figure 5: Model for Hxt6 regulation by the Rod1, Snf1 and Bmh1 pathway. (A) Stable expression of Hxt6 at the plasma membrane at low glucose concentration where Rod1 Is phosphorylated by Snf1, promoting the binding of Bmh1 (or Bmh2), decreasing Rod1 endocytic activity. (B) ubiquitination of Hxt6 by Rsp5 with the aid of the adaptor Rod1, (C) endosomal sorting complex required for transport and (D) multivesicular bodies (MVB), (E) final degradation at the vacuole. The figure was taken and modified from Llopis-Torregrosa et al. 2016.

2.6.3 Gene regulation of Rsp5 adaptors

Carbon sources changes and mainly glucose availability modulate Rsp5 adaptors expression in *S. cerevisiae*. In particular, the expression of *CSR2* (*ART8*) is induced when lactate is used as a carbon source, which is thought to mimic glucose starvation conditions; on the other hand, its expression is inhibited in glucose replete conditions. The mechanism underlying the expression of the *CSR2* gene is modulated by the Snf1 kinase and

transcriptional repressors Mig1 and Mig2 (Hovsepian et al., 2017) (see chapters 2.5.1 and 2.5.2). In cells growing in lactate as a carbon source, Snf1 kinase is active and targets Mig1 and Mig2 as substrates for phosphorylation, which impede them from entering the nucleus to exercise their repression on many genes, including *CSR2*. Upon expression, Csr2 protein is ubiquitinated by Rsp5 at the lysine 670; ubiquitination is necessary for its activation and is not involved in Csr2 degradation, like in many other ARTs, including the abovementioned Rod1. Active Csr2 acts as an adaptor of Rsp5 to achieve ubiquitination on the high and moderate affinity glucose transporters Hxt7, Hxt6, Hxt2, and Hxt4. When cells are shifted into a glucose-replete medium, *CSR2* transcription is repressed, and PKA phosphorylates Csr2, phosphorylated Csr2 bind 14-3-3 Bmh1/2 proteins, which probably leads to Csr2 deubiquitination and its consequent inactivation (Hovsepian et al., 2017).

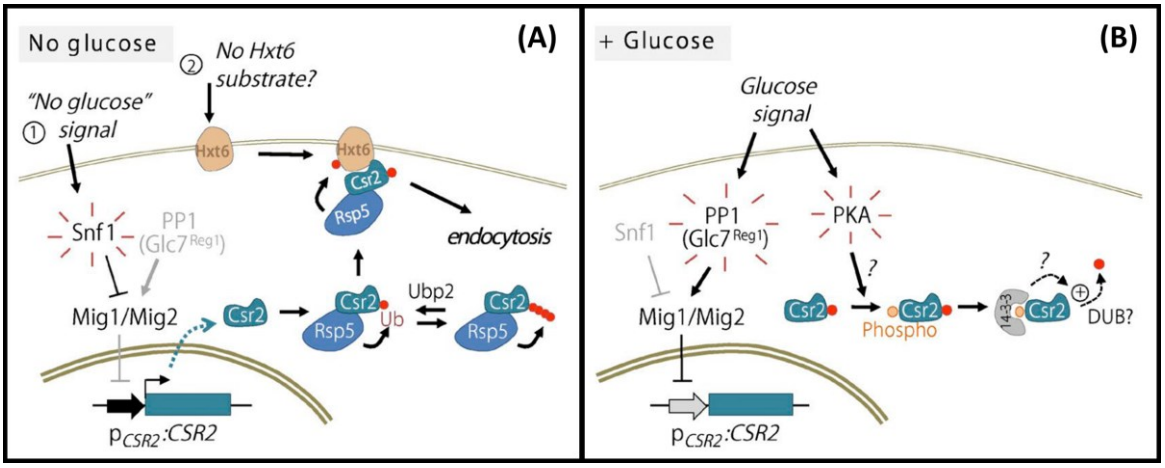

Figure 6: Model for regulation of Csr2 by glucose availability. (A) Glucose absence causes activation of Snf1, which inhibits the transcription factors Mig1 and Mig2, causing *CSR2* derepression. Rsp5 ubiquitinates Csr2, and the ubiquitin-specific protease Ubp2 regulates the ubiquitin chain elongation by deubiquitination. Active ubiquitinated Csr2 serves as an adaptor for the ubiquitination of Hxt6 by Rsp5. (B) The addition of glucose to the medium causes Mig1 and Mig2 repression on *CSR2* transcription, concomitant with Csr2 phosphorylation by protein kinase A, causing the binding of Bmh1 and Bmh2 proteins and the subsequent deactivation of Csr2. The figure was taken and modified from Hovsepian et al. 2017.

Rod1 abundance, in contrast to Csr2, is significantly high in glucose-grown cells and is repressed when cells are shifted into a lactate-containing medium. In this way, Rod1 and Csr2 modulate the degradation of the high-affinity glucose transporters Hxt6 and Hxt7 under lactate (or glucose-depleted conditions) as well as in high glucose concentrations (Becuwe et al., 2012; Llopis-Torregrosa et al., 2016; Hovsepian et al., 2017). Similar regulatory loop regulation could probably be observed in the high-affinity glucose transporters Hxt2 and Hxt4; however, there is no direct experimental proof that Rod1 is involved in the ubiquitination of Hxt2 and Hxt4 in glucose-depleted conditions.

2.6.4 Degradation of cargoes via multivesicular body (MVB) pathway

Ubiquitinated nutrient permeases (referred to as "cargos") are sent via plasma membrane invagination to *early* endosomes, where they encounter ESCRTs (endosomal sorting complex required for transport). There are five protein complexes ESCRT 0, ESCRT I, ESCRT II, ESCRT III, and the AAA ATPase Vps4 complex. The complexes ESCRT-0, I, and II, where each contains at least one protein with a ubiquitin-binding domain (UBD), recognize ubiquitinated cargoes and concentrate them into microdomains at the endosomal membrane; then the ESCRT III promotes the local membrane invagination at the site of cargo concentration, in this stage, the cargoes are deubiquitinated to allow recycling Ub and avoid its depletion. Finally, the Vps4 complex catalyzes ESCRT-III disassembly and intralumenal vesicle (ILV) released into the endosome lumen. After many cycles, several ILVs are formed and accumulated inside the endosome, turning it into a mature endosome called multivesicular body (MVB). The MVB then fuses with the vacuole to expose the protein content of the ILVs to lumenal hydrolases for degradation (Figure 7) (Lauwers et al., 2010; Finley et al., 2012; McNally & Brett, 2018).

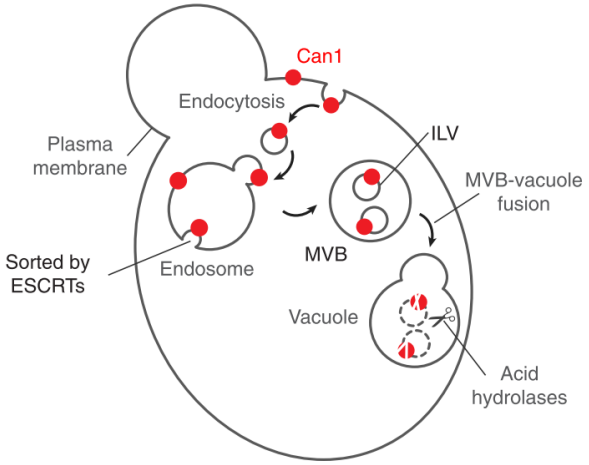

Figure 7: Route to the vacuole lumen for degradation of the arginine permease Can1. Invaginated membranes containing ubiquitinated Can1 (or other cargoes) accumulate at the lumen of endosomes as intralumenal vesicles (ILVs) via the endosomal sorting complex required for transport (ESCRTs). The accumulation of many ILV at the lumen of the endosome turns it into a mature endosome called multivesicular bodies (MVB). The figure was taken and modified from McNally and Brett 2018.

A degradative pathway, which bypasses the ESCRTs complex via cargoes accumulation on vacuolar membranes and subsequent internalization as an intralumenal fragment (ILF) for its degradation, was proposed for some nutrient permeases, like the hexose transporter Hxt3 (McNally & Brett, 2018). However, recent studies based on microfluidic imaging methods, which can capture the complete degradation process *in vivo*, showed that ESCRTs complexes on the vacuole membrane are responsible for sorting the cargoes into

the lumen for its degradation. Furthermore, the authors reveal that any ESCRT complex deletion in *S. cerevisiae* blocked the degradation of Hxt3, evidence that confirms the ESCRTs as the only pathway for the degradation of the nutrient permeases (Yang et al., 2021).

2.7 Cell response in the presence of xylose and arabinose

Xylose and arabinose are not natural substrates of *S. cerevisiae*; consequently, it is unclear how yeast responds to these carbon sources. For instance, xylose and arabinose do not activate a signaling cascade through plasma membrane glucose sensors Rgt2 and Snf3, measured by Mth1 degradation (Jouandot et al., 2011; Brink et al., 2016). in the same direction, xylose and probably arabinose do not trigger signaling via the plasma membrane G protein-coupled receptor Gpr1, which is responsible for triggering nutritional signals that modulate cell fate via PKA and cAMP synthesis (Rolland et al., 2000). Studies in recombinant yeast capable of consuming xylose showed that several genes, which are repressed via the Snf1/Mig1 pathway during growth on glucose, had higher expression in the cells grown on xylose. Nevertheless, the expression of these genes was lower than in glucose derepressed cells; that is to say, recombinant yeast cells capable of growing in xylose exhibit a metabolism that is neither represented by a fully glucose repressed state nor completely glucose derepressed condition (Salusjärvi et al., 2008).

High mRNA levels were detected from the genes that codify the transporters Hxt6 and Hxt7 in recombinant yeast cells growing in xylose under high aeration as well as oxygen limiting conditions; meanwhile, Hxt2 transcription was high in cells growing in xylose under high aeration (Jin et al., 2004).

2.7.1 Strategies to circumvent the lack of sensing of xylose and arabinose

Different strategies have been proposed to circumvent the lack of xylose and arabinose signaling pathways able to activate and deactivate the expression of hexose transporters in recombinant *S. cerevisiae*, capable of consuming these non-natural substrates, which include: promoter substitution in hexose transporters genes for constitutive promoters (Sedlak & Ho, 2004; Subtil & Boles, 2012), truncation of hexose transporters genes promoters to remove transcription factors binding regions (Hauf et al., 2000; Hamacher et al., 2002; Subtil & Boles, 2012; Shin et al., 2015), gene knockouts of components of the three primary sugar signaling pathways (Nijland & Driessen, 2020; Wu et al., 2020) and the creation of semi-synthetic signaling pathways able to react in the presence of xylose (Endalur Gopinarayanan & Nair, 2018).

Jeroen G. Nijland et al. (2016), investigated catabolite degradation of transporters in recombinant *S. cerevisiae* capable of consuming xylose and showed that the low-affinity hexose transporters Hxt1, and Hxt36 (a chimeric transporter formed by the N-terminus of Hxt3 (438 aa) and the C-terminus of Hxt6 (130 aa)), are rapidly degraded in a medium containing xylose as a sole carbon source, similar as in a depleted glucose medium. Meanwhile, the moderate affinity hexose transporters Hxt5 showed a slow degradation rate in xylose, although similar to the rate of degradation in a depleted glucose medium. Nevertheless, the trigger signal for the degradation of these transporters was not assessed; it could be due to glucose absence rather than the presence of xylose itself (Nijland et al., 2016). The authors suggest that the degradation of Hxt1 and Hxt3 is too fast in the xylose medium to enable its use as a sole carbon source in a strain, lacking the primary hexoses transporters (*HXT1-7* and *GAL2*) and endowed with the xylose catabolic pathway, where only Hxt1 or Hxt3 were expressed independently, even though these transporters feature high V_{max} values for xylose uptake, however, with a low affinity (Nijland et al., 2016; Nijland & Driessen, 2020).

A few strategies have been reported to avoid catabolite degradation of the hexose transporters, which are essential to consume non-physiological substrates like arabinose and xylose, including the use of recombinant strains with an Rsp5 E3 ubiquitin ligase variant carrying a mutation at the HECT domain (L733S) that impaired the catalysis of substrate ubiquitination (Wang et al., 1999; Snowdon & van der Merwe, 2012). In addition, knockout of Rsp5 adaptors had been reported to impair ubiquitination of hexose transporters (Nikko & Pelham, 2009; O'Donnell et al., 2015; Sen et al., 2016; Hovsepian et al., 2017). However, these approaches have not been proved in recombinant *S. cerevisiae* strains capable of consuming arabinose and xylose to assess possibly enhanced effects in the utilization of these non-physiological substrates.

Direct engineering of the hexose transporters by mutating or removing lysine residues from the amino acid sequence to eliminate the ubiquitination sites has been shown to disrupt catabolite inactivation of the transporters (Roy et al., 2014; Nijland et al., 2016). The benefit of this method is that the ubiquitination machinery remains intact, avoiding phenotype issues related to the deletion or insertion of mutant enzymatic variants impaired for ubiquitination. However, finding specific residues involved in the ubiquitination process may be time-consuming, considering hexose transporters have between 20 to 30 lysine residues, comprising 3.51% to 5.29% of the total amino acid composition of the transporters, where most of them are not involved in the ubiquitination; therefore, the lysine substitution or removal may harm the performance of the transporter. The lysine residues

involved in ubiquitination are usually located in the N-terminus, middle loop, and C-terminus, cytoplasmatic domains. Bioinformatics tools are available to predict ubiquitination sites and offer a good starting point to test different constructs of the transporters (Radivojac et al., 2010).

Lysine to arginine mutations in the transporter Hxt36 at the residues K12, K25, and K56, located at the N-terminus, turn the transporter stable at the plasma membrane independent of the carbon source (Nijland et al., 2016) (Figure 8). Fermentations with recombinant *S. cerevisiae*, lacking the *HXT1-7/GAL2* genes, harboring a xylose utilization pathway, and overexpressing the Hxt36 stable variant ($Hxt36_{3K}$), resulted in a strain able to rapid growth in medium including xylose as a sole carbon source in comparison to the same strain overexpressing Hxt36 wild-type (Nijland et al., 2016). Moreover, fermentations with the same strains in a glucose/xylose medium showed an overall decrease in the fermentation time for the strain overexpressing $Hxt36_{3K}$, however with a sequential utilization of glucose and xylose, respectively (Nijland et al., 2016).

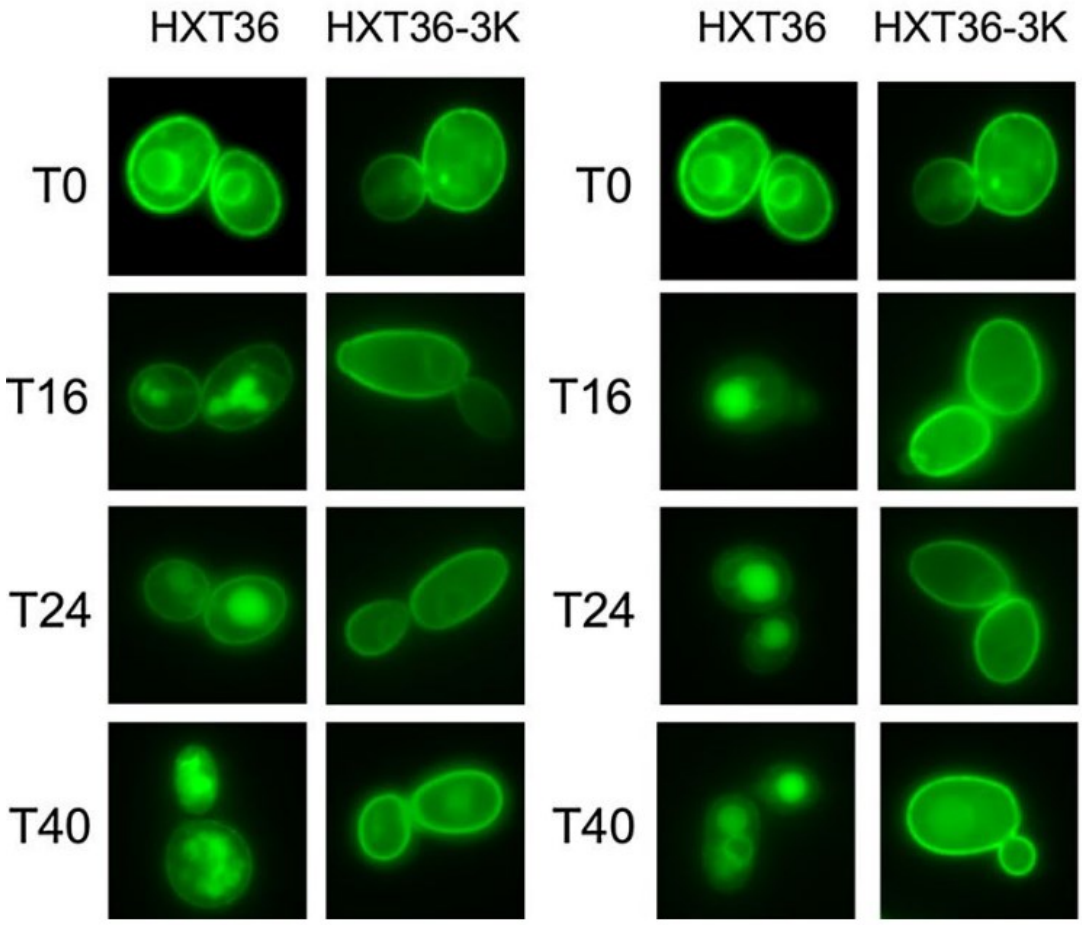

Figure 8: Membrane localization of the transporter Hxt36 and the variant Hxt36-3K fused to GFP. Micrographs of cells expressing the transporter $Hxt36_{GFP}$ and the variant $Hxt36_{3K\_GFP}$ (K12,25,56 to R) over time (T(h)). Cells were grown on minimal medium with 2% glucose (A) and 2% xylose (B). The figure was taken and modified from Nijland et al. 2016.

As mentioned in chapter 2.6, upstream phosphorylation signals may trigger ubiquitination at the target proteins; therefore, mutations or removal of the amino acids involved in phosphorylation could disrupt catabolite inactivation of the target permease (Marchal et al., 1998; Kelm et al., 2004; Nikko et al., 2008). For example, the plasma membrane ATP-binding cassette (ABC) transporter Ste6 is sequentially phosphorylated at the residues T613 and S623, ubiquitinated, and delivered to the vacuole for degradation; mutations of these residues to alanine successfully blocked its ubiquitination and endocytosis (Kelm et al., 2004). However, identifying phosphorylation residues directly involved in ubiquitination may be challenging due to the large number of residues that may be phosphorylated, as well for the wide range of amino acid consensus sequences used for the kinases to recognize their substrates (Kennelly & Krebs, 1991; Suzuki et al., 2015); for instance, the galactose permease Gal2 has 51 serine, 27 threonine, and 25 tyrosine residues, comprising together the 17.95% of the total amino acid composition of the transporter. Nevertheless, recently high-throughput mass spectrometry studies have verified *in vivo* phosphorylation sites in the *S. cerevisiae* proteome (Holt et al., 2009; Sadowski et al., 2013). These experimental data can be used to reduce the screening of phosphorylation sites directly involved in the internalization of the target transporter.

Hexose transporters are subjected to catabolite inactivation depending on the physiological state of the cells and the carbon source availability in the medium; however, not all of them exhibit the same degradation rate; for example, the low-affinity glucose transporter Hxt11 is stable at the plasma membrane over a wide range of glucose concentrations (Shin et al., 2015), the stability relay on its N-terminal where most of *S. cerevisiae* transporters harbor the degron signaling information; for instance, the truncation of the N-terminal of Hxt7 blocked its degradation in a high glucose medium (Krampe & Boles, 2002); nevertheless, the truncation also caused a significant loss in activity of the transporter. A way to circumvent these issues is to create chimeras harboring an N-terminal of a stable transporter with the rest of the peptide sequence corresponding to a transporter with suitable kinetic properties for the uptake of pentose sugars. Shin et al. (2017) successfully developed a chimeric transporter between Hxt11 and Hxt2 where the residues 1 to 49 of Hxt2 were replaced by the residues 1 to 54 of Hxt11, resulting in a chimera with stable plasma membrane expression with the identical kinetic properties of Hxt2. Fermentations with recombinant *S. cerevisiae*, lacking the *HXT1-7*/*GAL2* genes, harboring a xylose utilization pathway, and overexpressing the chimera Hxt11/Hxt2 resulted in a strain able to consume xylose faster in a medium containing xylose/glucose mixtures, with high concentrations of the inhibitor acetic acid, in comparison to the same strain overexpressing Hxt2 wild-type (Shin et al., 2017).

2.8 Steric inhibition of xylose and arabinose transport by glucose

The low affinity for xylose and arabinose in comparison to glucose is a significant disadvantage of the endogenous *S. cerevisiae* hexose transporters; as a result, glucose is the preferred substrate for uptake in mixed sugar fermentations, a phenomenon that causes a lack in the influx of pentoses which are competitively inhibited by glucose (Subtil & Boles, 2011; Farwick et al., 2014; Nijland et al., 2014). Furthermore, the heterologous expression in *S. cerevisiae* of known xylose and arabinose transporters showed similar results to the endogenous transporters, where neither of them is exclusively selective for these pentose sugars, leading to similar issues of competitive inhibition by glucose in mixed sugar fermentations (Henderson & Maiden, 1990; Subtil & Boles, 2011). Moreover, heterologous xylose transporter like the xylose/glucose/H^+ symporter *Ci*Gxs1 from *Candida intermedia* (Leandro et al., 2006) exhibit low xylose uptake rates in comparison with some *S. cerevisiae´s* endogenous transporters like Gal2, who exhibit a V_{max} value 16 times higher than CiGxs1 (5.68 vs. 91.3 nmol min^{-1} mg_{CDW}^{-1}, respectively) (Young et al., 2012; Farwick et al., 2014).

A few approaches have been used to engineer pentose transporters that are no longer inhibited by glucose, including evolutionary engineering, error-prone PCR, gene shuffling, and overexpression, among other techniques, with the aim to increase the availability of xylose and arabinose inside the cell, allowing co-consumption of glucose and pentoses in sugar mixed fermentations (Nijland & Driessen, 2020).

Using an error-prone PCR technique in conjunction with a screening *S. cerevisiae* strain, which lacks all hexose transporter (*hxt*^{0}), as well as all glucose hexokinases (*hxk*^{0}), and harbors a xylose utilization pathway, Farwick et al. (2014) were able to identify an asparagine residue (376) at the transmembrane helix 8 of the galactose permease Gal2, which is involved in the glucose affinity. This asparagine residue is conserved among all hexose transporters and plays a crucial role in glucose recognition (Farwick et al., 2014; Nijland et al., 2014). Gal2 asparagine´s 376 substitution by phenylalanine resulted in a transporter ($Gal2_{N376F}$) that completely abolished the uptake of glucose with decreased K_m values for xylose in comparison to the wild type (91mM and 225mM, respectively) (Farwick et al., 2014); similar results were obtained for the substitution of the asparagine 366 in Hxt11 (Shin et al., 2015), 367 in Hxt36 (Nijland et al., 2014), and 370 in Hxt7 (Farwick et al., 2014).

Structure analyses of Gal2 and Hxt36, based on the crystal structure of the proton-coupled sugar transporter XylE from *E. coli*, bound with glucose, showed the residue N376 in Gal2 and N367 in Hxt36, located at the sugar-binding pocket site in close proximity with the hydroxymethyl group of glucose, which is absent in xylose and arabinose (Farwick et al., 2014; Nijland et al., 2014). Substitution of this conserved asparagine by other amino acids that are more hydrophobic or bulkier could interfere with the proper binding of glucose (Nijland & Driessen, 2020). In particular, the N376F mutation in Gal2 drastically reduces the space in the transporter´s central cavity, which may probably be responsible for the complete abolishment of glucose uptake (Farwick et al., 2014).

2.9 Relevance of the galactose permease Gal2 in the uptake of non-physiological substrates in *S. cerevisiae*

Gal2, a member of the major facilitator superfamily, is one of the most studied hexose transporters in *S. cerevisiae*. Although its expression is repressed in the presence of glucose (chapter 2.5.4), it also transports this sugar with high affinity when constitutively expressed (Reifenberger et al., 1997). Recent efforts to engineer yeast strains for the utilization of plant biomass have unraveled the ability of Gal2 and Gal2 variants to transport non-physiological substrates (Table 1). Specifically, Gal2 was shown to transport xylose (Hamacher et al., 2002; Young et al., 2011), arabinose (Becker & Boles, 2003; Wisselink et al., 2007; Subtil & Boles, 2011), xylitol (Tani et al., 2016) and D-galacturonic acid (Protzko et al., 2018). As previously mentioned in chapter 2.8 improving its kinetic properties and substrate specificity, especially for pentoses, has become a crucial target in strain engineering (Farwick et al., 2014; Reznicek et al., 2015; Wang et al., 2017; Verhoeven et al., 2018).

This study will focus on the engineering of hexose transporters of *S. cerevisiae*, with a particular focus on Gal2, with the final goal of improving the utilization of the non-physiological substrates arabinose and xylose.

Table 1: Kinetic properties of different galactose permease Gal2 mutants and the respective wild type for different substrates.

	Main features	Glucose K_m (mM)	Reference
Gal2	Wild type	1.5 ± 0.2	(Farwick et al., 2014)
		1.9 ± 0.2	(Bracher et al., 2018)
Gal2$_{N376V}$	Decreased affinity for glucose	22.27 ± 0.2	(Farwick et al., 2014)
Gal2$_{N376F}$	Unable to transport glucose	-	(Farwick et al., 2014)
Gal2$_{N376I}$	Decreased affinity for glucose	101 ± 47	(Verhoeven et al., 2018)
Gal2$_{N376S}$	Decreased affinity for glucose	38 ± 1	(Verhoeven et al., 2018)
Gal2$_{N376T}$	Decreased affinity for glucose	57 ± 1	(Verhoeven et al., 2018)
Gal2$_{N376T_T89I}$	Unable to transport glucose	-	(Verhoeven et al., 2018)
Gal2$_{T89I}$	Decreased affinity for glucose	7 ± 0.2	Verhoeven 2021
	Main features	**Arabinose K_m (mM)**	**Reference**
Gal2	Wild type	57 ± 11	(Subtil & Boles, 2011)
		335 ± 21	(Bracher et al., 2018)
Gal2$_{N376I}$	Decreased affinity for glucose	117 ± 16	(Verhoeven et al., 2018)
Gal2$_{N376S}$	Decreased affinity for glucose	186 ± 33	(Verhoeven et al., 2018)
Gal2$_{N376T}$	Decreased affinity for glucose	171 ± 17	(Verhoeven et al., 2018)
Gal2$_{N376T_T89I}$	Unable to transport glucose	103 ± 40	(Verhoeven et al., 2018)
Gal2$_{T89I}$	Decreased affinity for glucose	99 ± 18	(Verhoeven et al., 2018)
	Main features	**Xylose K_m (mM)**	**Reference**
Gal2	Wild type	225.6 ± 15.8	(Farwick et al., 2014)
Gal2$_{N376V}$	Decreased affinity for glucose	168.3 ± 31.6	(Farwick et al., 2014)
Gal2$_{N376F}$	Unable to transport glucose	91.4 ± 8.9	(Farwick et al., 2014)
	Main features	**Galactose K_m (mM)**	**Reference**
Gal2	Wild type	5.3 ± 0.2	(Kasahara et al., 1996)

3 Aim of the thesis

The main goal of this study was to improve the utilization of the main pentose fraction of lignocellulosic feedstocks, D-xylose, and L-arabinose in *S. cerevisiae* by increasing the cell permeability of these non-physiological substrates by engineering the galactose permease Gal2.

First, we aim to stabilize the Gal2 transporter at the plasma membrane in the presence of glucose, the main component of lignocellulosic feedstocks, which triggers the Gal2 degradation, mediated by the covalent attachment of the small 76 amino acid protein ubiquitin (Ub) to a lysine residue at the targeted transporter; in a multi-step process called ubiquitination.

We evaluated the stability at the plasma membrane of the transporters as an indirect measurement of ubiquitination impairment. The technique was based on the *in vivo* subcellular localization by confocal laser scanning microscopy (CLSM) of the wild type transporters and their variants fused with GFP at the C-terminus. Using this approach, we screened for different Gal2 constructs where lysine residues were mutated or removed from the protein sequence to uncover which lysine residues are likely involved in ubiquitination and consequent turnover of the transporter. We furthermore evaluated upstream signals caused by phosphorylation which triggers ubiquitination and consequent turnover of the targeted protein by screening Gal2 constructs where serine residues were mutated to alanine in the protein sequence.

We aimed to identify E3 ubiquitin ligase adaptors involved in the recognition of Gal2 permease to attempt impair ubiquitination. We individually deleted the Rsp5 adaptors *BUL1* and *ROD1* ORFs and expressed Gal2 wild-type in these strains to assess its *in vivo* subcellular localization.

In this study, by using error-prone PCR (epPCR) and a screening system based on a recombinant strain AFY10 which lacks all hexose transporters and hexo-/glucokinases and is genetically engineered to use pentoses as a carbon source when the pathways are provided (Farwick et al., 2014), we aimed to find new mutations in Gal2 that enable the permease to transport pentoses without steric inhibition caused by glucose and an improved capacity for xylose and arabinose transport.

Finally, we aimed to determine how intracellular glucose interferes with the uptake of xylose and identify if glucose-insensitive transporters variants like $Gal2_{N376F}$ exhibit a symmetrically reduced affinity for glucose from both sides of the plasma membrane.

4 General discussion

The main goal of the thesis was to improve the utilization of xylose and arabinose by increasing the cell permeability of these sugars, mediated by the galactose permease Gal2. In the project's first stage, the objective was to stabilize the galactose permease Gal2 at the plasma membrane through different approaches, where some of them ended up in successfully stabilized Gal2 variants; these results can be seen in the first publication (Tamayo Rojas et al., 2021b) (see chapter 6.1). The second goal was to engineer the Gal2 permease to find mutations that render variants that exhibit a high transport rate of pentoses, which are less susceptible to competitive glucose inhibition; these results can be seen in the second publication (Tamayo Rojas et al., 2021a) (see chapter 6.2). Considering the overall results of the previously mentioned publications, we aimed to answer the influence of intracellular glucose in the uptake of xylose, which leads us to develop an *in vivo* assay for the analysis of glucose efflux. These results culminated in the last publication presented in this thesis (Tamayo Rojas et al., 2022) (see chapter 6.3).

Considering that all results and their discussions are already embedded in the publications, the following discussion chapters will focus mainly on the central results that interconnect the manuscripts, as well as future approaches that can be taken for the project continuity.

4.1 Identification of Gal2 lysine residues involved in ubiquitination

Gal2 contains 30 lysine residues, corresponding to 5.23% of the total amino acid composition of the peptide sequence. It is known that mono-ubiquitination by Rsp5 on multiple lysine residues is necessary to internalize Gal2 (Horak & Wolf, 2001) (see chapter 2.6). However, the authors did not identify the specific lysine residues involved in the ubiquitination processes. This study screened several Gal2 variants where lysine residues were mutated or removed from the peptide sequence to discover which lysine residues are likely involved in ubiquitination and consequent turnover of the transporter. The screening technique was based on the *in vivo* subcellular localization of the wild type transporters and their variants fused with GFP at the C-terminus by confocal laser scanning microscopy (CLSM) to evaluate the stability at the plasma membrane of the transporters, which is an indirect measurement of ubiquitination impairment.

The subcellular localization of Gal2 wild-type in cells growing in galactose showed a localization at the plasma membrane but partly also in the vacuole (Figure 9A), indicating

a constitutive degree of degradation (Tamayo Rojas et al., 2021b); However, the subcellular localization of the Gal2 wild-type in cells growing in glucose was mainly in the vacuole compartment (Figure 9B), which is consistent with previous observations (Horak et al., 2002).

After screening different Gal2 constructs with mutated or removed lysine residues, we found that mutations of the N-terminal lysine residues 27, 37, and 44 ($Gal2_{3KR}$) to arginine produced a functional transporter that, when fused with GFP ($Gal2_{3KR\_GFP}$), showed an exclusive localization at the plasma membrane in cells growing in galactose or glucose as a sole carbon source (Figure 9C and 9D). This result revealed how crucial are these lysine residues for the degradation of Gal2 (Tamayo Rojas et al., 2021b). However, future studies could examine if simultaneous ubiquitination must occur on all three lysine residues (K27, K37, and K44) in Gal2 as a pre-requisite for the transporter turnover or if each lysine residue's ubiquitination induces partial or complete transporter degradation.

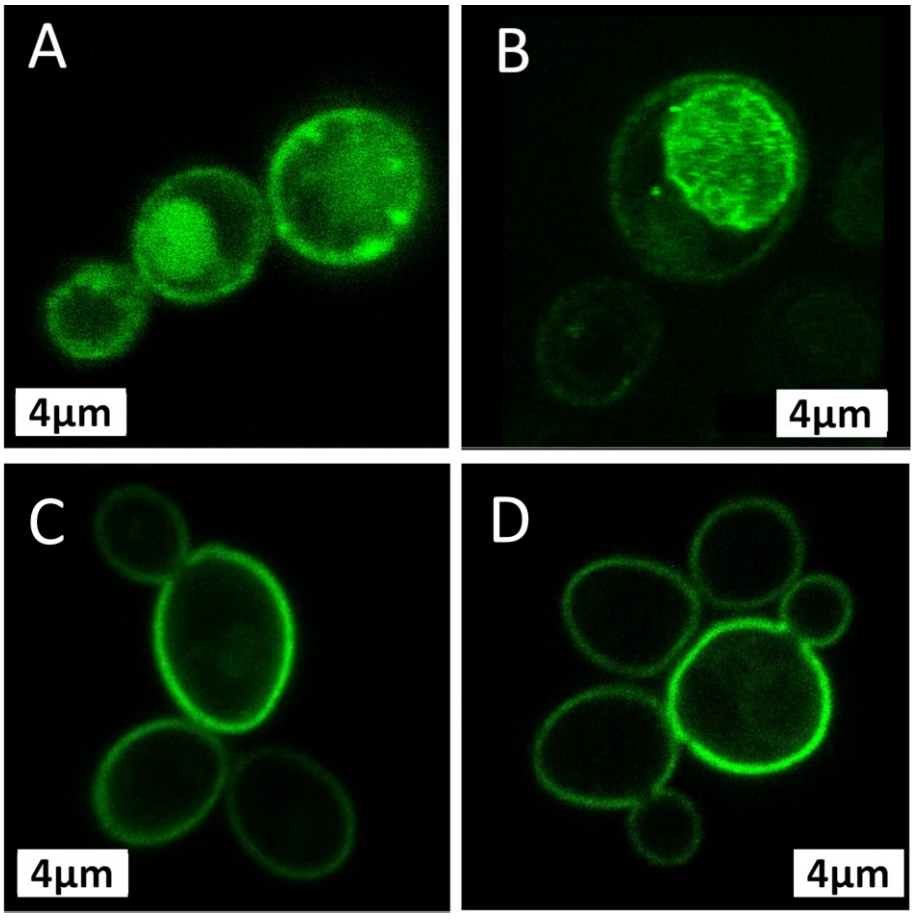

Figure 9: Subcellular localization of Gal2 with mutated lysine residues 27, 37, and 44. Representative micrographs of CEN.PK2-1C cells expressing GFP-tagged Gal2 wild-type (A, B) and $Gal2_{3KR}$ (C and D) from centromeric plasmids. The cells were grown in SC media with 2% galactose, left (A and C), or 2% glucose, right (B and D). The scale bar represents 4µM. The figure was taken and modified from Tamayo Rojas et al., 2021b.

The involvement in ubiquitination of the lysine residues 27, 37, and 44 was foreseen by the ubiquitination prediction tool UbPred (Radivojac et al., 2010), which identified only these residues with a high score of confidence as potential targets by ubiquitination; consequently, our empiric results validated the algorithm predictions, showing that most of the lysine residues in Gal2 are not involved in the ubiquitination process. The mutation or removal of lysine residues not involved in ubiquitination often leads to side effects associated with loss of functionality and miss localization of the transporters variants (Tamayo Rojas et al., 2021b). Nijland et al. 2016, using a similar approach, identified a degron region at the N-terminus of the chimeric transporter Hxt36, where lysine residues 12, 25, and 56 were recognized as a target of ubiquitination. Other authors mentioned the presence of a degron at the N-terminus in the hexose transporter Hxt7 and the amino acid permease Gap1 (Soetens et al., 2001; Krampe & Boles, 2002); however, the degron signal in permeases is not exclusively located at the N-terminus; as an example, the degradation of the cellobiose transporter CDT-2 from the filamentous fungus *Neurospora crassa* relies on the C-terminal lysine residues, this C-terminal region is also recognized in *S. cerevisiae* as a degron signal when CDT-2 is expressed in this host (Sen et al., 2016).

4.2 Identification of serine residues involved in phosphorylation signal for Gal2 degradation

It is known that upstream phosphorylation signals may trigger ubiquitination at target proteins (Marchal et al., 1998; Kelm et al., 2004; Nikko et al., 2008; Lundh et al., 2009) (see chapter 2.6); For this reason, we hypothesized that mutations of the amino acids involved in phosphorylation in Gal2 could disrupt its catabolite inactivation. Using a similar screening approach to assess the stabilization of Gal2, as mentioned in chapter 4.1, it could be shown that serine residues 32, 35, 39, 48, 53, and 55 are likely involved in the internalization of Gal2, since a Gal2 construct, where all these serine residues were mutated to alanine residues and tagged with GFP ($Gal2_{6SA\_GFP}$), showed practically complete localization at the plasma membrane in cells growing in galactose or glucose as a sole carbon source (Figure 10C and 10D) (Tamayo Rojas et al., 2021b). These results correlate with high-throughput proteomic studies which revealed that these serine residues in Gal2 are targets for phosphorylation (Holt et al., 2009).

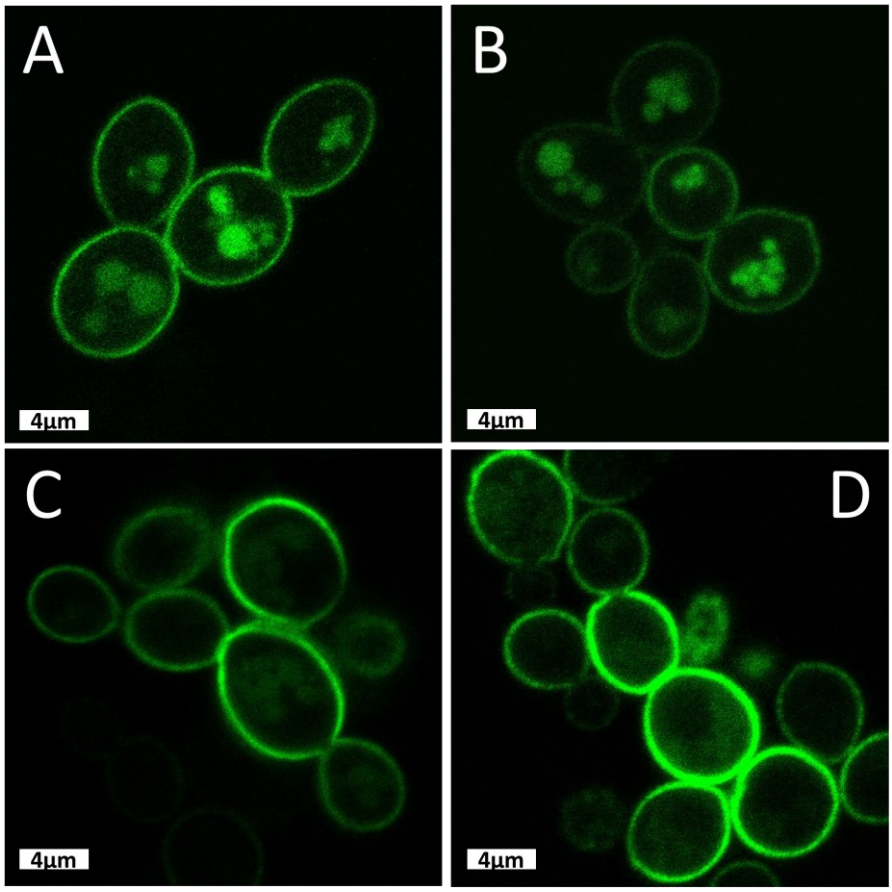

Figure 10. Subcellular localization of Gal2 with mutated serine residues 32, 35, 39, 48, 53, and 55. Representative micrographs of CEN.PK2-1C cells expressing GFP-tagged Gal2 wild-type (A, B) and Gal2^{6SA} (C and D) from centromeric plasmids. The cells were grown in SC media with 2% galactose, left (A and C), or 2% glucose, right (B and D). The scale bar represents 4µM. The figure was taken and modified from Tamayo Rojas et al., 2021b.

The open question for future studies will be to identify the kinase(s) responsible for the phosphorylation of the serine residues at the N-terminus of Gal2. The plasma-membrane-localized casein kinases 1 are encoded in *S. cerevisiae* by the genes *YCK1* and its paralog *YCK2*. Yck1/Yck2 kinases are activated by the plasma membrane glucose sensors Snf3 and Rgt2 as part of the glucose induction pathway (see chapter 2.5.1); these kinases are also involved in the phosphorylation of some Rsp5 adaptors (see chapter 2.6). Studies suggest that Yck1/Yck2 are responsible for the direct phosphorylation of the maltose permease Mal61 in response to glucose, acting as a primary signal for ubiquitination of the permease and its further degradation (Gadura et al., 2006). Similar results were found for the receptor for alpha-factor pheromone Ste2 (Hicke et al., 1998) and Ste3 (Panek et al., 1997) and the uracil permease Fur4 (Marchal et al., 1998).

Casein kinases 1 target proteins with an N-terminus rich in negatively charged residues, like aspartic acid or glutamic acid, as well as other phosphorylated residues, where one of

these residues is commonly located between 1 to 5 amino acids upstream (direction of N-terminus) of the phosphoacceptor (Kennelly & Krebs, 1991), criteria that are fulfilled by serine residues 32, 48 and 53 in Gal2; furthermore, phosphorylation of these residues will increase the number of negatively charged amino acids which will likely cause the subsequent phosphorylation of serine residues 35, 39 and 55 in the permease.

4.3 ARTs Rod1 and Bul1 involvement in Gal2 internalization

The knockout of Rsp5 adaptors had been reported to impair ubiquitination of hexose transporters (Nikko & Pelham, 2009; O'Donnell et al., 2015; Sen et al., 2016; Hovsepian et al., 2017). Our findings revealed that Rsp5 adaptors Bul1 and Rod1 are presumably involved in the ubiquitination of Gal2, as their individual deletion led to a stabilization of Gal2 at the plasma membrane in cells growing in glucose as a sole carbon source; however, the stabilization was not as strong as the variant $Gal2_{\mathbf{3KR}}$ or $Gal2_{\mathbf{6SA}}$, for this reason, we presumed that multiple Rsp5 adaptors may be involved in the internalization of Gal2 (Tamayo Rojas et al., 2021b).

Identifying all Rsp5 adaptors involved in the degradation of Gal2 was not in the scope of this study. Future research studies could assess the stability of Gal2 in several strains where multiple Rsp5 adaptors are deleted for the complete identification of adaptors that recognize Gal2 as a substrate for ubiquitination (Sen et al., 2016). Considering that Rsp5 adaptors are regulated at transcriptional and posttranscriptional levels, depending on the type of carbon source and its availability (see chapters 2.6.2 and 2.6.3), a broad set of Rsp5 adaptors should be able to recognize the N-terminus degron in Gal2, not only in different concentrations of glucose also in the absence of it or even in the presence of galactose, assuming Gal2 experiences a basal level of constitutive degradation regardless of the carbon source (Tamayo Rojas et al., 2021b).

4.4 Increase the stability of Gal2 by direct disruption of ubiquitination sites or phosphorylation sites, perspectives

The constructs $Gal2_{\mathbf{3KR}}$ and $Gal2_{\mathbf{6SA}}$ showed comparably higher stability at the plasma membrane and affinity for glucose, which was also similar to the wild type ($K_{\mathbf{m}}$ 2.46, 2.70, and 3.19 mM, respectively); however, the uptake rate of the construct $Gal2_{\mathbf{6SA}}$ was significantly higher than $Gal2_{\mathbf{3KR}}$ and this last one higher than the wild type ($V_{\mathbf{max}}$ 0.8330, 0.6698, and 0.3832 nmol min^{-1} $mg_{\mathbf{CDW}}^{-1}$, respectively); indicating these N-terminal modifications render in an increase in the uptake rate, probably due to the increasing

number of transporters at the plasma membrane, while keeping the same affinity for the substrate (Tamayo Rojas et al., 2021b).

Also, the growth conferred by the expression of $Gal2_{6SA}$ in the *hxt*^{0} strain EBY.VW4000 (Wieczorke et al., 1999) was superior in comparison with the expression of $Gal2_{3KR}$, which in turn was superior to the wild type, when the cells were growing in SC medium with 2% (w/v) glucose (Tamayo Rojas et al., 2021b).

The differences between the stable versions and the wild type seem to be clear and substantiated based on the fluorescent micrographs results (Figure 9, and Figure 10); however, the differences between the stable versions $Gal2_{3KR}$ and $Gal2_{6SA}$ were unexpected. Our hypothesis regarding the differences between these two stable versions is based on the assumption that phosphorylation preludes ubiquitination; therefore, the arrestin-Rsp5 complex could still bind $Gal2_{3KR}$ since all phosphorylation sites are present in this construct, partially impairing the transport rate of the permease, in which the arrestin-Rsp5 complex could act as a non-competitive inhibitor, a type of inhibition involved in the decreasing of V_{max} values.

Another hypothesis about the differences between $Gal2_{6SA}$ and $Gal2_{3KR}$ may be related to the subtle amino acid composition differences of the N-terminus between both constructs. A few amino acid changes at the cytosolic N-terminal domain in almost identical hexose transporters may cause long-range effects that create differences in transport activity/specificity between permeases (Jordan et al., 2016). For example, the active site of Hxt13 and Hxt17 or Hxt15 and Hxt16 are identical; both pairs share more than 97% sequence identity, whereas Hxt13 and Hxt17 differ only by 15 amino acids at the N-terminal tail, and Hxt15 and Hxt16 differ by only two amino acids at domain mentioned above. Studies suggest that these differences in the cytosolic modules result in different kinetic properties of each transporter, which are related to transporter dynamics rather than substrate binding (Jordan et al., 2016).

Prospective studies could also evaluate potential adverse side effects in the cells caused by the overexpression of Gal2 stable variants, considering that the general overexpression of membrane transporters decreases the overall fitness of the hosts due to membrane piercing or interferences with other plasma membrane proteins, among other causes (Tomala & Korona, 2013); therefore, excessive accumulation of stable Gal2 variants under high expression conditions, should be examined in different strains and expressions levels. In addition, the inability of the cell to degrade stable variants of Gal2 in the plasma membrane may cause competition for membrane space between Gal2 stable versions and

other vital membrane proteins, considering there is a limited membrane space (Casey & Follows, 2020). Also, the cell will not be able to remove damaged Gal2 stable variants from the plasma membrane regarding membrane proteins can be damaged, e.g., by oxidation (Hajieva et al., 2015).

4.5 Identification of glucose-insensitive Gal2 variants

As mentioned in chapter 2.8, impairments in the uptake of xylose or arabinose by steric inhibition of glucose result in a decreased uptake of these pentoses in glucose mixed sugar fermentations. In this study, by using error-prone PCR (epPCR) and a screening system based on a recombinant strain (AFY10), lacking all hexose transporters and glucose kinases and genetically engineered to use pentose as a carbon source when the pathways are provided (Farwick et al., 2014), we were able to find two mutations in Gal2 (N376Y/M435I) which together incorporate two properties highly desirable for fermentation of lignocellulosic hydrolysates, first the ability to transport pentoses in the presence of glucose and second an improved capacity for xylose and arabinose transport (Tamayo Rojas et al., 2021a). In addition, insertion of serine mutations at the residues 32, 35, 39, 48, 53, and 55 yielded a transporter ($Gal2_{6SA\_N376Y\_M435I}$) with the abovementioned features plus the increase in stability at the plasma membrane (see chapter 4.2), being one of the most advanced pentose transporters. The overexpression of this transporter in a recombinant industrial diploid strain, capable of consuming xylose, reduced the overall fermentation time of the total xylose consumption by approximately 20h, corresponding to 40% of the total fermentation course of a glucose/xylose mixture fermentation (Tamayo Rojas et al., 2021a); however, the strain was only able to consume glucose and xylose sequentially, proving that the xylose permeability is not the only determinant of co-consumption of both sugars (Tamayo Rojas et al., 2021a). This probably relies on metabolic constraints as well as glucose repression mechanisms (Papapetridis et al., 2018); despite the fact that, some studies support the hypothesis of the direct involvement of pentose permeability in co-consumption of xylose/glucose mixture fermentations (Nijland et al., 2014; Reznicek et al., 2015; Shin et al., 2015).

4.5.1 Relationship between the co-consumption of glucose/xylose and an improved pentose permeability

Economically feasible production of biofuels and other bulk chemicals from lignocellulosic hydrolysates requires an efficient co-fermentation of pentose and hexose sugars to increase the volumetric productivity of industrial processes. Recent strain engineering

strategies for enabling pentose utilization by *S. cerevisiae* commonly yield strains that ferment pentoses only after glucose is exhausted, causing a costly increase in the fermentation time. The reason for sequential utilization of glucose and pentose, as previously mentioned in chapter 4.5, can be related to metabolic constraints as well as glucose repression mechanisms (Papapetridis et al., 2018). However, many authors attributed the lack of co-fermentation based on uptake impairment of pentoses into the cells.

Reznicek et al. (2015), achieved co-consumption rates of glucose and xylose using a Gal2 variant with reduced affinity for glucose and increased affinity for xylose ($Gal2_{L301R\_K310R\_N314D\_M435T}$); however, the results were obtained from fermentations using a recombinant laboratory strain, able to use xylose, where all the main permeases were deleted (*HXT1-7* and *GAL2*, strain DS68625) (Nijland et al., 2014). Glucose/xylose mixtures fermentations with a strain lacking the main hexose transporters could influence the results since, in this strain, glucose is poorly uptaken by the remaining endogenous transporters (Hxt8-11 and Hxt13-17) (Reifenberger et al., 1995; Diderich et al., 1999), and the transient overexpression of a low glucose affinity transporter variant in the study, probably does not greatly contribute to glucose permeability, resulting in an overall slow glucose influx into the cell, which could cause the co-consumption titers of xylose and glucose. Similar co-consumption results, using the same setup mentioned above, were found for the overexpression of a low glucose affinity Hxt11 variant ($Hxt11_{N366T}$) (Shin et al., 2015), a stable chimeric transporter between the N-terminus of Hxt11 and Hxt2 with a reduced glucose affinity ($Hxt11/2_{N361F}$) (Shin et al., 2017) and a Hxt3/Hxt6 chimera with an asparagine mutation at position 376 ($HXT36_{N367A}$), which dramatically reduces the affinity for glucose (Nijland et al., 2014). It is tempting to speculate that the overexpression of the resistant to ubiquitination-mediated degradation, glucose-insensitive, and high xylose capacity transporter $Gal2_{6SA\_N376Y\_M435I}$ (Tamayo Rojas et al., 2021a) in the DS68625 strain could end in co-consumption rates of xylose and glucose. For this reason, more studies on different background strains are necessary to validate the hypothesis of the direct involvement of pentose permeability in the co-consumption of xylose and glucose in cofermentations.

Papapetridis et al. (2018), engineered a xylose-fermenting *S. cerevisiae* strain, where the genes *PGI1* and *RPE1* were deleted, to force the strain to co-consume xylose and glucose since the deletion of *PGI1* blocked glucose-6-phosphate to proceeding into glycolysis and *RPE1* deletion prevents the entry of ribulose-5-phosphate into the non-oxidative pentose phosphate pathway (noxPPP); therefore, the only way to utilize glucose as carbon and

energy source in this strain was by concomitant conversion of xylose into xylulose-5-phosphate, enabled by the heterologous expression of xylose isomerase (XylA) and the overexpression of the native xylulose kinase Xks1 (see Figure 11). In addition, to prevent a potential excessive formation of NADPH, the strain additionally included a replacement of the native *S. cerevisiae* $NADP^+$ dependent Gnd1 and Gnd2 by the NAD^+ dependent bacterial enzyme GndA to prevents a redox imbalance (Boles et al., 1993; Dickinson et al., 1995; Papapetridis et al., 2016), (see Figure 11). This strain, when submitted to laboratory evolution in xylose/glucose mixtures, yielded evolved variants harboring mutations in the genes that codify: the predominant hexokinase during growth on glucose Hxk2, one of three beta-subunits variants of the Snf1 kinase complex Gal83 and the NEDD4 family E3 ubiquitin ligase Rsp5. Introducing these gene mutations ($GAL83_{G673T}$) or deletions (*hxk2Δ, rsp5Δ*) into a non-evolved xylose-fermenting, *S. cerevisiae* strain strongly stimulated simultaneous utilization of xylose and glucose.

Even though in the study previously mentioned, were not found any mutations in the coding regions of the hexoses transporters (*HXT1–17* and *GAL2*), the mutations that caused the loss of function of Hxk2, an enzyme which plays a vital role in the regulation of multiple genes in *S. cerevisiae* including the hexose transporters Hxt4, Hxt6, Hxt7, and Gal2 (indirectly via Gal4), (see chapter 2.5.2), may indicate the role of the high-affinity transporters expression as an essential element to achieve co-fermentation, since it has been shown that the *hxk2Δ S. cerevisiae* mutants showed increase transcription levels of the high-affinity hexose transporters *HXT2* and *HXT7* (Petit et al., 2000); furthermore, the mutation in *GAL83* (*$GAL83_{G673T}$*) presumably allows the recruitment of Snf1 kinase to the nucleus, even in the presence of glucose (Papapetridis et al., 2018), where the complex perform the phosphorylation Mig1 and Hxk2 resulting in the nuclear export of these two proteins and the consequent disassociation of them with the transcription repressor complex with Ssn6 and Tup1 in the promoter regions of the earlier mentioned genes (DeVit & Johnston, 1999; Vincent et al., 2001; Fernańdez-García et al., 2012), (see chapter 2.5.2). In addition, the mutations in *RSP5*, which probably caused its loss of function (Papapetridis et al., 2018), may indicate the involvement of the disruption of hexose transporters turnover caused by Rsp5 misfunction (see chapter 2.6) as part of the crucial components to achieving the co-consumption of xylose and glucose. However, the authors mentioned that the deletion of *RSP5* yield in strains with reduced growth rates, which is probably due to Rsp5 is involved in the regulation of a multitude of cellular processes, including the mentioned role in protein trafficking as well as ribosome stability, regulation of the large subunit of RNA polymerase II, regulation of fatty acid synthesis and stress response (Wang et al., 1999; Hoppe et al., 2005; Shcherbik & Pestov, 2011). These results

support our approach in the present work, which avoided the deletion of *RSP5* in favor of the deletions of arrestine genes encoding Rsp5 adaptors, or the direct modification of the amino acids involved in the transporter turnover as better strategies to disrupt the internalization of hexose transporters.

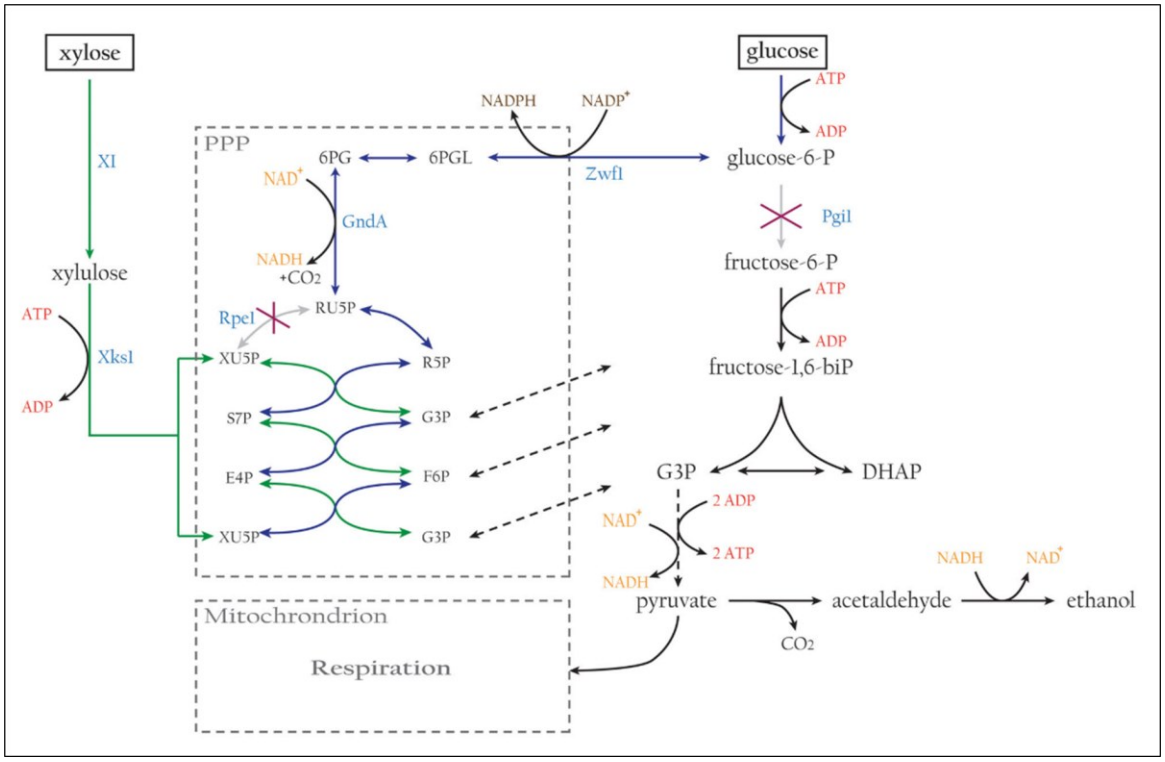

Figure 11. Schematic representation of the central carbon metabolism of *S. cerevisiae* engineered strain forced to co-consume xylose and glucose. *pgi12Δ rpe15Δ S. cerevisiae* strain expressing a heterologous xylose isomerase (XI). The native 6-phosphogluconate dehydrogenases (Gnd1 and Gnd2) were replaced by a bacterial NAD+-dependent enzyme (GndA). F6P fructose-6-phosphate; G3P glyceraldehyde-3-phosphate; DHAP dihydroxyacetone phosphate; 6PGL 6-phosphogluconolactone; 6PG 6-phosphogluconate; RU5P ribulose-5-phosphate; XU5P xylulose-5-phosphate; R5P ribose-5-phosphate; S7P sedoheptulose-7-phosphate; E4P erythrose-4-phosphate. The figure was taken from Papapetridis et al. 2018.

Futures studies could evaluate the expression of the resistant to ubiquitination-mediated degradation, glucose-insensitive, and high xylose capacity transporter $Gal2_{6SA\_N376Y\_M435I}$ (Tamayo Rojas et al., 2021a) in industrial xylose-fermenting strains harboring the deletion of *HXK2* and introduction of a $GAL83_{G673T}$ allele, with and without the deletion of *RSP5*, to evaluate potential improvement in co-consumption of xylose and glucose while expressing the construct mentioned above.

4.6 Intracellular glucose inhibition in xylose uptake

It is known that Gal2 asparagine's 376 substitution by phenylalanine resulted in a transporter variant ($Gal2_{N376F}$) that completely abolished the uptake of glucose, with a

concomitantly increased affinity for xylose, in comparison to the wild type (Farwick et al., 2014) (see chapter 2.8); moreover in this variant the uptake of xylose is not competitively inhibited by glucose during co-fermentation; that is to say, glucose present in the media will not use this transporter variant to enter into the cell in contraposition to xylose that will preferably enter into the cell via this glucose insensitive transporter (Figure 12B); however, if glucose enters into the cell using other hexose transporters available at the plasma membrane, it may accumulate inside and cause an intracellular inhibition of xylose transport, even in the glucose insensitive transporter variant above mentioned (Figure 12C), considering that it is not known if the decrease in the glucose affinity of Gal2$_{N376F}$ is symmetrical or asymmetrical regarding the glucose flux direction. To answer this question, we developed an assay platform that allows for qualitative and quantitative assessment of the glucose efflux mediated by facilitative hexose and pentose transporters (Tamayo Rojas et al., 2022).

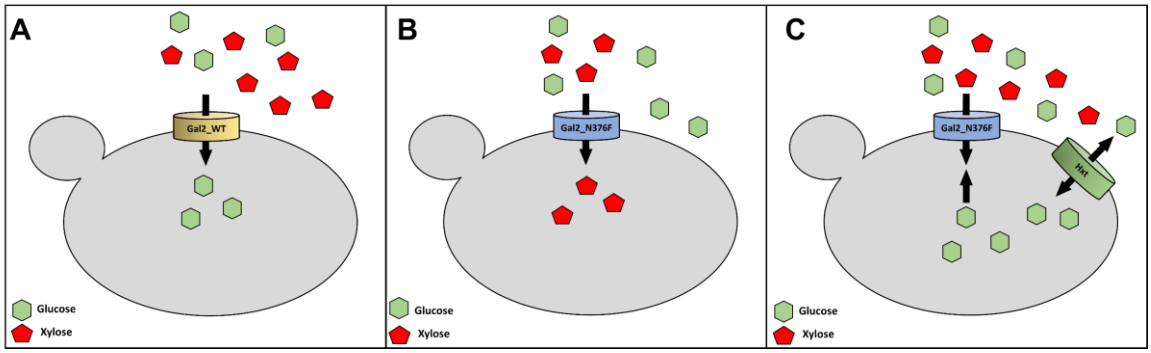

Figure 12: Transport dynamics of glucose and xylose in co-fermentation: (A) Gal2 wild-type has a higher affinity for glucose than xylose. Mainly, glucose is transported into the cell. (B) Gal2$_{N376F}$ variant has no affinity for glucose. Only xylose is transported into the cell. (C) System in which glucose and xylose are uptaken by different permeases, Gal2$_{N376F}$ variant, and any other hexose transporter. Glucose is transported into the cell and may internally inhibit the uptake of xylose.

The system uses an EBY.VW4000 (*hxt*^{0}) derivative strain AFY10, where the genes encoding the known enzymes with hexokinase activity, i.e., *HXK1*, *HXK2*, *GLK1*, and the putative hexokinase *YLR446W*, had been deleted (*hxk*^{0}) (Farwick et al., 2014). When this strain is fed with the disaccharide maltose, which is intracellularly hydrolyzed by maltases into two glucose moieties, glucose achieves growth-inhibitory levels inside the cells since it cannot be further metabolized, presumably due to osmotic mechanisms (Postma et al., 1990). When a permease mediating glucose efflux is expressed in this system, the inhibitory effect is relieved proportionally to the capacity of the introduced transporter (Tamayo Rojas et al., 2022). Feeding the system with maltose and xylose accompanied with the expression of the Gal2$_{N376F}$ variant and xylose isomerase (XylA from *Clostridium phytofermentans*), we saw that even though glucose probably achieved a high level inside

of the cell, it did not inhibit the uptake of xylose (Figure 13B), since we were able to measure xylose consumption over the fermentation; that is to say, we proved that $Gal2_{N376F}$, and probably other glucose insensitive variants, exhibit a symmetrically reduced affinity for glucose from both side of the plasma membrane in comparison to the wild type which is internally and externally inhibited by glucose probably due to its high bidirectional affinity for it (Figure 13A) (Tamayo Rojas et al., 2022). Symmetric glucose insensitivity is an essential feature in co-fermentations since it ensures the supply of xylose independent of glucose's extracellular or intracellular presence.

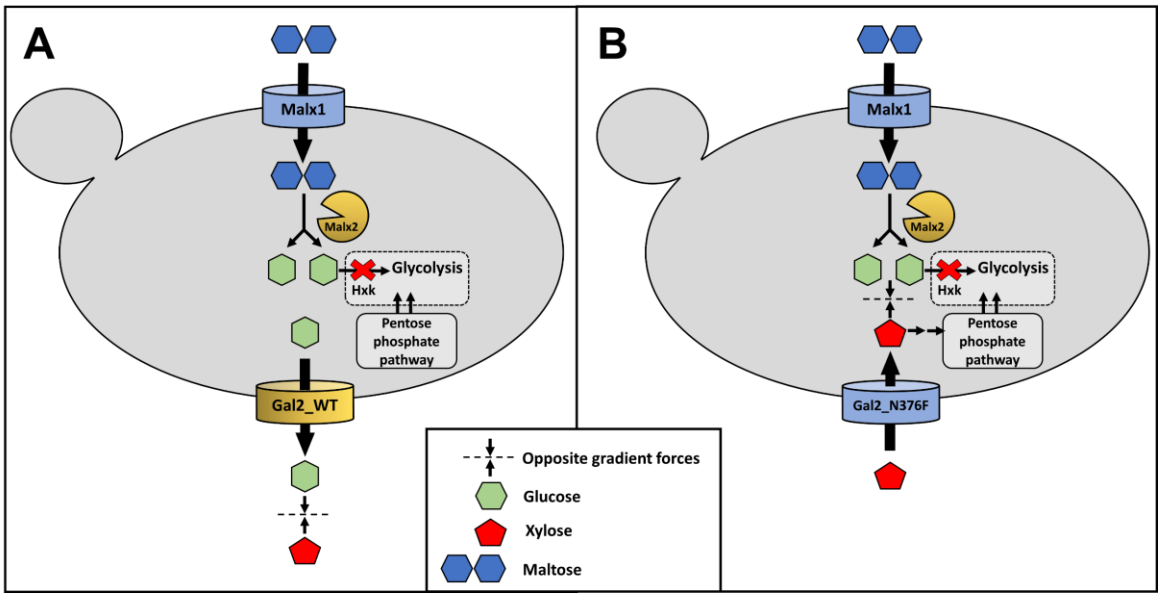

Figure 13: Design of the glucose efflux test system. The disaccharide maltose (blue) is taken up by specialized maltose/proton symporters Malx1 and intracellularly cleaved into two glucose molecules (green) by a maltase (Malx2). Glucose metabolism is prevented by deleting the hexokinase (*hxk*^{0}) genes, and glucose is intracellularly accumulated due to the absence of hexose transporters (*hxt*^{0}). Xylose is additionally provided (red). Xylose isomerase (not shown) is expressed in the system to allow xylose metabolism throughout the pentose phosphate pathway. (A) Expression of Gal2 wild-type relieves glucose growth-inhibitory levels inside the cells but does not facilitate xylose uptake into the cell. (B) $Gal2_{N376F}$ variant, even with probably high intracellular glucose levels inside the cell caused by maltose hydrolysis, poorly efflux glucose and mainly transports xylose into the cell. Opposite arrows indicate opposite gradient forces between glucose and xylose. The figure was taken and modified from (Tamayo Rojas et al., 2022).

As mentioned earlier, the assay development was focused on understanding the dynamics of intracellular inhibition caused by glucose efflux on xylose uptake, considering that this was the main field of this study; however, the screening system showed applicabilities beyond the given topic. This *in vivo* screening assay certainly will contribute to the characterization of endogenous and heterologous transporters in *S. cerevisiae*. Future studies could evaluate the efflux capacity of the human glucose facilitator family GLUTs, the equivalent to the Hxt transporters in *S. cerevisiae*. Functional GLUTs variants, actively expressed in yeast, like $GLUT1_{V69M}$, $GLUT2_{\Delta loopS\_Q455R}$, $GLUT3_{S66Y}$, $GLUT5_{S76I}$, and

GLUT5$_{S72Y}$ have been successfully characterized regarding their uptake kinetics (Wieczorke et al., 2003; Tripp et al., 2017; Schmidl et al., 2021a). Further GLUTs characterization considering their efflux capacity can be achieved with our *in vivo* assay, in particular for the low glucose affinity GLUT2 (K_M=~17 mM) (Uldry et al., 2002), which is responsible for the efflux of glucose from the basolateral membrane of the enterocytes to the blood vessels in the transepithelial glucose transport in the human intestine (Figure 14) (Merino et al., 2020). Furthermore, GLUT-interacting ligands, like the general GLUTs inhibitors phloretin and quercetin, and other more specific GLUT2 inhibitors (Schmidl et al., 2021b), can be investigated in our platform to asses the effectiveness of the inhibition, depending on the glucose flux direction. This could open a new viewpoint for GLUTs drug pharmacodynamics.

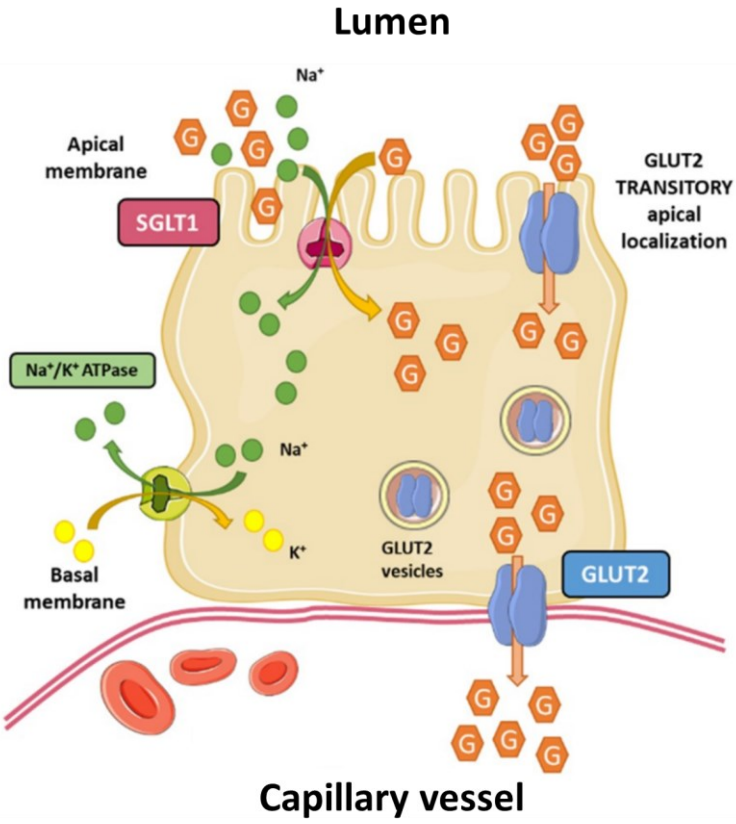

Figure 14: Glucose transport in enterocytes. Luminal glucose (G) is transported across the apical membrane by the sodium-glucose symporters (SGLT1), and sodium is transported out of the enterocyte cell through the basolateral membrane by the sodium-potassium ATPase. A portion of the intracellular glucose is phosphorylated and accumulates within the cell; the rest of it is passively transported out in the basolateral membrane by GLUT2 transporters. During high glucose luminal concentrations, part of endosomal GLUT2 transporters are rapidly and transiently translocated to the apical membrane to increase glucose uptake. The figure was taken and modified from Merino et al. 2020.

4.7 Conclusions and future perspectives

In this work, the galactose permease Gal2 was successfully stabilized at the plasma membrane; however, it was previously described that multiple mono-ubiquitination in lysine residues are enough to trigger its internalization; in this study, we locate the position of the targeted lysine residues, and additionally, we showed that its internalization also relays on serine residues, which may indicate that phosphorylation is an upstream signal that preludes ubiquitination (Tamayo Rojas et al., 2021b).

This study showed that the combination of the mutations N376Y and M435I in Gal2 together incorporates two properties highly desirable for fermentation of lignocellulosic hydrolysates, first the ability to transport pentoses without the competitive inhibition caused by glucose and second, an improved capacity for xylose and arabinose transport (Tamayo Rojas et al., 2021a). Altogether, the transporter $Gal2^{6SA\_N376Y\_M435I}$ included abovementioned features plus the increase in stability at the plasma membrane. This construct, when expressed in a diploid strain capable of consuming xylose, reduced the overall fermentation time of the total xylose consumption by approximately 20h, corresponding to 40% of the total fermentation course of a glucose/xylose mixture fermentation; however, the strain carrying this construct was only able to consume glucose and xylose sequentially (Tamayo Rojas et al., 2021a).

To further investigate the possible unfavorable effect of intracellular glucose competitive inhibition, a yeast-based *in vivo* assay system was further designed to analyze the efflux of sugars mediated by glucose transporters. With this assay, it was shown that the xylose transporter variant $Gal2^{N376F}$ is insensitive not only to extracellular but also to intracellular glucose (Tamayo Rojas et al., 2022). In addition, this assay showed that the main hexose permeases exhibited a bidirectional capacity for uptake or efflux of glucose. This assay has been proven to be suitable for screening transporters and quantitative analyses of their glucose efflux capacities.

Regarding the uptake of pentoses, in this study was possible to achieve notable improvements; nevertheless, even though there is always room for improvements; future studies should focus on disentangling metabolic constraints as well as glucose repression mechanisms that impede the co-consumption of xylose and glucose, which is the last missing remaining feature in *S. cerevisiae* engineered strains able to consume pentoses in glucose mixtures.

5 References

Barrett, L., Orlova, M., Maziarz, M., & Kuchin, S. (2012). Protein Kinase A Contributes to the Negative Control of Snf1 Protein Kinase in *Saccharomyces cerevisiae*. *Eukaryotic Cell*, *11*(2), 119–128. https://doi.org/10.1128/EC.05061-11

Baumann, L., Wernig, F., Born, S., & Oreb, M. (2020). *Engineering Saccharomyces cerevisiae for Production of Fatty Acids and Their Derivatives BT - Genetics and Biotechnology* (J. P. Benz & K. Schipper (eds.); pp. 339–368). Springer International Publishing. https://doi.org/10.1007/978-3-030-49924-2_14

Becker, J., & Boles, E. (2003). A modified *Saccharomyces cerevisiae* strain that consumes L -arabinose and produces ethanol. *Society*, *69*(7), 4144–4150. https://doi.org/10.1128/AEM.69.7.4144

Becuwe, M., Vieira, N., Lara, D., Gomes-Rezende, J., Soares-Cunha, C., Casal, M., Haguenauer-Tsapis, R., Vincent, O., Paiva, S., & Léon, S. (2012). A molecular switch on an arrestin-like protein relays glucose signaling to transporter endocytosis. *Journal of Cell Biology*, *196*(2), 247–259. https://doi.org/10.1083/jcb.201109113

Blondel, M.-O., Morvan, J., Dupré, S., Urban-Grimal, D., Haguenauer-Tsapis, R., & Volland, C. (2004). Direct Sorting of the Yeast Uracil Permease to the Endosomal System Is Controlled by Uracil Binding and Rsp5p-dependent Ubiquitylation. *Molecular Biology of the Cell*, *15*(2), 883–895. https://doi.org/10.1091/mbc.e03-04-0202

Boles, E., & Hollenberg, C. P. (1997). The molecular genetics of hexose transport in yeasts. *FEMS Microbiology Reviews*, *21*(1), 85–111. https://doi.org/10.1111/j.1574-6976.1997.tb00346.x

Boles, E., Lehnert, W., & Zimmermann, F. K. (1993). The role of the NAD-dependent glutamate dehydrogenase in restoring growth on glucose of a *Saccharomyces cerevisiae* phosphoglucose isomerase mutant. *European Journal of Biochemistry*, *217*(1), 469–477. https://doi.org/10.1111/j.1432-1033.1993.tb18266.x

Bracher, J. M., Verhoeven, M. D., Wisselink, H. W., Crimi, B., Nijland, J. G., Driessen, A. J. M., Klaassen, P., Van Maris, A. J. A., Daran, J. M. G., & Pronk, J. T. (2018). The Penicillium chrysogenum transporter PcAraT enables high-affinity, glucose-insensitive l-arabinose transport in *Saccharomyces cerevisiae*. *Biotechnology for Biofuels*, *11*(1), 1–16. https://doi.org/10.1186/s13068-018-1047-6

Brat, D., Boles, E., & Wiedemann, B. (2009). Functional expression of a bacterial xylose isomerase in *Saccharomyces cerevisiae*. *Applied and Environmental Microbiology*, *75*(8), 2304–2311. https://doi.org/10.1128/AEM.02522-08

Brink, D. P., Borgström, C., Tueros, F. G., & Gorwa-Grauslund, M. F. (2016). Real-time monitoring of the sugar sensing in *Saccharomyces cerevisiae* indicates endogenous mechanisms for xylose signaling. *Microbial Cell Factories*, *15*(1), 1–17. https://doi.org/10.1186/s12934-016-0580-x

Budhwar, R., Lu, A., & Hirsch, J. P. (2010). Nutrient control of yeast PKA activity involves opposing effects on phosphorylation of the Bcy1 regulatory subunit. *Molecular Biology of the Cell*, *21*(21), 3749–3758. https://doi.org/10.1091/mbc.E10-05-0388

Casey, J. R., & Follows, M. J. (2020). A steady-state model of microbial acclimation to substrate limitation. *PLoS Computational Biology*, *16*(8), 1–17. https://doi.org/10.1371/journal.pcbi.1008140

Castermans, D., Somers, I., Kriel, J., Louwet, W., Wera, S., Versele, M., Janssens, V., & Thevelein, J. M. (2012). Glucose-induced posttranslational activation of protein phosphatases PP2A and PP1 in yeast. *Cell Research*, *22*(6), 1058–1077. https://doi.org/10.1038/cr.2012.20

DeVit, M. J., & Johnston, M. (1999). The nuclear exportin Msn5 is required for nuclear export of the Mig1 glucose repressor of *Saccharomyces cerevisiae*. *Current Biology*, *9*(21), 1231–1241. https://doi.org/10.1016/S0960-9822(99)80503-X

Dickinson, J. R., Sobanski, M. A., & Hewlins, M. J. E. (1995). In *Saccharomyces cerevisiae* deletion of phosphoglucose isomerase can be suppressed by increased activities of enzymes of the hexose monophosphate pathway. *Microbiology*, *141*(2), 385–391. https://doi.org/10.1099/13500872-141-2-385

Diderich, J. A., Schepper, M., Van Hoek, P., Luttik, M. A. H., Van Dijken, J. P., Pronk, J. T., Klaassen, P., Boelens, H. F. M., De Mattos, M. J. T., Van Dam, K., et al. (1999). Glucose uptake kinetics and transcription of *HXT* genes in chemostat cultures of *Saccharomyces cerevisiae*. *Journal of Biological Chemistry*, *274*(22), 15350–15359. https://doi.org/10.1074/jbc.274.22.15350

Diderich, J. A., Schuurmans, J. M., Van Gaalen, M. C., Kruckeberg, A. L., & Van Dam, K. (2001). Functional analysis of the hexose transporter homologue *HXT5* in S*accharomyces cerevisiae*. *Yeast*, *18*(16), 1515–1524.

https://doi.org/10.1002/yea.779

Drew, D., North, R. A., Nagarathinam, K., & Tanabe, M. (2021). Structures and General Transport Mechanisms by the Major Facilitator Superfamily (MFS). *Chemical Reviews*, *121*(9), 5289–5335. https://doi.org/10.1021/acs.chemrev.0c00983

Endalur Gopinarayanan, V., & Nair, N. U. (2018). A semi-synthetic regulon enables rapid growth of yeast on xylose. *Nature Communications*, *9*(1). https://doi.org/10.1038/s41467-018-03645-7

Farwick, A., Bruder, S., Schadeweg, V., Oreb, M., & Boles, E. (2014). Engineering of yeast hexose transporters to transport d-xylose without inhibition by d-glucose. *Proceedings of the National Academy of Sciences*, *111*(14), 5159–5164. https://doi.org/10.1073/pnas.1323464111

Fernańdez-García, P., Peláez, R., Herrero, P., & Moreno, F. (2012). Phosphorylation of yeast hexokinase 2 regulates its nucleocytoplasmic shuttling. *Journal of Biological Chemistry*, *287*(50), 42151–42164. https://doi.org/10.1074/jbc.M112.401679

Finley, D., Ulrich, H. D., Sommer, T., & Kaiser, P. (2012). The Ubiquitin–Proteasome System of *Saccharomyces cerevisiae*. *Genetics*, *192*(2), 319–360. https://doi.org/10.1534/genetics.112.140467

Gadura, N., Robinson, L. C., & Michels, C. A. (2006). Glc7-Reg1 phosphatase signals to Yck1,2 casein kinase 1 to regulate transport activity and glucose-induced inactivation of saccharomyces maltose permease. *Genetics*, *172*(3), 1427–1439. https://doi.org/10.1534/genetics.105.051698

Gancedo, J. M. (2008). The early steps of glucose signalling in yeast. *FEMS Microbiology Reviews*, *32*(4), 673–704. https://doi.org/10.1111/j.1574-6976.2008.00117.x

Gárdonyi, M., Jeppsson, M., Lidén, G., Gorwa-Grauslund, M. F., & Hahn-Hägerdal, B. (2003). Control of xylose consumption by xylose transport in recombinant *Saccharomyces cerevisiae*. *Biotechnology and Bioengineering*, *82*(7), 818–824. https://doi.org/10.1002/bit.10631

Generoso, W. C., Schadeweg, V., Oreb, M., & Boles, E. (2015). Metabolic engineering of *Saccharomyces cerevisiae* for production of butanol isomers. *Current Opinion in Biotechnology*, *33*(Figure 1), 1–7. https://doi.org/10.1016/j.copbio.2014.09.004

Gírio, F. M., Fonseca, C., Carvalheiro, F., Duarte, L. C., Marques, S., & Bogel-Łukasik, R. (2010). Hemicelluloses for fuel ethanol: A review. *Bioresource Technology*, *101*(13), 4775–4800. https://doi.org/10.1016/j.biortech.2010.01.088

Hajieva, P., Bayatti, N., Granold, M., Behl, C., & Moosmann, B. (2015). Membrane protein oxidation determines neuronal degeneration. *Journal of Neurochemistry*, *133*(3), 352–367. https://doi.org/10.1111/jnc.12987

Hamacher, T., Becker, J., Gárdonyi, M., Hahn-Hägerdal, B., & Boles, E. (2002). Characterization of the xylose-transporting properties of yeast hexose transporters and their influence on xylose utilization. *Microbiology*, *148*(9), 2783–2788. https://doi.org/10.1099/00221287-148-9-2783

Hardie, D. G. (2007). AMP-activated/SNF1 protein kinases: conserved guardians of cellular energy. *Nature Reviews Molecular Cell Biology*, *8*(10), 774–785. https://doi.org/10.1038/nrm2249

Hauf, J., Zimmermann, F. K., & Müller, S. (2000). Simultaneous genomic overexpression of seven glycolytic enzymes in the yeast *Saccharomyces cerevisiae*. *Enzyme and Microbial Technology*, *26*(9–10), 688–698. https://doi.org/10.1016/S0141-0229(00)00160-5

Henderson, P. J., & Maiden, M. C. (1990). Homologous sugar transport proteins in Escherichia coli and their relatives in both prokaryotes and eukaryotes. *Philosophical Transactions of the Royal Society of London. Series B, Biological Sciences*, *326*(1236), 391–410. https://doi.org/10.1098/rstb.1990.0020

Herrador, A., Livas, D., Soletto, L., Becuwe, M., Léon, S., & Vincent, O. (2015). Casein kinase 1 controls the activation threshold of an α-arrestin by multisite phosphorylation of the interdomain hinge. *Molecular Biology of the Cell*, *26*(11), 2128–2138. https://doi.org/10.1091/mbc.E14-11-1552

Hettema, E. H., Valdez-Taubas, J., & Pelham, H. R. B. (2004). Bsd2 binds the ubiquitin ligase Rsp5 and mediates the ubiquitination of transmembrane proteins. *The EMBO Journal*, *23*(6), 1279–1288. https://doi.org/10.1038/sj.emboj.7600137

Hicke, L., Schubert, H. L., & Hill, C. P. (2005). Ubiquitin-binding domains. *Nature Reviews Molecular Cell Biology*, *6*(8), 610–621. https://doi.org/10.1038/nrm1701

Hicke, L., Zanolari, B., & Riezman, H. (1998). Cytoplasmic tail phosphorylation of the α-

factor receptor is required for its ubiquitination and internalization. *Journal of Cell Biology*, *141*(2), 349–358. https://doi.org/10.1083/jcb.141.2.349

Holt, L. J., Tuch, B. B., Villén, J., Johnson, A. D., Gygi, S. P., & Morgan, D. O. (2009). Global Analysis of Cdk1 Substrate Phosphorylation Sites Provides Insights into Evolution. *Science*, *325*(5948), 1682–1686. https://doi.org/10.1126/science.1172867

Hong, K. K., & Nielsen, J. (2012). Metabolic engineering of *Saccharomyces cerevisiae*: A key cell factory platform for future biorefineries. *Cellular and Molecular Life Sciences*, *69*(16), 2671–2690. https://doi.org/10.1007/s00018-012-0945-1

Hong, S. P., Leiper, F. C., Woods, A., Carling, D., & Carlson, M. (2003). Activation of yeast Snf1 and mammalian AMP-activated protein kinase by upstream kinases. *Proceedings of the National Academy of Sciences of the United States of America*, *100*(15), 8839–8843. https://doi.org/10.1073/pnas.1533136100

Hoppe, T., Matuschewski, K., Rape, M., Schlenker, S., Ulrich, H. D., & Jentsch, S. (2005). Contents, Ed. Board + Forthc. articles. *Trends in Biochemical Sciences*, *30*(3), i. https://doi.org/10.1016/S0968-0004(05)00043-5

Horak, J., Regelmann, J., & Wolf, D. H. (2002). Two distinct proteolytic systems responsible for glucose-induced degradation of fructose-1,6-bisphosphatase and the Gal2p transporter in the yeast *Saccharomyces cerevisiae* share the same protein components of the glucose signaling pathway. *Journal of Biological Chemistry*, *277*(10), 8248–8254. https://doi.org/10.1074/jbc.M107255200

Horak, J., & Wolf, D. H. (2001). Glucose-Induced Monoubiquitination of the *Saccharomyces cerevisiae* Galactose Transporter Is Sufficient To Signal Its Internalization. *Journal of Bacteriology*, *183*(10), 3083–3088. https://doi.org/10.1128/JB.183.10.3083-3088.2001

Hovsepian, J., Defenouillère, Q., Albanèse, V., Váchová, L., Garcia, C., Palková, Z., & Léon, S. (2017). Multilevel regulation of an α-arrestin by glucose depletion controls hexose transporter endocytosis. *Journal of Cell Biology*, *216*(6), 1811–1831. https://doi.org/10.1083/jcb.201610094

Hsu, J. W., Chen, K. J., & Lee, F. J. S. (2015). Snf1/AMP-activated protein kinase activates Arf3p to promote invasive yeast growth via a non-canonical GEF domain. *Nature Communications*, *6*, 1–8. https://doi.org/10.1038/ncomms8840

Jin, Y. S., Laplaza, J. M., & Jeffries, T. W. (2004). *Saccharomyces cerevisiae* engineered for xylose metabolism exhibits a respiratory response. *Applied and Environmental Microbiology*, *70*(11), 6816–6825. https://doi.org/10.1128/AEM.70.11.6816-6825.2004

Jordan, P., Choe, J.-Y., Boles, E., & Oreb, M. (2016). Hxt13, Hxt15, Hxt16 and Hxt17 from *Saccharomyces cerevisiae* represent a novel type of polyol transporters. *Scientific Reports*, *6*(1), 23502. https://doi.org/10.1038/srep23502

Jouandot, D., Roy, A., & Kim, J. H. (2011). Functional dissection of the glucose signaling pathways that regulate the yeast glucose transporter gene (*HXT*) repressor Rgt1. *Journal of Cellular Biochemistry*, *112*(11), 3268–3275. https://doi.org/10.1002/jcb.23253

Kaniak, A., Xue, Z., Macool, D., Kim, J. H., & Johnston, M. (2004). Regulatory Network Connecting Two Glucose Signal Transduction Pathways in *Saccharomyces cerevisiae*. *Eukaryotic Cell*, *3*(1), 221–231. https://doi.org/10.1128/EC.3.1.221-231.2004

Kasahara, M., Shimoda, E., & Maeda, M. (1996). Transmembrane segment 10 is important for substrate recognition in Gal2 and Hxt2 sugar transporters in the yeast *Saccharomyces cerevisiae*. *FEBS Letters*, *389*(2), 174–178. https://doi.org/10.1016/0014-5793(96)00567-4

Kelm, K. B., Huyer, G., Huang, J. C., & Michaelis, S. (2004). The Internalization of Yeast Ste6p Follows an Ordered Series of Events Involving Phosphorylation, Ubiquitination, Recognition and Endocytosis. *Traffic*, *5*(3), 165–180. https://doi.org/10.1111/j.1600-0854.2004.00168.x

Kennelly, P. J., & Krebs, E. G. (1991). Consensus sequences as substrate specificity determinants for protein kinases and protein phosphatases. *Journal of Biological Chemistry*, *266*(24), 15555–15558. https://doi.org/10.1016/s0021-9258(18)98436-x

Krampe, S., & Boles, E. (2002). Starvation-induced degradation of yeast hexose transporter Hxt7p is dependent on endocytosis, autophagy and the terminal sequences of the permease. *FEBS Letters*, *513*(2–3), 193–196. https://doi.org/10.1016/S0014-5793(02)02297-4

Kumar, R., Singh, S., & Singh, O. V. (2008). Bioconversion of lignocellulosic biomass: Biochemical and molecular perspectives. *Journal of Industrial Microbiology and*

Biotechnology, *35*(5), 377–391. https://doi.org/10.1007/s10295-008-0327-8

Lauwers, E., Erpapazoglou, Z., Haguenauer-Tsapis, R., & André, B. (2010). The ubiquitin code of yeast permease trafficking. *Trends in Cell Biology*, *20*(4), 196–204. https://doi.org/10.1016/j.tcb.2010.01.004

Lauwers, E., Jacob, C., & André, B. (2009). K63-linked ubiquitin chains as a specific signal for protein sorting into the multivesicular body pathway. *Journal of Cell Biology*, *185*(3), 493–502. https://doi.org/10.1083/jcb.200810114

Leandro, M. J., Gonçalves, P., & Spencer-Martins, I. (2006). Two glucose/xylose transporter genes from the yeast Candida intermedia : first molecular characterization of a yeast xylose–H+ symporter. *Biochemical Journal*, *395*(3), 543–549. https://doi.org/10.1042/BJ20051465

Limayem, A., & Ricke, S. C. (2012). Lignocellulosic biomass for bioethanol production: Current perspectives, potential issues and future prospects. *Progress in Energy and Combustion Science*, *38*(4), 449–467. https://doi.org/10.1016/j.pecs.2012.03.002

Llopis-Torregrosa, V., Ferri-Blázquez, A., Adam-Artigues, A., Deffontaines, E., van Heusden, G. P. H., & Yenush, L. (2016). Regulation of the Yeast Hxt6 Hexose Transporter by the Rod1 α-Arrestin, the Snf1 Protein Kinase, and the Bmh2 14-3-3 Protein. *Journal of Biological Chemistry*, *291*(29), 14973–14985. https://doi.org/10.1074/jbc.M116.733923

Lucero, P., Peñalver, E., Vela, L., & Lagunas, R. (2000). Monoubiquitination Is Sufficient To Signal Internalization of the Maltose Transporter in *Saccharomyces cerevisiae*. *Journal of Bacteriology*, *182*(1), 241–243. https://doi.org/10.1128/JB.182.1.241-243.2000

Lundh, F., Mouillon, J. M., Samyn, D., Stadler, K., Popova, Y., Lagerstedt, J. O., Thevelein, J. M., & Persson, B. L. (2009). Molecular mechanisms controlling phosphate-induced downregulation of the yeast Pho84 phosphate transporter. *Biochemistry*, *48*(21), 4497–4505. https://doi.org/10.1021/bi9001198

MacGurn, J. A., Hsu, P.-C., Smolka, M. B., & Emr, S. D. (2011). TORC1 Regulates Endocytosis via Npr1-Mediated Phosphoinhibition of a Ubiquitin Ligase Adaptor. *Cell*, *147*(5), 1104–1117. https://doi.org/10.1016/j.cell.2011.09.054

Marchal, C., Haguenauer-Tsapis, R., & Urban-Grimal, D. (1998). A PEST-Like Sequence

Mediates Phosphorylation and Efficient Ubiquitination of Yeast Uracil Permease. *Molecular and Cellular Biology*, *18*(1), 314–321. https://doi.org/10.1128/mcb.18.1.314

McNally, E. K., & Brett, C. L. (2018). The intralumenal fragment pathway mediates ESCRT-independent surface transporter down-regulation. *Nature Communications*, *9*(1). https://doi.org/10.1038/s41467-018-07734-5

Merino, B., Fernández-Díaz, C. M., Cózar-Castellano, I., & Perdomo, G. (2020). Intestinal fructose and glucose metabolism in health and disease. *Nutrients*, *12*(1), 1–35. https://doi.org/10.3390/nu12010094

Muir, A., Ramachandran, S., Roelants, F. M., Timmons, G., & Thorner, J. (2014). TORC2-dependent protein kinase Ypk1 phosphorylates ceramide synthase to stimulate synthesis of complex sphingolipids. *ELife*, *3*, 1–34. https://doi.org/10.7554/eLife.03779

Nath, N., McCartney, R. R., & Schmidt, M. C. (2003). Yeast Pak1 Kinase Associates with and Activates Snf1. *Molecular and Cellular Biology*, *23*(11), 3909–3917. https://doi.org/10.1128/mcb.23.11.3909-3917.2003

Nijland, J. G., & Driessen, A. J. M. (2020). Engineering of Pentose Transport in *Saccharomyces cerevisiae* for Biotechnological Applications. *Frontiers in Bioengineering and Biotechnology*, *7*(January), 1–13. https://doi.org/10.3389/fbioe.2019.00464

Nijland, J. G., Shin, H. Y., de Jong, R. M., de Waal, P. P., Klaassen, P., & Driessen, A. J. M. (2014). Engineering of an endogenous hexose transporter into a specific D-xylose transporter facilitates glucose-xylose co-consumption in *Saccharomyces cerevisiae*. *Biotechnology for Biofuels*, *7*(1), 168. https://doi.org/10.1186/s13068-014-0168-9

Nijland, J. G., Vos, E., Shin, H. Y., de Waal, P. P., Klaassen, P., & Driessen, A. J. M. (2016). Improving pentose fermentation by preventing ubiquitination of hexose transporters in *Saccharomyces cerevisiae*. *Biotechnology for Biofuels*, *9*(1), 158. https://doi.org/10.1186/s13068-016-0573-3

Nikko, E., & Pelham, H. R. B. (2009). Arrestin-Mediated Endocytosis of Yeast Plasma Membrane Transporters. *Traffic*, *10*(12), 1856–1867. https://doi.org/10.1111/j.1600-0854.2009.00990.x

Nikko, E., Sullivan, J. A., & Pelham, H. R. B. (2008). Arrestin-like proteins mediate ubiquitination and endocytosis of the yeast metal transporter Smf1. *EMBO Reports*, *9*(12), 1216–1221. https://doi.org/10.1038/embor.2008.199

Novoselova, T. V., Zahira, K., Rose, R.-S., & Sullivan, J. A. (2012). Bul Proteins, a Nonredundant, Antagonistic Family of Ubiquitin Ligase Regulatory Proteins. *Eukaryotic Cell*, *11*(4), 463–470. https://doi.org/10.1128/EC.00009-12

O'Donnell, A. F., Apffel, A., Gardner, R. G., & Cyert, M. S. (2010). α-Arrestins Aly1 and Aly2 Regulate Intracellular Trafficking in Response to Nutrient Signaling. *Molecular Biology of the Cell*, *21*(20), 3552–3566. https://doi.org/10.1091/mbc.e10-07-0636

O'Donnell, A. F., McCartney, R. R., Chandrashekarappa, D. G., Zhang, B. B., Thorner, J., & Schmidt, M. C. (2015). 2-Deoxyglucose Impairs *Saccharomyces cerevisiae* Growth by Stimulating Snf1-Regulated and α-Arrestin-Mediated Trafficking of Hexose Transporters 1 and 3. *Molecular and Cellular Biology*, *35*(6), 939–955. https://doi.org/10.1128/MCB.01183-14

O'Donnell, A. F., & Schmidt, M. C. (2019). AMPK-Mediated Regulation of Alpha-Arrestins and Protein Trafficking. *International Journal of Molecular Sciences*, *20*(3), 515. https://doi.org/10.3390/ijms20030515

Ozcan, S., Leong, T., & Johnston, M. (1996). Rgt1p of *Saccharomyces cerevisiae*, a key regulator of glucose-induced genes, is both an activator and a repressor of transcription. *Molecular and Cellular Biology*, *16*(11), 6419–6426. https://doi.org/10.1128/mcb.16.11.6419

Özcan, S., & Johnston, M. (1999). Function and Regulation of Yeast Hexose Transporters. *Microbiology and Molecular Biology Reviews*, *63*(3), 554–569. https://doi.org/10.1128/mmbr.63.3.554-569.1999

Palma, M., Seret, M. L., & Baret, P. V. (2009). Combined phylogenetic and neighbourhood analysis of the hexose transporters and glucose sensors in yeasts. *FEMS Yeast Research*, *9*(4), 526–534. https://doi.org/10.1111/j.1567-1364.2009.00511.x

Panek, H. R., Stepp, J. D., Engle, H. M., Marks, K. M., Tan, P. K., Lemmon, S. K., & Robinson, L. C. (1997). Suppressors of YCK-encoded yeast casein kinase 1 deficiency define the four subunits of a novel clathrin AP-like complex. *EMBO Journal*, *16*(14), 4194–4204. https://doi.org/10.1093/emboj/16.14.4194

Papapetridis, I., van Dijk, M., Dobbe, A. P. A., Metz, B., Pronk, J. T., & van Maris, A. J. A. (2016). Improving ethanol yield in acetate-reducing *Saccharomyces cerevisiae* by cofactor engineering of 6-phosphogluconate dehydrogenase and deletion of *ALD6*. *Microbial Cell Factories*, *15*(1), 67. https://doi.org/10.1186/s12934-016-0465-z

Papapetridis, I., Verhoeven, M. D., Wiersma, S. J., Goudriaan, M., Van Maris, A. J. A., & Pronk, J. T. (2018). Laboratory evolution for forced glucose-xylose co-consumption enables identification of mutations that improve mixed-sugar fermentation by xylose-fermenting *Saccharomyces cerevisiae*. *FEMS Yeast Research*, *18*(6), 1–17. https://doi.org/10.1093/femsyr/foy056

Petit, T., Diderich, J. A., Kruckeberg, A. L., Gancedo, C., & Van Dam, K. (2000). Hexokinase Regulates Kinetics of Glucose Transport and Expression of Genes Encoding Hexose Transporters in *Saccharomyces cerevisiae*. *Journal of Bacteriology*, *182*(23), 6815–6818. https://doi.org/10.1128/JB.182.23.6815-6818.2000

Pitkänen, J.-P., Aristidou, A., Salusjärvi, L., Ruohonen, L., & Penttilä, M. (2003). Metabolic flux analysis of xylose metabolism in recombinant *Saccharomyces cerevisiae* using continuous culture. *Metabolic Engineering*, *5*(1), 16–31. https://doi.org/10.1016/S1096-7176(02)00012-5

Platt, A., & Reece, R. J. (1998). The yeast galactose genetic switch is mediated by the formation of a Gal4p-Gal80p-Gal3p complex. *EMBO Journal*, *17*(14), 4086–4091. https://doi.org/10.1093/emboj/17.14.4086

Portela, P., Howell, S., Moreno, S., & Rossi, S. (2002). *In vivo* and *in vitro* phosphorylation of two isoforms of yeast pyruvate kinase by protein kinase A. *Journal of Biological Chemistry*, *277*(34), 30477–30487. https://doi.org/10.1074/jbc.M201094200

Portela, P., Moreno, S., & Rossi, S. (2006). Characterization of yeast pyruvate kinase 1 as a protein kinase A substrate, and specificity of the phosphorylation site sequence in the whole protein. *Biochemical Journal*, *396*(1), 117–126. https://doi.org/10.1042/BJ20051642

Postma, E., Verduyn, C., Kuiper, A., Scheffers, W. A., & Van Dijken, J. P. (1990). Substrate-accelerated death of *Saccharomyces cerevisiae* CBS 8066 under maltose stress. *Yeast*, *6*(2), 149–158. https://doi.org/10.1002/yea.320060209

Protzko, R. J., Latimer, L. N., Martinho, Z., de Reus, E., Seibert, T., Benz, J. P., & Dueber,

J. E. (2018). Engineering *Saccharomyces cerevisiae* for co-utilization of d-galacturonic acid and d-glucose from citrus peel waste. *Nature Communications*, *9*(1). https://doi.org/10.1038/s41467-018-07589-w

Radivojac, P., Vacic, V., Haynes, C., Cocklin, R. R., Mohan, A., Heyen, J. W., Goebl, M. G., & Iakoucheva, L. M. (2010). Identification, analysis, and prediction of protein ubiquitination sites. *Proteins: Structure, Function, and Bioinformatics*, *78*(2), 365–380. https://doi.org/10.1002/prot.22555

Reifenberger, E., Freidel, K., & Ciriacy, M. (1995). Identification of novel *HXT* genes in *Saccharomyces cerevisiae* reveals the impact of individual hexose transporters on qlycolytic flux. *Molecular Microbiology*, *16*(1), 157–167. https://doi.org/10.1111/j.1365-2958.1995.tb02400.x

Reifenberger, E., Boles, E., & Ciriacy, M. (1997). Kinetic characterization of individual hexose transporters of *Saccharomyces cerevisiae* and their relation to the triggering mechanisms of glucose repression. *European Journal of Biochemistry*, *245*(2), 324–333. https://doi.org/10.1111/j.1432-1033.1997.00324.x

Reznicek, O., Facey, S. J., de Waal, P. P., Teunissen, A. W. R. H., de Bont, J. A. M., Nijland, J. G., Driessen, A. J. M., & Hauer, B. (2015). Improved xylose uptake in *Saccharomyces cerevisiae* due to directed evolution of galactose permease Gal2 for sugar co-consumption. *Journal of Applied Microbiology*, *119*(1), 99–111. https://doi.org/10.1111/jam.12825

Richard, P., Putkonen, M., Väänänen, R., Londesborough, J., & Penttilä, M. (2002). The missing link in the fungal L-arabinose catabolic pathway, identification of the L-xylulose reductase gene. *Biochemistry*, *41*(20), 6432–6437. https://doi.org/10.1021/bi025529i

Rolland, F., De Winde, J. H., Lemaire, K., Boles, E., Thevelein, J. M., & Winderickx, J. (2000). Glucose-induced cAMP signalling in yeast requires both a G-protein coupled receptor system for extracellular glucose detection and a separable hexose kinase-dependent sensing process. *Molecular Microbiology*, *38*(2), 348–358. https://doi.org/10.1046/j.1365-2958.2000.02125.x

Rotin, D., & Kumar, S. (2009). Physiological functions of the HECT family of ubiquitin ligases. *Nature Reviews Molecular Cell Biology*, *10*(6), 398–409. https://doi.org/10.1038/nrm2690

Roy, A., Kim, Y.-B., Cho, K. H., & Kim, J.-H. (2014). Glucose starvation-induced turnover of the yeast glucose transporter Hxt1. *Biochimica et Biophysica Acta (BBA) - General Subjects*, *1840*(9), 2878–2885. https://doi.org/10.1016/j.bbagen.2014.05.004

Runquist, D., Hahn-Hägerdal, B., & Rådström, P. (2010). Comparison of heterologous xylose transporters in recombinant *Saccharomyces cerevisiae*. *Biotechnology for Biofuels*, *3*(1), 1–7. https://doi.org/10.1186/1754-6834-3-5

Sadowski, I., Breitkreutz, B. J., Stark, C., Su, T. C., Dahabieh, M., Raithatha, S., Bernhard, W., Oughtred, R., Dolinski, K., Barreto, K., et al. (2013). The PhosphoGRID *Saccharomyces cerevisiae* protein phosphorylation site database: Version 2.0 update. *Database*, *2013*, 1–10. https://doi.org/10.1093/database/bat026

Saier, M. H. (2000). A Functional-Phylogenetic Classification System for Transmembrane Solute Transporters. *Microbiology and Molecular Biology Reviews*, *64*(2), 354–411. https://doi.org/10.1128/mmbr.64.2.354-411.2000

Salusjärvi, L., Kankainen, M., Soliymani, R., Pitkänen, J. P., Penttilä, M., & Ruohonen, L. (2008). Regulation of xylose metabolism in recombinant *Saccharomyces cerevisiae*. *Microbial Cell Factories*, *7*, 1–16. https://doi.org/10.1186/1475-2859-7-18

Schmidl, S., Tamayo Rojas, S. A., Iancu, C. V., Choe, J. Y., & Oreb, M. (2021a). Functional Expression of the Human Glucose Transporters GLUT2 and GLUT3 in Yeast Offers Novel Screening Systems for GLUT-Targeting Drugs. *Frontiers in Molecular Biosciences*, *7*(February), 1–13. https://doi.org/10.3389/fmolb.2020.598419

Schmidl, S., Ursu, O., Iancu, C. V., Oreb, M., Oprea, T. I., & Choe, J. yong. (2021b). Identification of new GLUT2-selective inhibitors through in silico ligand screening and validation in eukaryotic expression systems. *Scientific Reports*, *11*(1), 1–13. https://doi.org/10.1038/s41598-021-93063-5

Sedlak, M., & Ho, N. W. Y. (2004). Characterization of the effectiveness of hexose transporters for transporting xylose during glucose and xylose co-fermentation by a recombinant Saccharomyces yeast. *Yeast*, *21*(8), 671–684. https://doi.org/10.1002/yea.1060

Sen, A., Acosta-Sampson, L., Alvaro, C. G., Ahn, J. S., Cate, J. H. D., & Thorner, J. (2016). Internalization of Heterologous Sugar Transporters by Endogenous α-Arrestins in the Yeast *Saccharomyces cerevisiae*. *Applied and Environmental Microbiology*, *82*(24), 7074–7085. https://doi.org/10.1128/AEM.02148-16

Shcherbik, N., & Pestov, D. G. (2011). The ubiquitin ligase Rsp5 is required for ribosome stability in *Saccharomyces cerevisiae*. *RNA*, *17*(8), 1422–1428. https://doi.org/10.1261/rna.2615311

Shin, H. Y., Nijland, J. G., de Waal, P. P., de Jong, R. M., Klaassen, P., & Driessen, A. J. M. (2015). An engineered cryptic Hxt11 sugar transporter facilitates glucose–xylose co-consumption in *Saccharomyces cerevisiae*. *Biotechnology for Biofuels*, *8*(1), 176. https://doi.org/10.1186/s13068-015-0360-6

Shin, H. Y., Nijland, J. G., de Waal, P. P., & Driessen, A. J. M. (2017). The amino-terminal tail of Hxt11 confers membrane stability to the Hxt2 sugar transporter and improves xylose fermentation in the presence of acetic acid. *Biotechnology and Bioengineering*, *114*(9), 1937–1945. https://doi.org/10.1002/bit.26322

Shinoda, J., & Kikuchi, Y. (2007). Rod1, an arrestin-related protein, is phosphorylated by Snf1-kinase in *Saccharomyces cerevisiae*. *Biochemical and Biophysical Research Communications*, *364*(2), 258–263. https://doi.org/10.1016/j.bbrc.2007.09.134

Smith, A., Ward, M. P., & Garrett, S. (1998). Yeast PKA represses Msn2p/Msn4p-dependent gene expression to regulate growth, stress response and glycogen accumulation. *EMBO Journal*, *17*(13), 3556–3564. https://doi.org/10.1093/emboj/17.13.3556

Snowdon, C., & van der Merwe, G. (2012). Regulation of Hxt3 and Hxt7 Turnover Converges on the Vid30 Complex and Requires Inactivation of the Ras/cAMP/PKA Pathway in *Saccharomyces cerevisiae*. *PLoS ONE*, *7*(12), e50458. https://doi.org/10.1371/journal.pone.0050458

Soetens, O., De Craene, J.-O., & André, B. (2001). Ubiquitin Is Required for Sorting to the Vacuole of the Yeast General Amino Acid Permease, Gap1. *Journal of Biological Chemistry*, *276*(47), 43949–43957. https://doi.org/10.1074/jbc.M102945200

Stimpson, H. E. M., Lewis, M. J., & Pelham, H. R. B. (2006). Transferrin receptor-like proteins control the degradation of a yeast metal transporter. *The EMBO Journal*, *25*(4), 662–672. https://doi.org/10.1038/sj.emboj.7600984

Subtil, T., & Boles, E. (2011). Improving L-arabinose utilization of pentose fermenting *Saccharomyces cerevisiae* cells by heterologous expression of L-arabinose transporting sugar transporters. *Biotechnology for Biofuels*, *4*, 1–10. https://doi.org/10.1186/1754-6834-4-38

Subtil, T., & Boles, E. (2012). Competition between pentoses and glucose during uptake and catabolism in recombinant *Saccharomyces cerevisiae*. *Biotechnology for Biofuels*, *5*(1), 14. https://doi.org/10.1186/1754-6834-5-14

Sutherland, C. M., Hawley, S. A., McCartney, R. R., Leech, A., Stark, M. J. R., Schmidt, M. C., & Hardie, D. G. (2003). Elm1p Is One of Three Upstream Kinases for the *Saccharomyces cerevisiae* SNF1 Complex. *Current Biology*, *13*(15), 1299–1305. https://doi.org/10.1016/S0960-9822(03)00459-7

Suzuki, K., Sako, K., Akiyama, K., Isoda, M., Senoo, C., Nakajo, N., & Sagata, N. (2015). Identification of non-Ser/Thr-Pro consensus motifs for Cdk1 and their roles in mitotic regulation of C2H2 zinc finger proteins and Ect2. *Scientific Reports*, *5*, 1–9. https://doi.org/10.1038/srep07929

Tamayo Rojas, S. A., Schadeweg, V., Kirchner, F., Boles, E., & Oreb, M. (2021a). Identification of a glucose-insensitive variant of Gal2 from *Saccharomyces cerevisiae* exhibiting a high pentose transport capacity. *Scientific Reports*, *11*(1), 24404. https://doi.org/10.1038/s41598-021-03822-7

Tamayo Rojas, S. A., Schmidl, S., Boles, E., & Oreb, M. (2021b). Glucose-induced internalization of the *S. cerevisiae* galactose permease Gal2 is dependent on phosphorylation and ubiquitination of its aminoterminal cytoplasmic tail. *FEMS Yeast Research*, *21*(3), 1–10. https://doi.org/10.1093/femsyr/foab019

Tamayo Rojas, S. A., Boles, E., & Oreb, M. (2022). A yeast-based *in vivo* assay system for analyzing efflux of sugars mediated by glucose and xylose transporters. *FEMS Yeast Research*, *21*(1), foac038. https://doi.org/10.1093/femsyr/foac038

Tani, T., Taguchi, H., Fujimori, K. E., Sahara, T., Ohgiya, S., Kamagata, Y., & Akamatsu, T. (2016). Isolation and characterization of xylitol-assimilating mutants of recombinant *Saccharomyces cerevisiae*. *Journal of Bioscience and Bioengineering*, *122*(4), 446–455. https://doi.org/10.1016/j.jbiosc.2016.03.008

Tanino, T., Ito, T., Ogino, C., Ohmura, N., Ohshima, T., & Kondo, A. (2012). Sugar consumption and ethanol fermentation by transporter-overexpressed xylose-metabolizing *Saccharomyces cerevisiae* harboring a xyloseisomerase pathway. *Journal of Bioscience and Bioengineering*, *114*(2), 209–211. https://doi.org/10.1016/j.jbiosc.2012.03.004

Toivari, M. H., Salusjärvi, L., Ruohonen, L., & Penttilä, M. (2004). Endogenous xylose

pathway in *Saccharomyces cerevisiae*. *Applied and Environmental Microbiology*, *70*(6), 3681–3686. https://doi.org/10.1128/AEM.70.6.3681-3686.2004

Tomala, K., & Korona, R. (2013). Evaluating the fitness cost of protein expression in *Saccharomyces cerevisiae*. *Genome Biology and Evolution*, *5*(11), 2051–2060. https://doi.org/10.1093/gbe/evt154

Träff, K. L., Jönsson, L. J., & Hahn-Hägerdal, B. (2002). Putative xylose and arabinose reductases in *Saccharomyces cerevisiae*. *Yeast*, *19*(14), 1233–1241. https://doi.org/10.1002/yea.913

Tripp, J., Essl, C., Iancu, C. V., Boles, E., Choe, J. Y., & Oreb, M. (2017). Establishing a yeast-based screening system for discovery of human GLUT5 inhibitors and activators. *Scientific Reports*, *7*(1), 1–9. https://doi.org/10.1038/s41598-017-06262-4

Uldry, M., Ibberson, M., Hosokawa, M., & Thorens, B. (2002). GLUT2 is a high affinity glucosamine transporter. *FEBS Letters*, *524*(1–3), 199–203. https://doi.org/10.1016/S0014-5793(02)03058-2

Verhoeven, M. D., Bracher, J. M., Nijland, J. G., Bouwknegt, J., Daran, J.-M. G., Driessen, A. J. M., van Maris, A. J. A., & Pronk, J. T. (2018). Laboratory evolution of a glucose-phosphorylation-deficient, arabinose-fermenting *S. cerevisiae* strain reveals mutations in *GAL2* that enable glucose-insensitive l-arabinose uptake. *FEMS Yeast Research*, *18*(6), 1–15. https://doi.org/10.1093/femsyr/foy062

Vincent, O., Townley, R., Kuchin, S., & Carlson, M. (2001). Subcellular localization of the Snf1 kinase is regulated by specific β subunits and a novel glucose signaling mechanism. *Genes and Development*, *15*(9), 1104–1114. https://doi.org/10.1101/gad.879301

Wang, C., Li, Y., Qiu, C., Wang, S., Ma, J., Shen, Y., Zhang, Q., Du, B., Ding, Y., & Bao, X. (2017). Identification of important amino acids in Gal2p for improving the L-arabinose transport and metabolism in *Saccharomyces cerevisiae*. *Frontiers in Microbiology*, *8*(JUL), 1–11. https://doi.org/10.3389/fmicb.2017.01391

Wang, G., Yang, J., & Huibregtse, J. M. (1999). Functional Domains of the Rsp5 Ubiquitin-Protein Ligase. *Molecular and Cellular Biology*, *19*(1), 342–352. https://doi.org/10.1128/MCB.19.1.342

Weber, C., Farwick, A., Benisch, F., Brat, D., Dietz, H., Subtil, T., & Boles, E. (2010).

Trends and challenges in the microbial production of lignocellulosic bioalcohol fuels. *Applied Microbiology and Biotechnology*, *87*(4), 1303–1315. https://doi.org/10.1007/s00253-010-2707-z

Wess, J., Brinek, M., & Boles, E. (2019). Improving isobutanol production with the yeast *Saccharomyces cerevisiae* by successively blocking competing metabolic pathways as well as ethanol and glycerol formation. *Biotechnology for Biofuels*, *12*(1), 1–16. https://doi.org/10.1186/s13068-019-1486-8

Westholm, J. O., Nordberg, N., Murén, E., Ameur, A., Komorowski, J., & Ronne, H. (2008). Combinatorial control of gene expression by the three yeast repressors Mig1, Mig2 and Mig3. *BMC Genomics*, *9*(1), 601. https://doi.org/10.1186/1471-2164-9-601

Wieczorke, R., Dlugai, S., Krampe, S., & Boles, E. (2003). Characterisation of Mammalian GLUT Glucose Transporters in a Heterologous Yeast Expression System. *Cellular Physiology and Biochemistry*, *13*(3), 123–134. https://doi.org/10.1159/000071863

Wieczorke, R., Krampe, S., Weierstall, T., Freidel, K., Hollenberg, C. P., & Boles, E. (1999). Concurrent knock-out of at least 20 transporter genes is required to block uptake of hexoses in *Saccharomyces cerevisiae*. *FEBS Letters*, *464*(3), 123–128. https://doi.org/10.1016/S0014-5793(99)01698-1

Wiedemann, B., & Boles, E. (2008). Codon-optimized bacterial genes improve L-arabinose fermentation in recombinant *Saccharomyces cerevisiae*. *Applied and Environmental Microbiology*, *74*(7), 2043–2050. https://doi.org/10.1128/AEM.02395-07

Wisselink, H. W., Toirkens, M. J., Berriel, M. D. R. F., Winkler, A. A., Van Dijken, J. P., Pronk, J. T., & Van Maris, A. J. A. (2007). Engineering of *Saccharomyces cerevisiae* for efficient anaerobic alcoholic fermentation of L-arabinose. *Applied and Environmental Microbiology*, *73*(15), 4881–4891. https://doi.org/10.1128/AEM.00177-07

Wu, M., Li, H., Wei, S., Wu, H., Wu, X., Bao, X., Hou, J., Liu, W., & Shen, Y. (2020). Simulating extracellular glucose signals enhances xylose metabolism in recombinant *Saccharomyces cerevisiae*. *Microorganisms*, *8*(1). https://doi.org/10.3390/microorganisms8010100

Yan, N. (2013). Structural advances for the major facilitator superfamily (MFS) transporters. *Trends in Biochemical Sciences*, *38*(3), 151–159. https://doi.org/10.1016/J.TIBS.2013.01.003

Yang, X., Reist, L., Chomchai, D. A., Chen, L., Arines, F. M., & Li, M. (2021). ESCRT, not intralumenal fragments, sorts ubiquitinated vacuole membrane proteins for degradation. *Journal of Cell Biology*, *220*(8). https://doi.org/10.1083/jcb.202012104

Yashiroda, H., Oguchi, T., Yasuda, Y., Toh-E, A., & Kikuchi, Y. (1996). Bul1, a new protein that binds to the Rsp5 ubiquitin ligase in *Saccharomyces cerevisiae*. *Molecular and Cellular Biology*, *16*(7), 3255–3263. https://doi.org/10.1128/mcb.16.7.3255

Yashiroda, H., Kaida, D., Toh-e, A., & Kikuchi, Y. (1998). The PY-motif of Bul1 protein is essential for growth of *Saccharomyces cerevisiae* under various stress conditions. *Gene*, *225*(1–2), 39–46. https://doi.org/10.1016/S0378-1119(98)00535-6

Young, E. M., Comer, A. D., Huang, H., & Alper, H. S. (2012). A molecular transporter engineering approach to improving xylose catabolism in *Saccharomyces cerevisiae*. *Metabolic Engineering*, *14*(4), 401–411. https://doi.org/10.1016/j.ymben.2012.03.004

Young, E., Poucher, A., Comer, A., Bailey, A., & Alper, H. (2011). Functional survey for heterologous sugar transport proteins, using *Saccharomyces cerevisiae* as a host. *Applied and Environmental Microbiology*, *77*(10), 3311–3319. https://doi.org/10.1128/AEM.02651-10

Zabed, H., Sahu, J. N., Boyce, A. N., & Faruq, G. (2016). Fuel ethanol production from lignocellulosic biomass: An overview on feedstocks and technological approaches. *Renewable and Sustainable Energy Reviews*, *66*, 751–774. https://doi.org/10.1016/j.rser.2016.08.038

Zoghlami, A., & Paës, G. (2019). Lignocellulosic Biomass: Understanding Recalcitrance and Predicting Hydrolysis. *Frontiers in Chemistry*, *7*(December). https://doi.org/10.3389/fchem.2019.00874

6 Publications

6.1 Glucose-induced internalization of the *S. cerevisiae* galactose permease Gal2 is dependent on phosphorylation and ubiquitination of its aminoterminal cytoplasmic tail

Declaration of author contributions to the publication:
Glucose-induced internalization of the *S. Cerevisiae* galactose permease Gal2 is dependent on phosphorylation and ubiquitination of its aminoterminal cytoplasmic tail

Status: Published, May 2021
Journal: FEMS Yeast Research
Type of publication: research article
Contributing authors: Sebastian A. Tamayo Rojas (SR), Sina Schmidl (SS), Eckhard Boles (EB), and Mislav Oreb (MO)

Contributions of doctoral candidate and co-authors
(1) Concept and design
Doctoral candidate SR: 60%
Co-authors EB, MO: 20%, 20%
(2) Conducting tests and experiments
Doctoral candidate SR: 85%, yeast molecular biology, fluorescence microscopy and fermentations
Co-authors SS: 15%, radiolabeled glucose uptake assay
(3) Compilation of data sets and figures
Doctoral candidate SR: 100%, microscopy micrographs and growth curves
(4) Analysis and interpretation of data
Doctoral candidate SR: 70%, microscopy micrographs and growth curves
Co-authors SS: 10 %, kinetics; EB, MO: 10 %, 10%, supervision and advice
(5) Drafting of manuscript
Doctoral candidate SR: 60%
Co-authors EB, MO: 5%, 35%

Copyright information:

The following article is reprinted with permission from Oxford University Press

The article is available online:
https://doi.org/10.1093/femsyr/foab019

FEMS Yeast Research, 21, 2021, foab019

doi: 10.1093/femsyr/foab019
Advance Access Publication Date: 31 March 2021
Research Article

RESEARCH ARTICLE

Glucose-induced internalization of the *S. cerevisiae* galactose permease Gal2 is dependent on phosphorylation and ubiquitination of its aminoterminal cytoplasmic tail

Sebastian A. Tamayo Rojas, Sina Schmidl[†], Eckhard Boles and Mislav Oreb[*,‡]

Faculty of Biological Sciences, Institute of Molecular Biosciences, Goethe University Frankfurt, Max-von-Laue Straße 9, Frankfurt am Main 60438, Germany

[*]**Corresponding author:** Faculty of Biological Sciences, Institute of Molecular Biosciences, Goethe University Frankfurt, Max-von-Laue Straße 9, 60438 Frankfurt am Main, Germany. Tel: +49 (0)69 798 29331; Fax: +49 (0)69 798 29527; E-Mail: m.oreb@bio.uni-frankfurt.de

One sentence summary: Phosphorylation and ubiquitination are required for the glucose-induced internalization and degradation of the galactose permease Gal2.

Editor: John Morrissey
[†]Sina Schmidl, http://orcid.org/0000-0002-4643-0722
[‡]Mislav Oreb, http://orcid.org/0000-0002-6118-1517

ABSTRACT

The hexose permease Gal2 of *Saccharomyces cerevisiae* is expressed only in the presence of its physiological substrate galactose. Glucose tightly represses the *GAL2* gene and also induces the clearance of the transporter from the plasma membrane by ubiquitination and subsequent degradation in the vacuole. Although many factors involved in this process, especially those responsible for the upstream signaling, have been elucidated, the mechanisms by which Gal2 is specifically targeted by the ubiquitination machinery have remained elusive. Here, we show that ubiquitination occurs within the N-terminal cytoplasmic tail and that the arrestin-like proteins Bul1 and Rod1 are likely acting as adaptors for docking of the ubiquitin E3-ligase Rsp5. We further demonstrate that phosphorylation on multiple residues within the tail is indispensable for the internalization and possibly represents a primary signal that might trigger the recruitment of arrestins to the transporter. In addition to these new fundamental insights, we describe Gal2 mutants with improved stability in the presence of glucose, which should prove valuable for engineering yeast strains utilizing complex carbohydrate mixtures present in hydrolysates of lignocellulosic or pectin-rich biomass.

Keywords: Gal2; catabolite degradation; permease phosphorylation; permease ubiquitination

INTRODUCTION

Gal2, a member of the major facilitator superfamily, is the only galactose permease among the hexose transporters (HXT) in *Saccharomyces cerevisiae* (Boles and Hollenberg 1997; Özcan and Johnston 1999). Although its expression is repressed in the presence of glucose, it also transports this sugar with high affinity when constitutively expressed (Reifenberger, Boles and Ciriacy 1997). Moreover, recent efforts to engineer yeast for utilization of plant biomass have unraveled the capability of Gal2 to transport non-physiological substrates as well. Specifically, Gal2 was shown to transport arabinose (Becker and Boles 2003; Wisselink *et al.* 2007; Subtil and Boles 2011) xylose (Hamacher *et al.* 2002; Young *et al.* 2011), xylitol (Tani *et al.* 2016) and D-galacturonic

Received: 3 February 2021; **Accepted:** 29 March 2021

© The Author(s) 2021. Published by Oxford University Press on behalf of FEMS. All rights reserved. For permissions, please e-mail: journals.permissions@oup.com

acid (Protzko *et al.* 2018). Improving its kinetics and specificity, especially for pentoses, has therefore become an important target in strain engineering (Farwick *et al.* 2014; Reznicek *et al.* 2015; Wang *et al.* 2017; Verhoeven *et al.* 2018).

The expression of the *GAL2* gene is tightly regulated at the transcriptional level, whereby galactose (Horák 2013) and, as more recently found, the structurally similar arabinose (Oehling *et al.* 2018) act as inducers. Even in the presence of the inducers, glucose, the preferred carbon source of *S. cerevisiae*, acts as a strict repressor (for review, see Campbell *et al.* 2008; Conrad *et al.* 2014). To overcome this, the *GAL2* ORF is usually placed under the control of a constitutive promoter in strains engineered for utilization of non-physiological substrates (Becker and Boles 2003; Farwick *et al.* 2014). However, the presence of glucose not only represses the transcription of *GAL2*, but also triggers the Gal2 protein ubiquitination, endocytosis and degradation in the vacuole (Horak and Wolf 1997). This phenomenon is referred to as catabolite degradation and has attracted a significant research effort to understand the mechanisms driving catabolite-regulated protein turnover (for review, see Dupré, Urban-Grimal and Haguenauer-Tsapis 2004; Horák 2013). The degradation of Gal2 is insensitive to rapamycin and independent of the Gid/Vid family proteins (Horák 2013). Mono-ubiquitination of Gal2 occurs on multiple lysine residues through the action of Ubc1p-Ubc4p-Ubc5p triad of ubiquitin conjugating enzymes and Npi1/Rsp5p ubiquitin-protein ligase (Horak and Wolf 2001). However, the identity of the ubiquitinated lysines is not known. Also, the mechanism for recruiting Rsp5 to Gal2 was not investigated until now, but it is well established that arrestin-like adaptor proteins (ART, arrestin-related trafficking) are necessary to mediate the interaction between the ubiquitin ligase and other yeast permeases, including some related HXTs (for review, see Lauwers *et al.* 2010). However, it is generally not well understood how these adapters recognize their target proteins and what primary signals trigger the interaction. Regarding the upstream signal cascade, it was shown that glucose-induced degradation of Gal2 is independent both of the Gpr1-Gpa2 G protein-coupled receptor system and of glucose sensors Snf3p and Rgt2 (Horak, Regelmann and Wolf 2002). Intriguingly, the presence of intracellular glucose and the activity of the major hexokinase Hxk2 (yielding glucose-6-phosphate) are necessary for the signal initiating Gal2 degradation (Horak, Regelmann and Wolf 2002). Whether or not the downstream signal for Gal2 degradation proceeds through fructose-1,6-bisphosphate, a stimulator of Ras-signaling (Peeters *et al.* 2017), is unclear at present.

Since the regulation of the Gal2 turnover is interesting both from a fundamental point of view and in terms of biotechnological applications, we investigated the signals necessary for Gal2 degradation in more depth in the present work. In particular, we investigated the localization of lysines targeted by the ubiquitin ligase, the potential involvement of prominent ARTs Rod1 and Bul1 and the role of phosphorylation in regulating the endocytosis of Gal2.

MATERIALS AND METHODS

Strains and media

The strains CEN.PK2–1C (Entian and Kötter 2007) and EBY.VW4000 (Wieczorke *et al.* 1999) used in this study were previously described. The knock out of the open reading frames (ORFs) of *ROD1* and *BUL1* in CEN.PK2–1C was performed using the CRISPR-Cas9 system (Generoso *et al.* 2016), resulting in strains SRY001 and SRY002 respectively. The genotypes of the strains are listed in Table 1.

For the preparation of competent cells, plasmid-free cells were grown in standard YEP-media (1% (w/v) yeast extract, 2% (w/v) peptone) supplemented with 1% (w/v) maltose for EBY.VW4000 and 2% (w/v) of glucose for CEN.PK2–1C, SRY001 and SRY002. Frozen competent cells were prepared and transformed according to Gietz and Schiestl (2007). The transformants were plated on solid, selective synthetic complete (SC) medium with 1% (w/v) maltose or 2% (w/v) glucose, where uracil was absent (-URA) to maintain the selection pressure. Amino acids were added as stated in Bruder *et al.* (2016). For subcloning of plasmids, *E. coli* strain DH10B (Gibco BRL, Gaithersburg, MD) was used. It was grown either solid or liquid broth medium with carbenicillin as a selective marker.

PCR and plasmid construction

Genomic DNA of CEN.PK2–1C was used as template for PCR amplification of yeast ORF sequences of *GAL2* and *HXT11*. GAL2_30KR, GAL2_23KR and GAL2_25SA sequences were ordered as string DNA fragments from GeneArt Thermo Fisher Scientific (Waltham, MA). All synthetic DNA fragments are listed in Table S1 (Supporting Information). The synthetic genes or the wild-type *GAL2* sequence were used as template to introduce individual point mutations by PCR-based site directed mutagenesis. PCRs were performed with Phusion polymerase (New England Biolabs GmbH, Ipswich, MA) and the primers are listed in Table S2 (Supporting Information). The resulting fragments were transformed together with the XhoI/BamHI linearized multicopy (2μ) p426H7 and HindIII-HF/EcoRI-HF linearized low-copy CEN6/ARS4 pUCP1 vectors in CEN.PK2–1C frozen competent cells, respectively, to allow for plasmid assembly via homologous recombination. Cells were plated on SC -URA with 2% (w/v) glucose agar plates and incubated for 3 days at 30°C. Single colonies from these plates were picked, sub-cultivated and plasmids were recovered by the standard alkaline lysis protocol. For propagation and amplification, plasmids were transformed via electroporation into *E. coli* strain DH10B. Plasmid isolation from overnight *E. coli* cultures was carried out using a GeneJET Plasmid Miniprep Kit (Thermo Fisher Scientific, Waltham, MA) according to the manufacturer's instructions and sequenced at Microsynth (Balgach, Switzerland).

GFP (Slubowski *et al.* 2015) was fused to the C-terminus of transporter constructs via homologous recombination of PCR fragments carrying the specific overhangs. All plasmids used in this study are listed in Table S3 (Supporting Information).

Growth tests

For growth tests on agar solid medium, drop tests were performed on minimal SC-URA medium, containing the indicated sugar. Pre-cultures were grown over night in 10 mL SC -URA medium with 1% (w/v) maltose at 30°C and 180 rpm, centrifuged (3000 *g*, 3 min, 20°C) and washed twice in sterile water. Cells were resuspended in sterile water and $OD_{600nm} = 1$ was adjusted. Dilutions of $OD_{600\ nm} = 0.1$, 0.01 and 0.001 were prepared and 5 μL of each dilution was dropped onto the agar plate. Plates were incubated at 30°C for 3 days.

Cell growth in liquid SC-URA 2% (w/v) glucose medium was measured with the Cell Growth Quantifier (Aquila Biolabs, Baesweiler, Germany; Bruder *et al.* 2016). Pre-cultures of cells expressing the transporters in the low-copy CEN6/ARS4 pUCP1 vector were grown over night in 50 mL SC -URA 1% (w/v) maltose

Table 1. Strains used in this study.

Strain	Relevant genotype	Source
CEN.PK2–1C	*MATa leu2–3 112 ura3–52 trp1–289 his3Δ1 MAL2–8c SUC2*	Entian and Kötter (2007)
EBY.VW4000	CEN.PK2–1C *Δhxt1–17 gal2Δ::loxP stl1Δ::loxP agt1Δ::loxP mph2Δ::loxP mph3Δ::loxP*	Wieczorke *et al.* (1999)
SRY001	CEN.PK2–1C *Δrod1*	This study
SRY002	CEN.PK2–1C *Δbul1*	This study

medium, the cells were harvested by centrifugation (3000 *g*, 3 min, 20°C) and washed twice with sterile water. Washed cells were used to inoculate 50 mL SC-URA 2% (w/v) glucose medium to an $OD_{600\,nm}$ of ≈ 0.2 in 300 mL Erlenmeyer flasks, which were mounted onto the sensor plate. Quantification of cell growth was performed as previously described (Bruder *et al.* 2016).

Fluorescence microscopy

For fluorescence microscopy, CEN.PK2–1C, SRY001 and SRY002 cells expressing the GFP-tagged constructs were grown over night in 50 mL filter-sterilized, low fluorescent SC medium with 2% (w/v) galactose lacking uracil (lf-SC-URA), containing 6.9 g/L yeast nitrogen base with ammonium sulfate, without amino acids, without folic acid and without riboflavin (MP Biomedicals, Santa Ana, CA). Subsequently, the cells were washed twice with sterile water and re-suspended in parallel in a 50 mL fresh lf-SC-URA 2% (w/v) galactose or 50 mL lf-SC-URA 2% (w/v) glucose to an $OD_{600\,nm}$ between 1.5 and 3. From these main cultures, after 4 h of cultivation at 30°C with shaking (180 rpm), an aliquot of each one was mixed separately with 500 µL lf-SC -URA medium with the respective sugar, containing 1.2% (w/v) low melting agarose (Roth) to reach a final suspension of 0.6% (w/v) low melting agarose for immobilization of cells. The final cell density in the suspension was $OD_{600\,nm} \approx 2$. A total of 6 µL of it were applied to an object plate and sealed with a cover slip. GFP fluorescence was detected with the Confocal Laser Scanning Microscope Zeiss LSM 780 (Jena, Germany).

Radiolabeled glucose uptake assay

EBY.VW4000 yeast cells expressing GAL2_WT, Gal2_3KR and Gal2_6SA in the low-copy pUCP1 vector, were grown overnight at 30°C and 180 rpm in SC -URA with 1% maltose (w/v) medium. The next day, cells were centrifuged (4000 *g*, 5 min, 20°C) in 50 mL Falcon tubes. Pellets were washed twice in ice-cold 0.1 M potassium phosphate buffer (KH_2PO_4, pH 6.5, adjusted with KOH), weighed and resuspended in 0.1 M potassium phosphate buffer to a wet-weight concentration of 60 mg/mL. Aliquots of 110 µL were prepared and cooled on ice. The leftover cell suspension (of determined volume) was centrifuged (4000 *g*, 5 min, 4°C) and the pellet was frozen at -80°C overnight before it was freeze-dried to determine the cell dry weight. For the uptake assay with radiolabeled glucose the detailed protocol as described by Boles and Oreb (2018) was followed, in which transport activity was halted after 5 s. The measured uptake velocity was expressed as nmol ^{14}C glucose taken up per minute per milligram cell dry weight (nmol min^{-1} mg_{CDW}^{-1}). Uptake was measured at glucose concentrations 0.2, 0.5, 1, 2, 5, 20 and 50 mM. Calculation of the K_M and the V_{max} was done by nonlinear regression analysis and global curve fitting in Prism 5 (GraphPad Software) with values from technical triplicates according to Boles and Oreb (2018).

RESULTS

Identification of ubiquitination target residues in Gal2

It has been demonstrated by others (Peng *et al.* 2003) that the ubiquitination of HXTs (represented by Hxt6 and Hxt7) in yeast can occur on lysine residues located within the N- and C-terminal tails or within the large hydrophilic loop that connects the 6th and 7th transmembrane domain (TMD). To identify lysines that are exposed to the cytosol and are thereby potential targets for ubiquitination, we analyzed the Gal2 protein sequence using the TMD prediction tool *Philius* (Reynolds *et al.* 2008), which revealed that 23 (out of total 30) lysines are likely accessible from the cytosolic side (Table S4, Supporting Information). To further support this analysis, we simulated the membrane insertion of the structure model of Gal2 (Thomik *et al.* 2017) using the PPM-Server (Lomize *et al.* 2012; Figure S5, Supporting Information). The results of both approaches were in good agreement, except for Lys 141, 149, 150 and 394, which are rather inserted into the lipid bilayer according to the homology model. Nevertheless, they are located close to the membrane/cytosol interface and are therefore likely to be at least temporarily exposed to the cytosol, considering the conformational dynamics of sugar transporters.

We additionaly analysed the Gal2 sequence with the ubiquitination prediction online tool UbPred (Radivojac *et al.* 2010). Among eight residues that were recognized as potential ubiquitination targets (see Table S4, Supporting Information), only Lys 27, 37 and 44 in the N-terminal cytoplasmic tail had a high score and we therefore created a construct (3KR), in which they were mutated to arginine. Since it is well-known that alternative lysines can become ubiquitinated if the actual target residues are removed or mutated, we generated a construct (23KR), in which all cytosolically exposed lysines were substituted. Although the TMD or extracellularly localized residues obviously cannot be accessed by ubiquitin ligases, we further mutated all 30 lysines of Gal2 (30KR), driven by curiosity to see if the protein function is still retained. In addition to amino acid exchange mutations, we also deleted the N- (Δ64) and C-terminal (Δ523) tails as well as a large stretch (flanked by Lys 274 and Lys 326) of the cytosolic loop connecting TMD6 and TMD7 (Δ274–326). The deletion constructs were intended to investigate not only the involvement of the respective modules in Gal2 ubiquitination, but—more generally—their importance for the trafficking and function of the transporter.

To analyze the subcellular localization of these mutants by fluorescence microscopy (Fig. 1), we expressed them from multicopy plasmids under the control of the strong constitutive promoter $HXT7p^{-1-392}$ (Hamacher *et al.* 2002) as fusion proteins with C-terminal GFP in the strain CEN.PK2–1C. Low-fluorescence synthetic media (SC) lacking uracil were used for the cultivation. The cells were first cultivated on galactose and subsequently transferred to glucose containing medium to induce the internalization of the transporter. On galactose, Gal2 showed a clear localization in the plasma membrane but partly also in the

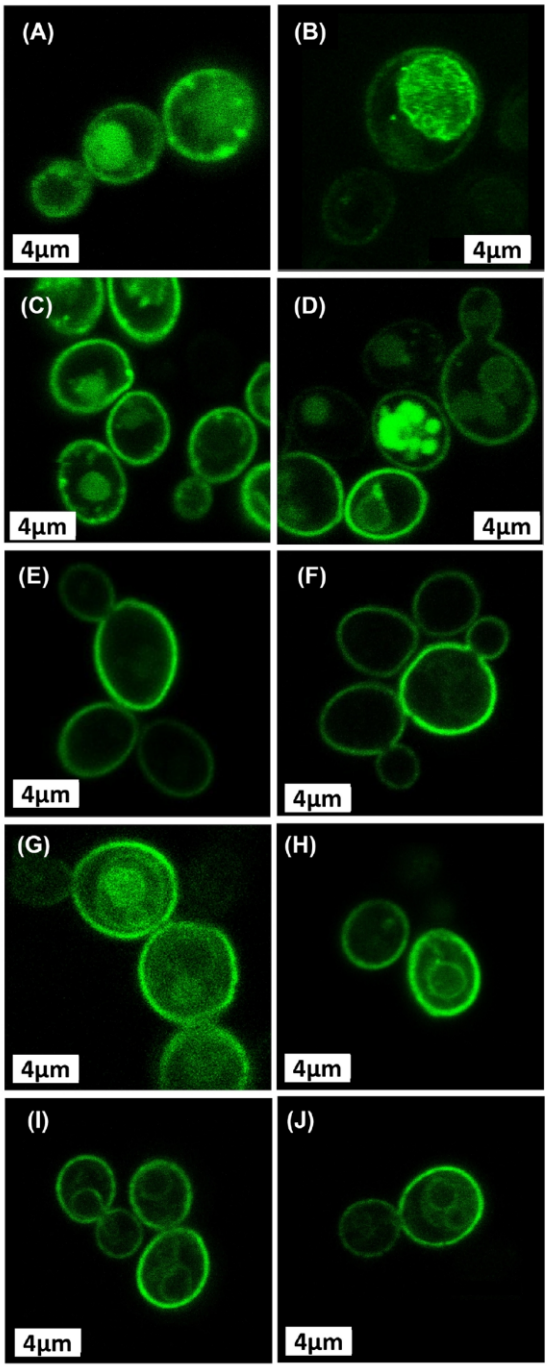

Figure 1. Mapping the lysines targeted by ubiquitination. Representative (about 70% of the fluorescent population) confocal images of CEN.PK2–1C cells expressing GFP-tagged Gal2 wildtype (**A** and **B**), Gal2_Δ64 (**C** and **D**), Gal2_3KR (**E** and **F**), Gal2_23KR (**G** and **H**) and Gal2 30KR (**I** and **J**) from multicopy plasmids are shown. The cells were grown in SC media with 2% galactose on the left (A, C, E, G and I) or 2% glucose media on the right (B, D, F, H and J). Scale bar represents 4 μm.

vacuole, which indicates a certain degree of constitutive internalization. Nevertheless, when the cells were shifted to glucose, the signal mainly resided in the vacuole, which is consistent with previous observations (Horak, Regelmann and Wolf 2002). In contrast, the 3KR mutant was almost exclusively localized in the plasma membrane on both sugars, demonstrating that the first three N-terminal lysines are crucial for the degradation of Gal2, in acordance with the UbPred score. The 23KR, 30KR and Δ64 also were more stable at the plasma membrane on glucose compared to the wildtype, but at the same time showed increased intracellular signal compared to 3KR. For all three constructs, a partial localization in a ring surrounding the nucleus was observed, which is indicative of misfolding and accumulation of the protein in the (perinuclear) endoplasmic reticulum, as frequently observed when heterologous membrane proteins are (over)expressed in yeast (O'Malley *et al.* 2009; Tripp *et al.* 2017), due to the limited capacity of the secretory pathway. To test the functionality of the mutant transporters, we expressed them in EBY.VW4000, a strain deficient for all endogenous permeases capable of hexose uptake (Wieczorke *et al.* 1999), which is frequently used for functional characterization of endogenous and heterologous hexose transporters (Boles and Oreb 2018). For strain maintenance and to control the viability of the transformants, the disaccharide maltose is used as a permissive carbon source that is taken up by specific permeases (Mal21 and Mal31). Supporting the results from fluorescence microscopy, the ability of 23KR and Δ64 constructs to transport glucose was strongly impaired, whereas the 30KR mutant completely lost the activity (Figure S6, Supporting Information). The latter result demonstrates that the lysines in the extracellular loops (K108, K110, K172, K233, K358, K423 and K429) are important for the function of Gal2. The deletion (Δ274–326) within 6th hydrophilic loop expectedly also abolished the transporter function (not shown) and severely affected its trafficking to the plasma membrane even on galactose (Figure S7, Supporting Information). This is consistent with the importance of this large loop, connecting the N- and C-terminal halves in all major facilitator superfamily members, for the structural integrity of the transporter (Forrest, Krämer and Ziegler 2011). The deletion of the C-terminal tail led to a complete loss of function (not shown) and a rather diffuse fluorescence signal on galactose, resembling cytosolic localization (Figure S7, Supporting Information), which suggests that the C-terminal tail is indispensible for the correct membrane insertion of the transporter.

Involvement of ARTs Rod1 and Bul1 in Gal2 internalization

ARTs are important regulators of the endocytic pathway in yeast, facilitating selective ubiquitination of target transporters by the E3 ubiquitin ligase, Rsp5 (Llopis-Torregrosa *et al.* 2016). It was reported that the internalization of glucose transporters (Hxt1, Hxt3 and Hxt6) and of the monocarboxylate transporter Jen1 is mediated by the ART Rod1 (Fujita *et al.* 2018). More recently, it was found that Bul1, another ART, is required for the internalization of Jen1, acting in response to glucose availability at the plasma membrane, whereas Rod1 is involved further downstream in the endocytic process (Hovsepian *et al.* 2018). We therefore assumed that Rod1 and Bul1 are potential candidate ARTs that mediate the glucose-induced internalization of Gal2 as well.

We knocked out *ROD1* and *BUL1* genes individually in CEN.PK2–1C using CRISPR-Cas9 (Generoso *et al.* 2016). Then we transformed the resultant strains SRY001 and SRY002 with

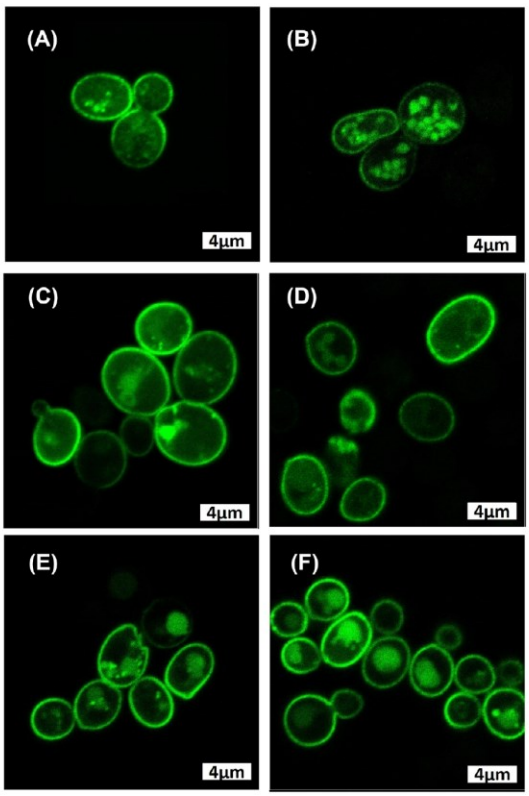

Figure 2. The effect of *ROD1* and *BUL1* deletion on internalization of Gal2. Representative fluorescence micrographs of CEN.PK2–1C (**A** and **B**) CEN.PK2–1C_ΔROD1 (**C** and **D**) and CEN.PK2–1C_ΔBUL1 (**E** and **F**) expressing wildtype Gal2-GFP from a multicopy plasmid are shown. The cells were grown in SC media with 2% galactose on the left (A, C and E) or 2% glucose media on the right (B, D and F) Scale bar represents 4 μm.

GAL2-GFP constructs. In fluorescence micrographs, when the cells were growing in galactose medium, we did not observe differences between the parental strain CEN.PK2–1C and both deletion strains Δ*rod1* and Δ*bul1* in terms of localization of Gal2. The fluorescence signal was mainly at the membrane with only partial vacuolar localization, resembling the pattern in wildtype cells (see Fig. 1). When the cells were exposed to glucose, we could observe a stabilization of Gal2 in both Δ*rod1* and Δ*bul1* background compared to the wildtype, but a large proportion of the protein was still localized in the vacuoles (Fig. 2). This suggests that Bul1 and Rod1 are both possibly involved in the internalization of Gal2, but other ART family members likely can, at least partly, take over their function in the knock-out mutants. Consistent with this hypothesis, deletion of multiple ARTs was necessary to fully abolish the internalization of heterologous cellodextrin transporters in yeast (Sen *et al.* 2016).

Phosphorylation as a potential primary signal for Gal2 internalization

One of the major unresolved questions regarding the internalization of permeases—not only in yeast—relates to the nature of the primary signal(s) that trigger the recruitment of adaptors to the appropriate target protein (Lauwers *et al.* 2010). Phosphorylation was found to precede ubiquitination of the uracil permease Fur4 (Marchal, Haguenauer-Tsapis and Urban-Grimal 1998) and of the phosphate transporter Pho84 (Lundh *et al.* 2009) in yeast. Strikingly, in high-throughput proteomic approaches (Holt *et al.* 2009; Oliveira *et al.* 2012), phosphoserine residues were identified within the N-terminal tail of Gal2, which is also targeted by ubiquitination, as shown above. To test their relevance for Gal2 internalization, we mutated only Ser 32 (Oliveira *et al.* 2012) or six serines (at positions 32, 35, 39, 48, 53 and 55 in the CEN.PK2–1C Gal2 variant; note that Gal2 from S288C has an additional Ser50 that is also phosphorylated) (Holt *et al.* 2009) to alanine (named S32A and 6SA constructs, respectively). In a third construct, we mutated all eleven serines (11SA) in the N-terminal tail to prevent potential promiscuous phosphorylation of neighboring serine residues. The mutants were expressed as GFP fusions from centromeric plasmids in CEN.PK2–1C cells to study their subcellular localization by fluorescence microscopy. We switched to the low copy plasmids to ensure that possible subtle differences between different mutants are not masked by overexpression. The S32A mutant was partly localized to the vacuole after glucose exposure but slightly more stable at the plasma membrane than the wildtype Gal2 (Fig. 3), which suggests an important role of S32 in regulating Gal2 internalization. However, the signals of both the 6SA and the 11SA mutant were virtually exclusively localized at the plasma membrane on both sugars, supporting the finding that multiple serine residues are targeted by phosphorylation (Holt *et al.* 2009). Taken together, these observations suggest that phosphorylation could be an upstream signal for recruiting the adaptors and subsequently the Rsp5 ubiquitin ligase to the N-terminal tail of Gal2.

Glucose transport by stabilized Gal2 variants

We finally sought to functionally analyze the consequences of Gal2 stabilization. We reasoned that Gal2 variants that are resistant to glucose-induced degradation should confer higher glucose uptake rates in EBY.VW4000. We first measured the uptake kinetics of ^{14}C-labelled glucose in this strain expressing the wildtype, 3KR and 6SA variants from centromeric plasmids. The cells were pre-grown on maltose, so that their growth was independent of Gal2. It is important to note that maltose, like glucose, induces the internalization of Gal2 (Horak, Regelmann and Wolf 2002). Thus, mutations that prevent Gal2 degradation should also affect the abundance of the transporter in the cells that are subjected to the uptake assay. In accordance with the expectation, the mutations did not significantly affect the K_M value, which is an intrinsic kinetic constant, but the maximum velocity (V_{max})—a parameter that is directly proportional to the protein abundance—was approximately 1.8- and 2.2-fold increased for the 3KR and 6SA mutant, respectively (Fig. 4 and Table 2). We further performed growth tests with the same transformants (again pre-grown on maltose) in liquid glucose-containing media. The growth behavior, with 3KR and 6SA exhibiting much shorter lag phases, reflected the result of the glucose uptake assay. Together, these results strongly support the conclusion that the 3KR and 6SA mutations prevent the internalization of Gal2 and thereby increase its abundance in the plasma membrane.

Transfer of the amino-terminal tail of Gal2 to Hxt11

We hypothesized that, if the N-terminal tail of Gal2 is necessary and sufficient to drive glucose-induced internalization of the permease, transferring it to another transporter should replicate

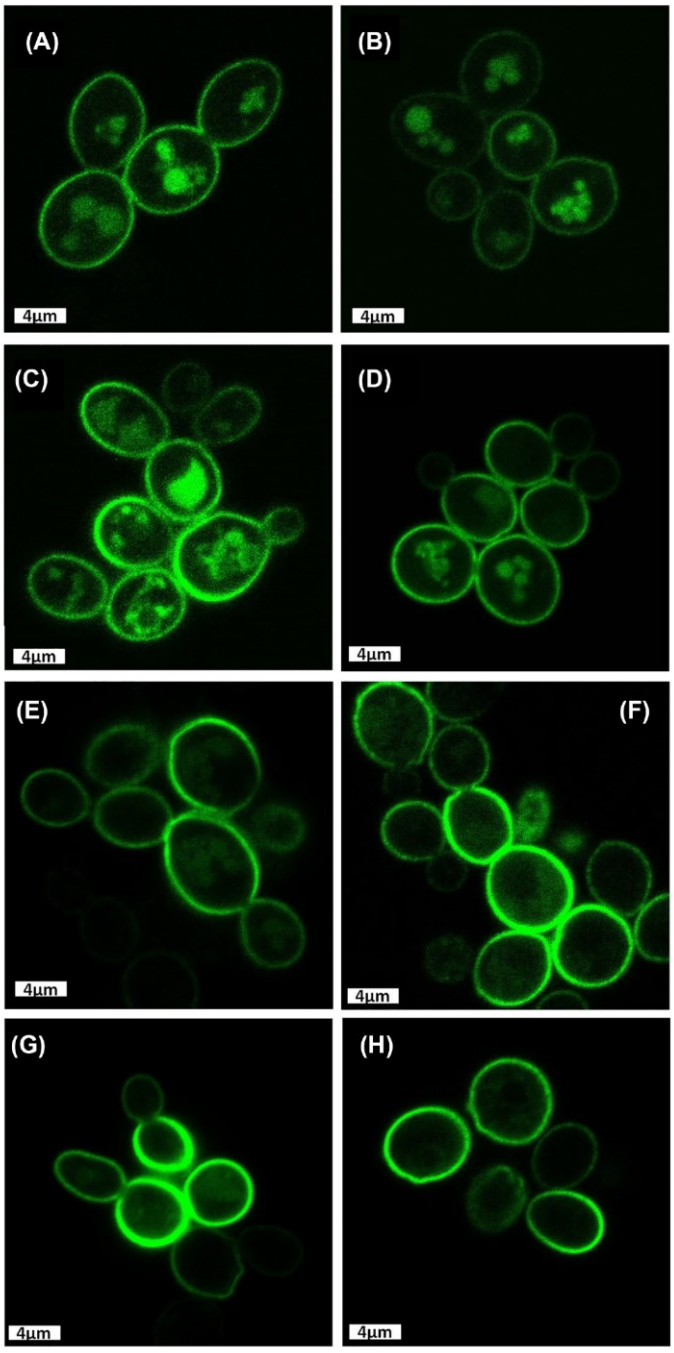

Figure 3. Subcellular localization of Gal2 with mutated phosphorylation sites. Representative micrographs of CEN.PK2–1C expressing GFP-tagged Gal2 wildtype (**A** and **B**), Gal2_S32A (**C** and **D**), Gal2_6SA (**E** and **F**) and Gal2_11SA (**G** and **H**) from centromeric plasmids are shown. The cells were grown in SC media with 2% galactose on the left (A, C, E and G) or 2% glucose media on the right (B, D, F and H) Scale bar represents 4 μm.

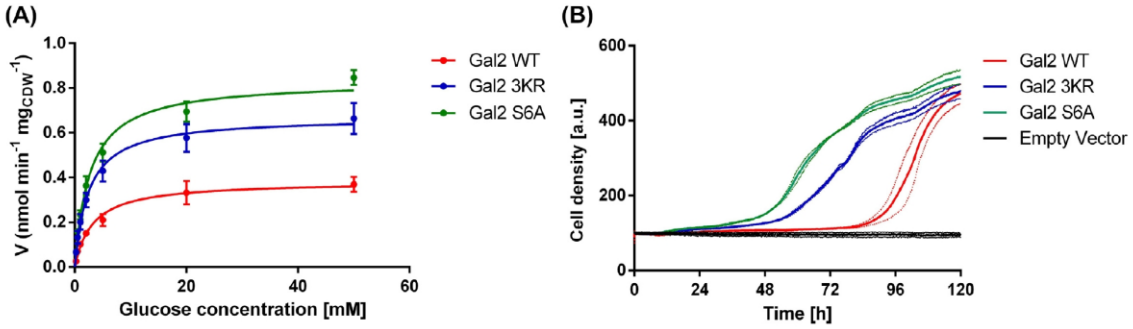

Figure 4. Functional characterization of stabilized Gal2 variants. **(A)** A ^{14}C-glucose uptake assay was performed in EBY.VW4000 cells with indicated Gal2 variants. The initial velocity is plotted against glucose concentration. The mean values and standard deviations were calculated from four replicates at each concentration. The kinetic parameters (shown in Table 2) were determined by a non-linear fit to the Michaelis–Menten equation. **(B)** EBY.VW4000 cells transformed with the Gal2 constructs or with the empty vector as a negative control (centromeric plasmids) were tested for growth in SC medium with 2% (w/v) glucose. The cell density increase over time was monitored with the Cell Growth Quantifier (Aquila Biolabs). The mean values (solid lines) and standard deviations (dotted lines) were calculated from three independent cultures.

Table 2. The kinetic parameters of Gal2 variants were calculated from data shown in Fig. 4.

	Kinetic parameters	
Transporter variant	Km [mM]	Vmax [nmol/min/mg]
Gal2 wildtype	3.194 ± 0.386	0.383 ± 0.014
Gal2_3KR	2.460 ± 0.259	0.670 ± 0.019
Gal2_6SA	2.701 ± 0.227	0.832 ± 0.020

the behavior of Gal2 on different sugars. For this, we selected Hxt11, a transporter that is not degraded in the presence of glucose. When overexpressed, it transports the hexoses glucose, fructose, mannose and galactose (Wieczorke *et al.* 1999), the pentose xylose (Shin *et al.* 2015) and the pentitol xylitol (Jordan *et al.* 2016). It was shown that a chimeric construct, in which the N-terminal cytosolic part of Hxt2 was replaced by the corresponding region of Hxt11 was not degraded on glucose, in contrast to the native Hxt2 (Shin *et al.* 2017). We first investigated the behavior of wildtype Hxt11 with C-terminally fused GFP on galactose and glucose, which was opposite to Gal2 (i.e. the internalization being induced on galactose; compare Figs 1 and 5). When we removed the N-terminus (Δ38), Hxt11 was clearly localized at the plasma membrane on both sugars (Fig. 5). As the minimal sequence including all ubiquitinated lysines and phosphorylated serines, we fused the N-terminal aminoacids 1–55 of Gal2 as wildtype, 3KR and 6SA variant to the Δ38-Hxt11 construct. Unexpectedly, the chimera with the wildtype Gal2-tail was internalized not only on glucose, but even more on galactose (Fig. 5). The mutants, however, were stable at the plasma membrane on both carbon sources, comparable to the Δ38. This confirms the crucial role of the lysines and serines in the N-terminus of Gal2 for its internalization. On the other hand, the observation that both transporters behave differently with the wildtype tail of Gal2 also suggests that not only the N-terminal tail, but also other sequence elements of Gal2 and Hxt11 may be contributing to recognition by the phosphorylation and/or ubiquitination machineries.

DISCUSSION

It was known for long time that mono-ubiquitination by Rsp5 on multiple lysine residues is necessary for the internalization of Gal2 (Horak and Wolf 2001). In this work, we mapped the ubiquitination sites to the N-terminal tail. Whether or not the simultaneous ubiquitination must occur on all three lysines that we mutated in the 3KR construct (at positions 27, 37 and 44) remains to be established in the future. It is intriguing that the mutant with the complete deletion of the N-terminal tail (Δ64), although more stable on glucose, still partly enters the vacuole. Its partial retention in the ER indicates some degree of incorrect folding, which is likely recognized by the ER-associated quality control. ER-associated protein degradation (ERAD) occurs in the proteasome (Thibault and Ng 2012), but a part of the conformationally damaged Gal2 presumably escapes ERAD and becomes recognized in the post-ER compartments, e.g. by the plasma membrane quality control, which involves different mechanism than the nutrient-induced internalization (Okiyoneda, Apaja and Lukacs 2011). Thus, ubiquitination of the misfolded Δ64 mutant on alternative lysine residues might trigger the clearance from the plasma membrane and transport to the vacuole. This conclusion is supported by the observation that 23KR and 30KR mutants, which are also partly retained in the endomembrane systems, apparently do not enter the vacuole.

The identification of the full set of ARTs that may mediate the ubiquitination of Gal2 was not in the scope of this study. For an unambiguous conclusion, it would be necessary to study the behavior of Gal2 in deletion mutants of multiple ARTs (Sen *et al.* 2016). Nevertheless, we found that Bul1 and Rod1 are likely candidates for this role, as their individual deletion led to a stabilization of Gal2 at the plasma membrane on glucose. This would be reminiscent of their involvement in Jen1 internalization (Hovsepian *et al.* 2018), which is likewise induced by glucose.

We show that phosphorylation of the N-terminal tail of Gal2 is an additional, previously unknown mechanism involved in the signal cascade that leads to Gal2 internalization. Although

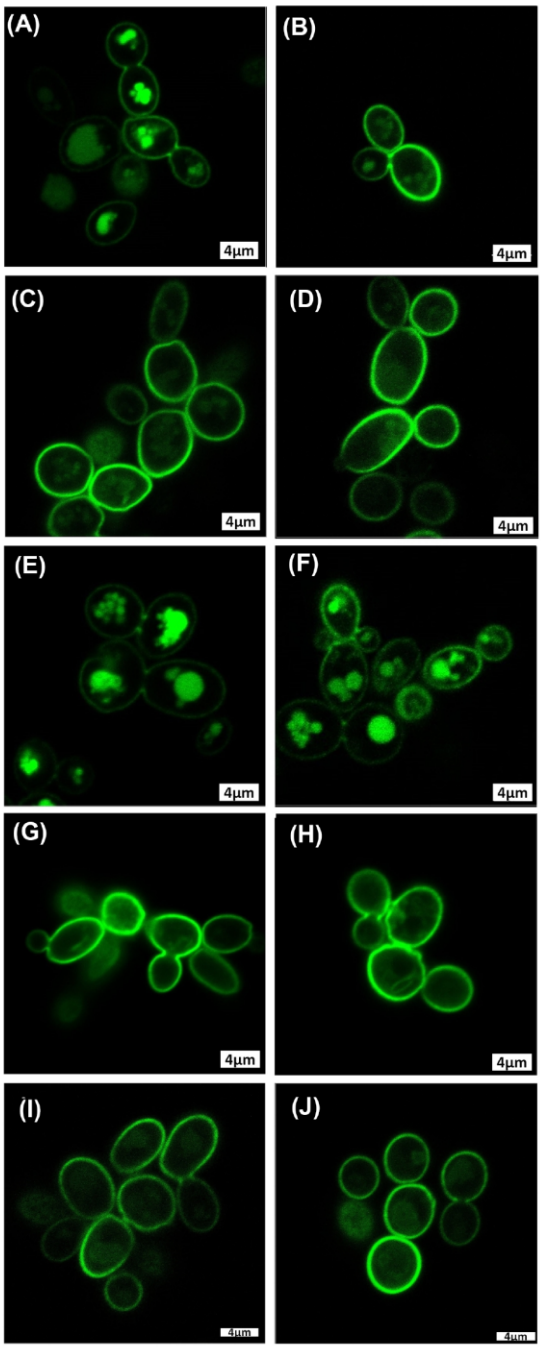

Figure 5. Subcellular localization of chimeric Hxt11 constructs. Representative confocal images of CEN.PK2–1C cells expressing different GFP-tagged Hxt11 constructs: wildtype Hxt11 (**A** and **B**), the N-terminal deletion mutant alone (Δ38) (**C** and **D**) or fused with the N-terminal amino acids 1–55 of Gal2 as wildtype (WT) (**E** and **F**), 3KR (**G** and **H**) or 6SA (**I** and **J**) variant from centromeric plasmids are shown. The cells were grown in SC media with 2% galactose on the left (A, C, E, G and I) or 2% glucose media on the right (B, D, F, H and J). Scale bar represents 4 μm.

our experiments allow no conclusions regarding the sequence of events, it is very likely that phosphorylation occurs first, as a 'label' for recruitment of ARTs, since phosphorylation has been reported to occur prior to ubiquitination of Fur4 and Pho84 permeases in yeast (Marchal, Haguenauer-Tsapis and Urban-Grimal 1998; Lundh *et al.* 2009). An important next step will be the identification of responsible kinase(s). Although the Gal2 phosphorylation sites were identified in a global analysis of Cdk1 substrates, Gal2 can be clearly ruled out as a target of this cyclin-dependent kinase, as it neither fulfills the consensus sequence criteria, nor does the phosphorylation pattern sufficiently change after Cdk1 inhibition (Holt *et al.* 2009). The intriguing observation that the wildtype (but not 6SA) N-terminal tail of Gal2 drives the internalization of Hxt11 on both glucose and galactose suggests either that different kinases can phosphorylate the same sequence or that the same kinase is present on both sugars. The latter assumption would imply that additional factors are involved in the recognition of the N-terminal tail depending on the physiological conditions. Considering that wildtype Gal2 and chimeric Hxt11 with the wildtype Gal2 tail are differently internalized (compare Figs 1 and 5), it is reasonable to assume that other sequence elements—presumably the cytosolic loops—could contribute to the recognition of the appropriate substrate, regardless of the identity of the involved kinase(s).

Interestingly, the glucose uptake rate (and the growth conferred by it) were higher with the 6SA mutant than with the 3KR variant (Fig. 4), although their stability at the plasma membrane was comparable (compare Figs 1 and 3). We cannot rule out that this is caused by the differences of the amino acid sequence, but it is tempting to speculate that the effect is due to the binding of other proteins (e.g. ARTs) to the N-terminal tail. If phosphorylation is the primary signal, as assumed, then binding of ARTs would occur only on the 3KR mutant, but not on the 6SA mutant. Binding of other proteins might negatively affect the transport rate, e.g. by affecting the conformational changes by so-called long-distance effects (Smirnova, Kasho and Kaback 2011). Thus, this observation might indirectly support the idea that phosphorylation drives the binding of ARTs to Gal2.

Besides these exciting scientific aspects, the stabilized Gal2 variants that we described in this work have a potential for biotechnological applications. As outlined in the introduction, Gal2 can be used as a transporter for arabinose, xylose or D-galacturonic acid. Our preliminary experiments have shown that the stabilized Gal2 variants can transport galactose, xylose and arabinose comparably to the wildtype transporter, indicating that the mutations within the N-terminal tail have not changed the substrate specificity. These carbohydrates are abundant in industrially relevant hydrolysates of plant biomass, e.g. lignocellulose (Jansen *et al.* 2017) or pectin (Schmitz *et al.* 2019). Since these feedstocks commonly contain glucose as the predominant sugar, preventing glucose-induced degradation of the transporter would be beneficial for the simultaneous uptake and fermentation of the abovementioned carbohydrates in engineered yeast strains.

AUTHOR CONTRIBUTIONS

The project was initiated by MO. STR performed most of the experiments, analyzed the data and drafted the manuscript. SS performed the radiolabeled glucose uptake including data analysis. EB and MO contributed to experimental design and supervised the project. All authors edited and approved the manuscript.

ACKNOWLEDGMENTS

We thank Fernando Garcés Daza, for inspirational discussions and support. We are grateful to Katharina Happel and Chiara Nenninger, who helped with plasmid construction.

SUPPLEMENTARY DATA

Supplementary data are available at *FEMSYR* online.

FUNDING

This work was supported by DAAD/BECAS Chile, 2016, grant number 57221134 (to STR).

Conflicts of interest. None declared.

REFERENCES

Becker J, Boles E. A modified *Saccharomyces cerevisiae* strain that consumes L-arabinose and produces ethanol. *Appl Environ Microbiol* 2003;**69**:4144–50.

Boles E, Hollenberg CP. The molecular genetics of hexose transport in yeasts. *FEMS Microbiol Rev* 1997;**21**:85–111.

Boles E, Oreb M. A growth-based screening system for hexose. *Methods Mol Biol* 2018;**1713**:123–35.

Bruder S, Reifenrath M, Thomik T *et al.* Parallelised online biomass monitoring in shake flasks enables efficient strain and carbon source dependent growth characterisation of *Saccharomyces cerevisiae*. *Microb Cell Fact* 2016;**15**:1–14.

Campbell RN, Leverentz MK, Ryan LA *et al.* Metabolic control of transcription: paradigms and lessons from *Saccharomyces cerevisiae*. *Biochem J* 2008;**414**:177–87.

Conrad M, Schothorst J, Kankipati HN *et al.* Nutrient sensing and signaling in the yeast *Saccharomyces cerevisiae*. *FEMS Microbiol Rev* 2014;**38**:254–99.

Dupré S, Urban-Grimal D, Haguenauer-Tsapis R. Ubiquitin and endocytic internalization in yeast and animal cells. *Biochimica et Biophysica Acta (BBA) - Molecular Cell Research* 2004;**1695**:89–111.

Entian KD, Kötter P. 25 yeast genetic strain and plasmid collections. *Methods Microbiol* 2007;**36**:629–66.

Farwick A, Bruder S, Schadeweg V *et al.* Engineering of yeast hexose transporters to transport D-xylose without inhibition by D-glucose. *Proc Natl Acad Sci* 2014;**111**:5159–64.

Forrest LR, Krämer R, Ziegler C. The structural basis of secondary active transport mechanisms. *Biochimica et Biophysica Acta (BBA) - Bioenergetics* 2011;**1807**:167–88.

Fujita S, Sato D, Kasai H *et al.* The C-terminal region of the yeast monocarboxylate transporter Jen1 acts as a glucose signal-responding degron recognized by the α-arrestin Rod1. *J Biol Chem* 2018;**293**:10926–36.

Generoso WC, Gottardi M, Oreb M *et al.* Simplified CRISPR-Cas genome editing for *Saccharomyces cerevisiae*. *J Microbiol Methods* 2016;**127**:203–5.

Gietz RD, Schiestl RH. Frozen competent yeast cells that can be transformed with high efficiency using the LiAc/SS carrier DNA/PEG method. *Nat Protoc* 2007;**2**:1–4.

Hamacher T, Becker J, Gárdonyi M *et al.* Characterization of the xylose-transporting properties of yeast hexose transporters and their influence on xylose utilization. *Microbiology* 2002;**148**:2783–8.

Holt LJ, Tuch BB, Villén J *et al.* Global analysis of Cdk1 substrate phosphorylation sites provides insights into evolution. *Science* 2009;**325**:1682–6.

Horak J, Regelmann J, Wolf DH. Two distinct proteolytic systems responsible for glucose-induced degradation of fructose-1,6-bisphosphatase and the Gal2p transporter in the yeast *Saccharomyces cerevisiae* share the same protein components of the glucose signaling pathway. *J Biol Chem* 2002;**277**:8248–54.

Horak J, Wolf DH. Catabolite inactivation of the galactose transporter in the yeast *Saccharomyces cerevisiae* : ubiquitination, endocytosis and degradation in the vacuole. *J Bacteriol* 1997;**179**:1541–9.

Horak J, Wolf DH. Glucose-induced monoubiquitination of the *Saccharomyces cerevisiae* galactose transporter is sufficient to signal its internalization. *J Bacteriol* 2001;**183**:3083–8.

Horák J. Regulations of sugar transporters: insights from yeast. *Curr Genet* 2013;**59**:1–31.

Hovsepian J, Albanèse V, Becuwe M *et al.* The yeast arrestin-related protein Bul1 is a novel actor of glucose-induced endocytosis. *Mol Biol Cell* 2018;**33**:mbc.E17–07-0466.

Jansen MLA, Bracher JM, Papapetridis I *et al.* *Saccharomyces cerevisiae* strains for second-generation ethanol production: from academic exploration to industrial implementation. *FEMS Yeast Res* 2017;**17**:1–20.

Jordan P, Choe J-Y, Boles E *et al.* Hxt13, Hxt15, Hxt16 and Hxt17 from *Saccharomyces cerevisiae* represent a novel type of polyol transporters. *Sci Rep* 2016;**6**:23502.

Lauwers E, Erpapazoglou Z, Haguenauer-Tsapis R *et al.* The ubiquitin code of yeast permease trafficking. *Trends Cell Biol* 2010;**20**:196–204.

Llopis-Torregrosa V, Ferri-Blázquez A, Adam-Artigues A *et al.* Regulation of the yeast Hxt6 hexose transporter by the Rod1 α-Arrestin, the Snf1 protein kinase, and the Bmh2 14-3-3 protein. *J Biol Chem* 2016;**291**:14973–85.

Lomize MA, Pogozheva ID, Joo H *et al.* OPM database and PPM web server: resources for positioning of proteins in membranes. *Nucleic Acids Res* 2012;**40**:D370–6.

Lundh F, Mouillon JM, Samyn D *et al.* Molecular mechanisms controlling phosphate-induced downregulation of the yeast Pho84 phosphate transporter. *Biochemistry* 2009;**48**:4497–505.

Marchal C, Haguenauer-Tsapis R, Urban-Grimal D. A PEST-Like sequence mediates phosphorylation and efficient ubiquitination of yeast uracil permease. *Mol Cell Biol* 1998;**18**:314–21.

O'Malley MA, Mancini JD, Young CL *et al.* Progress toward heterologous expression of active G-protein-coupled receptors in *Saccharomyces cerevisiae*: linking cellular stress response with translocation and trafficking. *Protein Sci* 2009;**18**:2356–70.

Oehling V, Klaassen P, Frick O *et al.* I-Arabinose triggers its own uptake via induction of the arabinose-specific Gal2p transporter in an industrial *Saccharomyces cerevisiae* strain. *Biotechnol Biofuels* 2018;**11**:1–16.

Okiyoneda T, Apaja PM, Lukacs GL. Protein quality control at the plasma membrane. *Curr Opin Cell Biol* 2011;**23**:483–91.

Oliveira AP, Ludwig C, Picotti P *et al.* Regulation of yeast central metabolism by enzyme phosphorylation. *Mol Syst Biol* 2012;**8**:623.

Özcan S, Johnston M. Function and regulation of yeast hexose transporters. *Microbiol Mol Biol Rev* 1999;**63**:554–69.

Peeters K, Van Leemputte F, Fischer B *et al.* Fructose-1,6-bisphosphate couples glycolytic flux to activation of Ras. *Nat Commun* 2017;**8**:922.

Peng J, Schwartz D, Elias JE *et al.* A proteomics approach to understanding protein ubiquitination. *Nat Biotechnol* 2003;**21**:921.

Protzko RJ, Latimer LN, Martinho Z *et al.* Engineering *Saccharomyces cerevisiae* for co-utilization of d-galacturonic acid and d-glucose from citrus peel waste. *Nat Commun* 2018; **9**:5059.

Radivojac P, Vacic V, Haynes C *et al.* Identification, analysis, and prediction of protein ubiquitination sites. *ProteinsProteins: Struct, Funct, Bioinf* 2010;**78**:365–80.

Reifenberger E, Boles E, Ciriacy M. Kinetic characterization of individual hexose transporters of *Saccharomyces cerevisiae* and their relation to the triggering mechanisms of glucose repression. *Eur J Biochem* 1997;**245**:324–33.

Reynolds SM, Käll L, Riffle ME *et al.* Transmembrane topology and signal peptide prediction using dynamic Bayesian networks. *PLoS Comput Biol* 2008;**4**:e1000213.

Reznicek O, Facey SJ, de Waal PP *et al.* Improved xylose uptake in *Saccharomyces cerevisiae* due to directed evolution of galactose permease Gal2 for sugar co-consumption. *J Appl Microbiol* 2015;**119**:99–111.

Schmitz K, Protzko R, Zhang L *et al.* Spotlight on fungal pectin utilization—from phytopathogenicity to molecular recognition and industrial applications. *Appl Microbiol Biotechnol* 2019;**103**:2507–24.

Sen A, Acosta-Sampson L, Alvaro CG *et al.* Internalization of heterologous sugar transporters by endogenous alpha-arrestins in the yeast *Saccharomyces cerevisiae*. *Appl Environ Microbiol* 2016;**82**:7074–85.

Shin HY, Nijland JG, de Waal PP *et al.* An engineered cryptic Hxt11 sugar transporter facilitates glucose–xylose co-consumption in *Saccharomyces cerevisiae*. *Biotechnol Biofuels* 2015; **8**:176.

Shin HY, Nijland JG, de Waal PP *et al.* The amino-terminal tail of Hxt11 confers membrane stability to the Hxt2 sugar transporter and improves xylose fermentation in the presence of acetic acid. *Biotechnol Bioeng* 2017;**114**:1937–45.

Slubowski CJ, Funk AD, Roesner JM *et al.* Plasmids for C-terminal tagging in *Saccharomyces cerevisiae* that contain improved GFP proteins, Envy and Ivy. *Yeast* 2015;**32**:379–87.

Smirnova I, Kasho V, Kaback HR. Lactose permease and the alternating access mechanism. *Biochemistry* 2011;**50**:9684–93.

Subtil T, Boles E. Improving L-arabinose utilization of pentose fermenting *Saccharomyces cerevisiae* cells by heterologous expression of L-arabinose transporting sugar transporters. *Biotechnol Biofuels* 2011;**4**:1–10.

Tani T, Taguchi H, Fujimori KE *et al.* Isolation and characterization of xylitol-assimilating mutants of recombinant *Saccharomyces cerevisiae*. *J Biosci Bioeng* 2016;**122**:446–55.

Thibault G, Ng DTW. The endoplasmic reticulum-associated degradation pathways of budding yeast. *Cold Spring Harb Perspect Biol* 2012;**4**:a013193–.

Thomik T, Wittig I, Choe J *et al.* An artificial transport metabolon facilitates improved substrate utilization in yeast. *Nat Chem Biol* 2017;**13**:1158–63.

Tripp J, Essl C, Iancu C V. *et al.* Establishing a yeast-based screening system for discovery of human GLUT5 inhibitors and activators. *Sci Rep* 2017;**7**:1–9.

Verhoeven MD, Bracher JM, Nijland JG *et al.* Laboratory evolution of a glucose-phosphorylation-deficient, arabinose-fermenting *S. cerevisiae* strain reveals mutations in GAL2 that enable glucose-insensitive l-arabinose uptake. *FEMS Yeast Res* 2018:1–15. DOI: 10.1093/femsyr/foy062.

Wang C, Li Y, Qiu C *et al.* Identification of important amino acids in Gal2p for improving the L-arabinose transport and metabolism in *Saccharomyces cerevisiae*. *Front Microbiol* 2017;**8**:1–11.

Wieczorke R, Krampe S, Weierstall T *et al.* Concurrent knock-out of at least 20 transporter genes is required to block uptake of hexoses in *Saccharomyces cerevisiae*. *FEBS Lett* 1999;**464**:123–8.

Wisselink HW, Toirkens MJ, Berriel MDRF *et al.* Engineering of *Saccharomyces cerevisiae* for efficient anaerobic alcoholic fermentation of L-arabinose. *Appl Environ Microbiol* 2007;**73**:4881–91.

Young E, Poucher A, Comer A *et al.* Functional survey for heterologous sugar transport proteins, using *Saccharomyces cerevisiae* as a host. *Appl Environ Microbiol* 2011;**77**:3311–9.

Supplementary Information

Glucose-induced internalization of the *S. cerevisiae* galactose permease Gal2 is dependent on phosphorylation and ubiquitination of its aminoterminal cytoplasmic tail

Sebastian A. Tamayo Rojas, Sina Schmidl, Eckhard Boles and Mislav Oreb*

Institute of Molecular Biosciences, Faculty of Biological Sciences, Goethe University Frankfurt, Frankfurt am Main, Germany

*Corresponding author
Mislav Oreb
Goethe University Frankfurt
Institute of Molecular Biosciences
Max-von-Laue Straße 9
60438 Frankfurt
Germany
Telephone +49 (0)69 798 29331
Telefax +49 (0)69 798 29527
E-Mail m.oreb@bio.uni-frankfurt.de

Supplementary Tables

Supplementary Table S1 | Synthetic genes used in this study.

Name of the gene	Sequence 5′-3′
Gal2 23KR	ATGGCAGTTGAGGAGAACAATATGCCTGTTGTTTCACAGCAACCCCAAGCTGGTGAAGACGTGATCTCTTCACTCAGTCGTGATTCCCATTTAAGCG CACAATCTCAAAGATATTCCAATGATGAATTGCGTGCCGGTGAGTCAGGGCCTGAAGGCTCCCAAAGTGTTCCTATAGAGATACCCAGAAGACCCAT GTCTGAATATGTTACCGTTTCCTTGCTTTGTTTGTGTGTTGCCTTCGGCGGCTTCATGTTTGGCTGGGATACCGGTACTATTTCTGGGTTTGTTGTC CAAACAGACTTTTTGAGAAGGTTTGGTATGAAACATAAGGATGGTACCCACTATTTGTCAAACGTCAGAACAGGTTTAATCGTCGCCATTTTCAATA TTGGCTGTGCCTTTGGTGGTATTATACTTTCCCGTGGTGGAGATATGTATGGCCGTCGTAGAGGTCTTTCGATTGTCGTCTCGGTTTATATAGTTGG TATTATCATTCAAATTGCCTCTATCAACAAGTGGTACCAATATTTCATTGGTAGAATCATATCTGGTTTGGGTGTCGGCGGCATCGCCGTCTTATGT CCTATGTTGATCTCTGAAATTGCTCCAAGACACTTGAGAGGCACACTAGTTTCTTGTTATCAGCTGATGATTACTGCAGGTATCTTTTTGGGCTACT GTACTAATTACGGTACAAAGAGCTATTCGAACTCAGTTCAATGGAGAGTTCCATTAGGGCTATGTTTCGCTTGGTCATTATTTATGATTGGCGCTTT GACGTTAGTTCCTGAATCCCCACGTTATTTATGTGAGGTGAATAGAGTAGAAGACGCCAGACTTTCCATTGCTAGATCTAACAGAGTGTCACCAGAG GATCCTGCCGTCCAGGCAGAGTTAGATCTGATCATGGCCGGTATAGAAGCTGAACGTCTGGCTGGCAATGCGTCCTGGGGGGAATTATTTTCCACCA GAACCCGTGTATTTCAACGTTTGTTGATGGGTGTATTTGTTCAAATGTTCCAACAATTAACCGGTAACAATTATTTTTTCTACTACGGTACCGTTAT TTTCAAGTCAGTTGGCCTGGATGATTCCTTTGAAACATCCATTGTCATTGGTGTAGTCAACTTTGCCTCCACTTTCTTTAGTTTGTGGACTGTCGAA AACTTGGGGCGTCGTCGTTGTTTACTTTTGGGCGCTGCCACTATGATGGCTTGTATGGTCATCTACGCCTCTGTTGGTGTTACCAGATTATATCCTC ACGGTAAAAGCCAGCCATCTTCTAAAGGTGCCGGTAACTGTATGATTGTCTTTACCTGTTTTTATATTTTCTGTTATGCCACAACCTGGGCGCCAGT TGCCTGGGTCATCACAGCAGAATCATTCCCACTGAGAGTCAGATCGCGTTGTATGGCGTTGGCCTCTGCTTCCAATTGGGTATGGGGGTTCTTGATT GCATTTTTCACCCCATTCATCACATCTGCCATTAACTTCTACTACGGTTATGTCTTCATGGGCTGTTTGGTTGCCATGTTTTTTTATGTCTTTTTCT TTGTTCCAGAAACTCGTGGCCTATCGTTAGAAGAAATTCAAGAATTATGGGAAGAAGGTGTTTTACCTTGGCGTTCTGAAGGCTGGATTCCTTCATC CAGAAGAGGTAATAATTACGATTTAGAGGATTTACAACATGACGACCGTCCGTGGTACAGAGCCATGCTAGAATAA
Gal2 30KR	ATGGCAGTTGAGGAGAACAATATGCCTGTTGTTTCACAGCAACCCCAAGCTGGTGAAGACGTGATCTCTTCACTCAGTCGTGATTCCCATTTAAGCG CACAATCTCAAAGATATTCCAATGATGAATTGCGTGCCGGTGAGTCAGGGCCTGAAGGCTCCCAAAGTGTTCCTATAGAGATACCCAGAAGACCCAT GTCTGAATATGTTACCGTTTCCTTGCTTTGTTTGTGTGTTGCCTTCGGCGGCTTCATGTTTGGCTGGGATACCGGTACTATTTCTGGGTTTGTTGTC CAAACAGACTTTTTGAGAAGGTTTGGTATGCGTCATAGAGATGGTACCCACTATTTGTCAAACGTCAGAACAGGTTTAATCGTCGCCATTTTCAATA TTGGCTGTGCCTTTGGTGGTATTATACTTTCCCGTGGTGGAGATATGTATGGCCGTCGTAGAGGTCTTTCGATTGTCGTCTCGGTTTATATAGTTGG TATTATCATTCAAATTGCCTCTATCAACAGATGGTACCAATATTTCATTGGTAGAATCATATCTGGTTTGGGTGTCGGCGGCATCGCCGTCTTATGT CCTATGTTGATCTCTGAAATTGCTCCAAGACACTTGAGAGGCACACTAGTTTCTTGTTATCAGCTGATGATTACTGCAGGTATCTTTTTGGGCTACT GTACTAATTACGGTACAAGAAGCTATTCGAACTCAGTTCAATGGAGAGTTCCATTAGGGCTATGTTTCGCTTGGTCATTATTTATGATTGGCGCTTT GACGTTAGTTCCTGAATCCCCACGTTATTTATGTGAGGTGAATAGAGTAGAAGACGCCAGACTTTCCATTGCTAGATCTAACAGAGTGTCACCAGAG GATCCTGCCGTCCAGGCAGAGTTAGATCTGATCATGGCCGGTATAGAAGCTGAACGTCTGGCTGGCAATGCGTCCTGGGGGGAATTATTTTCCACCA GAACCCGTGTATTTCAACGTTTGTTGATGGGTGTATTTGTTCAAATGTTCCAACAATTAACCGGTAACAATTATTTTTTCTACTACGGTACCGTTAT TTTCAGATCAGTTGGCCTGGATGATTCCTTTGAAACATCCATTGTCATTGGTGTAGTCAACTTTGCCTCCACTTTCTTTAGTTTGTGGACTGTCGAA AACTTGGGGCGTCGTCGTTGTTTACTTTTGGGCGCTGCCACTATGATGGCTTGTATGGTCATCTACGCCTCTGTTGGTGTTACCAGATTATATCCTC ACGGTCGTAGCCAGCCATCTTCTCGTGGTGCCGGTAACTGTATGATTGTCTTTACCTGTTTTTATATTTTCTGTTATGCCACAACCTGGGCGCCAGT TGCCTGGGTCATCACAGCAGAATCATTCCCACTGAGAGTCAGATCGCGTTGTATGGCGTTGGCCTCTGCTTCCAATTGGGTATGGGGGTTCTTGATT GCATTTTTCACCCCATTCATCACATCTGCCATTAACTTCTACTACGGTTATGTCTTCATGGGCTGTTTGGTTGCCATGTTTTTTTATGTCTTTTTCT TTGTTCCAGAAACTCGTGGCCTATCGTTAGAAGAAATTCAAGAATTATGGGAAGAAGGTGTTTTACCTTGGCGTTCTGAAGGCTGGATTCCTTCATC CAGAAGAGGTAATAATTACGATTTAGAGGATTTACAACATGACGACCGTCCGTGGTACAGAGCCATGCTAGAATAA
Gal2 25SA	ATGGCAGTTGAGGAGAACAATATGCCTGTTGTTGCACAGCAACCCCAAGCTGGTGAAGACGTGATCGCTGCACTCGCAAAAGATGCCCATTTAGCAG CACAAGCTCAAAAGTATGCCAATGATGAATTGAAAGCCGGTGAGGCAGGGCCTGAAGGCGCCCAAGCAGTTCCTATAGAGATACCCAAGAAGCCCAT GGCTGAATATGTTACCGTTTCCTTGCTTTGTTTGTGTGTTGCCTTCGGCGGCTTCATGTTTGGCTGGGATACCGGTACTATTTCTGGGTTTGTTGTC CAAACAGACTTTTTGAGAAGGTTTGGTATGAAACATAAGGATGGTACCCACTATTTGTCAAACGTCAGAACAGGTTTAATCGTCGCCATTTTCAATA TTGGCTGTGCCTTTGGTGGTATTATACTTTCCAAAGGTGGAGATATGTATGGCCGTAAAAAGGGTCTTTCGATTGTCGTCTCGGTTTATATAGTTGG TATTATCATTCAAATTGCCTCTATCAACAAGTGGTACCAATATTTCATTGGTAGAATCATATCTGGTTTGGGTGTCGGCGGCATCGCCGTCTTATGT CCTATGTTGATCGCTGAAATTGCTCCAAAGCACTTGAGAGGCACACTAGTTTCTTGTTATCAGCTGATGATTACTGCAGGTATCTTTTTGGGCTACT GTACTAATTACGGTACAAAGAGCTATTCGAACTCAGTTCAATGGAGAGTTCCATTAGGGCTATGTTTCGCTTGGTCATTATTTATGATTGGCGCTTT GACGTTAGTTCCTGAAGCCCCACGTTATTTATGTGAGGTGAATAAGGTAGAAGACGCCAAGCTTGCCATTGCTAAGGCTAACAAGGTGGCACCAGAG GATCCTGCCGTCCAGGCAGAGTTAGATCTGATCATGGCCGGTATAGAAGCTGAAAAACTGGCTGGCAATGCGGCCTGGGGGGAATTATTTGCCACCA AGACCAAAGTATTTCAACGTTTGTTGATGGGTGTATTTGTTCAAATGTTCCAACAATTAACCGGTAACAATTATTTTTTCTACTACGGTACCGTTAT TTTCAAGTCAGTTGGCCTGGATGATTCCTTTGAAACATCCATTGTCATTGGTGTAGTCAACTTTGCCTCCACTTTCTTTAGTTTGTGGACTGTCGAA AACTTGGGGCGTCGTAAATGTTTACTTTTGGGCGCTGCCACTATGATGGCTTGTATGGTCATCTACGCCTCTGTTGGTGTTACCAGATTATATCCTC ACGGTAAAAGCCAGCCATCTTCTAAAGGTGCCGGTAACTGTATGATTGTCTTTACCTGTTTTTATATTTTCTGTTATGCCACAACCTGGGCGCCAGT TGCCTGGGTCATCACAGCAGAAGCATTCCCACTGAGAGTCAAGGCGAAATGTATGGCGTTGGCCTCTGCTTCCAATTGGGTATGGGGGTTCTTGATT GCATTTTTCACCCCATTCATCACATCTGCCATTAACTTCTACTACGGTTATGTCTTCATGGGCTGTTTGGTTGCCATGTTTTTTTATGTCTTTTTCT TTGTTCCAGAAACTAAAGGCCTAGCGTTAGAAGAAATTCAAGAATTATGGGAAGAAGGTGTTTTACCTTGGAAAGCTGAAGGCTGGATTCCTGCAGC CAGAAGAGGTAATAATTACGATTTAGAGGATTTACAACATGACGACAAACCGTGGTACAAGGCCATGCTAGAATAA

Supplementary Table S2 | Primers used in this study.

Primer name	Application	Sequence 5'-3'
MOP 280	Forward primer for cloning GAL2_WT	AACACAAAAACAAAAAGTTTTTTTAATTTTAATCAAAAAATGGCAGTTGAGGAGAAC
MOP 281	Reverse primer for cloning GAL2_WT	GAATGTAAGCGTGACATAACTAATTACATGACTCGAGTTATTCTAGCATGGCCTTGTACC
SRp 0009	Forward primer for amplification of GFP ORF	ATGAGTAAAGGAGAAGAACTTTTCAC
SRp 0010	Reverse primer for amplification of GFP ORF	TTATTTGTATAGTTCATCCATGCCATGTG
SRp 0001	Forward primer for fusing GFP to GAL2	GGTACAAGGCCATGCTAGAAATGAGTAAAGGAGAAGAACTTTTCAC
SRp 0002	Reverse primer for fusing GFP to GAL2	AACTAATTACATGACTCGAGTTATTTGTATAGTTCATCCATGCCATG
MOP 282	Forward primer for cloning GAL2_Δ64	AACAAAAAGTTTTTTTAATTTTAATCAAAAAATGTCTGAATATGTTACCGTTTCC
SRp 0007	Reverse primer for cloning GAL2_Δ523	CGTGACATAACTAATTACATGACTCGAGTTAAGTTTCTGGAACAAAGAAAAAGAC
SRp 0048	Forward primer for cloning GAL2_Δ274-326	GTTATTTATGTGAGGTGAATGTATTTCAACGTTTGTTGATGGGTG
SRp 0049	Reverse primer for cloning GAL2_Δ274-326	ATCAACAAACGTTGAAATACATTCACCTCACATAAATAACGTG
MOP 270	Forward primer for cloning GAL2_3KR	GCGCACAATCTCAAAGATATTCCAATGATGAATTGAGAGCCGGTGAGTCAGGGCCTG
MOP 271	Reverse primer for cloning GAL2_3KR	ACGTGATCTCTTCACTCAGTAGAGATTCCCATTTAAGCGCACAATCTCAAAGATATTC
SRp 0052	Reverse primer for cloning GAL2_30KR and GAL2_23KR	AATGTAAGCGTGACATAACTAATTACATGACTCGAGTTATTCTAGCATGGCTCTGTACC
SRp 0013	Forward primer for fusing GFP to GAL2_Δ523	TTTTCTTTGTTCCAGAAACTATGAGTAAAGGAGAAGAACTTTTCAC
SRp 0053	Reverse primer for fusing GFP to GAL2_30KR	GTGAAAAGTTCTTCTCCTTTACTCATTTCTAGCATGGCTCTGTACC
SRp 0060	Reverse primer for deletion of ROD1 with CRISPR Cas9 (gRNA)	AAGCAGCCCGACTTGATCTGGATCATTTATCTTTCACTGCGGAG
SRp 0061	Forward primer for deletion of ROD1 with CRISPR Cas9 (gRNA)	CAGATCAAGTCGGGCTGCTTGTTTTAGAGCTAGAAATAGCAAGTTAAAATAAGG
SRp 0062	Donor DNA for repairing ROD1 locus (forward strand)	TTTCATCACACCATTCGCTTCTCTTCCTCCATAAGTAATAACTGCTTTATTTTTTGTCTTCGAAATTTCGACAAAAAGAT
SRp 0063	Donor DNA for repairing ROD1 locus (reverse strand)	ATCTTTTTGTCGAAATTTCGAAGACAAAAAATAAAGCAGTTATTACTTATGGAGGAAGAGAAGCGAATGGTGTGATGAAA
SRp 0069	Reverse primer for verification of ROD1 deletion	CCGAGTAAGACCACTTAACAAAATCTATGAGAAG
SRp 0070	Forward primer for verification of ROD1 deletion	GTTTTAATGCGGATGAATGTCTAACCCCAG
SRp 0127	Forward primer for deletion of BUL1 with CRISPR Cas9 (gRNA)	AATAGCACTGGGGTCCGGTGGTTTTAGAGCTAGAAATAGCAAGTTAAAATAAGG
SRp 0128	Reverse primer for: For deletion of BUL1 with CRISPR Cas9 (gRNA)	CCACCGGACCCCAGTGCTATTGATCATTTATCTTTCACTGCGGAG

SRp 0129	Donor DNA for repairing BUL1 locus (forward strand)	GGAAAGAAGCTCTTAGCAAGGGCGAAAAGAGAC TGTTCGTGTGTGTGTCAACAGGTATATTGTACG CTAAAAAAACATTAGAAAAAATTCTCGTTACTT TTCTTATAGATATAGATATATGTATGGTTTGCG TATAGATG
SRp 0130	Donor DNA for repairing BUL1 locus (reverse strand)	CATCTATACGCAAACCATACATATATCTATATC TATAAGAAAAGTAACGAGAATTTTTTCTAATGT TTTTTTAGCGTACAATATACCTGTTGACACACA CACGAACAGTCTCTTTTCGCCCTTGCTAAGAGCT TCTTTCC
SRp 0121	Forward primer for verification of BUL1 deletion	TGCTAGTATGATTCGGTGTC
SRp 0122	Reverse primer for verification of BUL1 deletion	TGACAAAGAAAATTCTATGTTTTG
SRp 0264	Forward primer for cloning of GAL2_6SA	GCAGCACAAGCTCAAAAGTATG
SRp 0265	Reverse primer for cloning GAL2_6SA	ATCATTGGCATACTTTTGAGCTTGTGCTGCTAA ATGGGAATCTTTACTGAGTGAAGAG
SRp 0178	Forward primer for cloning GAL2_11SA	GAAACGGTAACATATTCAGACATGGGCTTCTTG GGTATCTCTATAG
SRp 0179	Reverse primer for cloning GAL2_11SA	AGATACCCAAGAAGCCCATGTCTGAATATGTTA CCGTTTCCTTGC
MOP 279	Forward primer for cloning GAL2_S32A	GTAAAGATTCCCATTTAGCTGCACAATCTCAAA AGTATTCCAATGATG
MOP 278	Reverse primer for cloning GAL2_S32A	CATCATTGGAATACTTTTGAGATTGTGCAGATA AATGGGAATCTTTAC
PJ07	Forward primer for cloning HXT11_WT	AAAAACAAAAAGTTTTTTTAATTTTAATCAAAA AATGTCAGGTGTTAATAATACATCC
PJ08	Reverse primer for cloning HXT11_WT	GAATGTAAGCGTGACATAACTAATTACATGACT CGAGTCAGCTGGAAAAGAACCTC
SRp 0003	Forward primer for fusing GFP to HXT11	TTTACAAGAGGTTCTTTTCCAGCATGAGTAAAG GAGAAGAACTTTTCAC
SRp 0004	Reverse primer for fusing GFP to HXT11	TGACATAACTAATTACATGACTCGAGTTATTTG TATAGTTCATCCATGCCATGTG
SRp 0266	Reverse primer for cloning the chimera GAL2_6SA_Δ38-Hxt11	AATAGGTGGCTCATTGGCATCTAGGTTAAGTGC TTGGGCGCCTTC
SRp 0267	Forward primer for cloning Δ38-Hxt11	CACAAAAACAAAAAGTTTTTTTAATTTTAATCA AAAAATGCTTAACCTAGATGCCAATGAG
SRp 0268	Forward primer for cloning Δ38-Hxt11	CACAAAAACAAAAAGTTTTTTTAATTTTAATCA AAAAATGGTTCCTATAGAGATACCCAAG
SRp 0273	Forward primer for cloning the chimera GAL2_WT/3KR_Δ38-Hxt11	GTTCCTATAGAGATACCCAAGAAGC
SRp 0274	Reverse primer for cloning the chimera GAL2_WT/3KR_Δ38-Hxt11	CATGGGCTTCTTGGGTATCTCTATAGGAACGGA ATTTTTAGAGTCACCGTG

Supplementary Table S3 | Plasmids used in this study.

The standard nomenclature is used for the relevant genetic elements. Promotors and terminators are denoted with the suffixes "p" and "t", respectively.

Plasmid names	Relevant properties	Reference
p426H7	2µ, *URA3*, AmpR, *HXT7p*$^{-1--392}$, *CYC1t*	Hamacher et al., 2002
pUCP1	*CEN6/ARS4*, *URA3*, AmpR, *HXT7p*$^{-1--392}$, *CYC1t*	(this study)
pRCC-K	2µ-plasmid; *kanMX4* marker, employed for the CRISPR/Cas9 deletions; *ROX3p-cas9-CYC1t; SNR52p-gRNA-SUP4t*	Generoso et al., 2016
pRCC-N	As pRCC-K, but with the natMX resistance marker	Generoso et al., 2016
SRB021	*pRCC-N with a protospacer targeting ROD1*	(this study)
SRB043	*pRCC-K with a protospacer targeting BUL1*	(this study)
MOB92	*p426H7 GAL2 wildtype*	(this study)
SRB000	*p426H7 GAL2 wildtype GFP*	(this study)
SRB105	*pUCP1 GAL2 wildtype*	(this study)
SRB077	*pUCP1 GAL2 wildtype GFP*	(this study)
MOB95	*p426H7 GAL2 Δ64*	(this study)
SRB004	*p426H7 GAL2 Δ64 GFP*	(this study)
SRB067	*p426H7 GAL2 Δ273-326*	(this study)
SRB007	*p426H7 GAL2 Δ273-326 GFP*	(this study)
SRB012	*p426H7 GAL2 Δ523*	(this study)
SRB005	*p426H7 GAL2 Δ523 GFP*	(this study)
MOB93	*p426H7 GAL2 3KR*	(this study)
SRB001	*p426H7 GAL2 3KR GFP*	(this study)
SRB106	*pUCP1 GAL2 3KR*	(this study)
SRB078	*pUCP1 GAL2 3KR GFP*	(this study)
SRB016	*p426H7 GAL2 23KR*	(this study)
SRB015	*p426H7 GAL2 23KR GFP*	(this study)
SRB017	*p426H7 GAL2 30KR*	(this study)
SRB018	*p426H7 GAL2 30KR GFP*	(this study)
SRB107	*pUCP1 GAL2 6SA*	(this study)
SRB098	*pUCP1 GAL2 6SA GFP*	(this study)
SRB083	*pUCP1 GAL2 11SA N term GFP*	(this study)
MOB94	*p426H7 GAL2 S32A*	(this study)
SRB202	*pUCP1 GAL2 S32A GFP*	(this study)
SRB071	*p426H7 GAL2 _25SA GFP*	(this study)
SRB117	*pUCP1 HXT11 Δ38 GFP*	(this study)
SRB089	*pUCP1 HXT11 wildtype GFP*	(this study)
SRB094	*pUCP1 GAL2 wildtype /HXT11 GFP*	(this study)
SRB095	*pUCP1 GAL2 3KR/HXT11 GFP*	(this study)
SRB104	*pUCP1 GAL2 6SA/HXT11 GFP*	(this study)

Suplementary Table S4 | Localization and ubiquitination probability of lysine residues in Gal2. The topology of the protein was predicted based on the primary sequence or on the structure homology model using the online tools Philius (Reynolds *et al.*, 2008) or PPM server (Lomize *et al.*, 2012), respectively. The nomenclature for the localization is as follows: NT, N-terminal tail; CT, C-terminal tail; L#, consequtively numbered loops connecting transmembrane domains; the prefixes "c" and "e" denote cytosolic and extracellular exposition, respectively. NT and CT are not resolved in the homology model. For individual constructs, a lysine to arginine mutation is indicated by an "R" at the respective position. For truncated constructs, the range of deleted amino acids is indicated following the prefix "Δ" in the construct name and the absence of lysines is denoted by a "d" in the residue list.

Lysine residue position	Localization (Philius)	Localization (model/PPM)	Ubiquitination probability score (UbPred)	Construct name					
				3KR	23KR	30KR	Δ64	Δ523	Δ274-326
27	cNT	not resolved	high	R	R	R	d		
37	cNT	not resolved	high	R	R	R	d		
44	cNT	not resolved	high	R	R	R	d		
62	cNT	not resolved	low		R	R	d		
63	cNT	not resolved	-		R	R	d		
108	eL1	eL1	-			R			
110	eL1	eL1	-			R			
141	cL2	TM1/ cL2	-		R	R			
149	cL2	TM1/ cL2	-		R	R			
150	cL2	TM1/ cL2	-		R	R			
172	eL3	eL3	-			R			
204	cL4	cL4	-		R	R			
233	eL5	eL5	-			R			
274	cL6	cL6	-		R	R			d
279	cL6	cL6	-		R	R			d
284	cL6	cL6	-		R	R			d
287	cL6	cL6	-		R	R			d
310	cL6	cL6	low		R	R			d
324	cL6	cL6	-		R	R			d
326	cL6	cL6	-		R	R			d
358	eL7	eL7	-			R			
394	cL8	cL8/TM9	-		R	R			
423	eL9	eL9	-			R			
429	eL9	eL9	low			R			
467	cL10	cL10	-		R	R			
469	cL10	cL10	-		R	R			
523	cCT	not resolved	-		R	R		d	
542	cCT	not resolved	-		R	R		d	
566	cCT	not resolved	medium		R	R		d	
570	cCT	not resolved	medium		R	R		d	

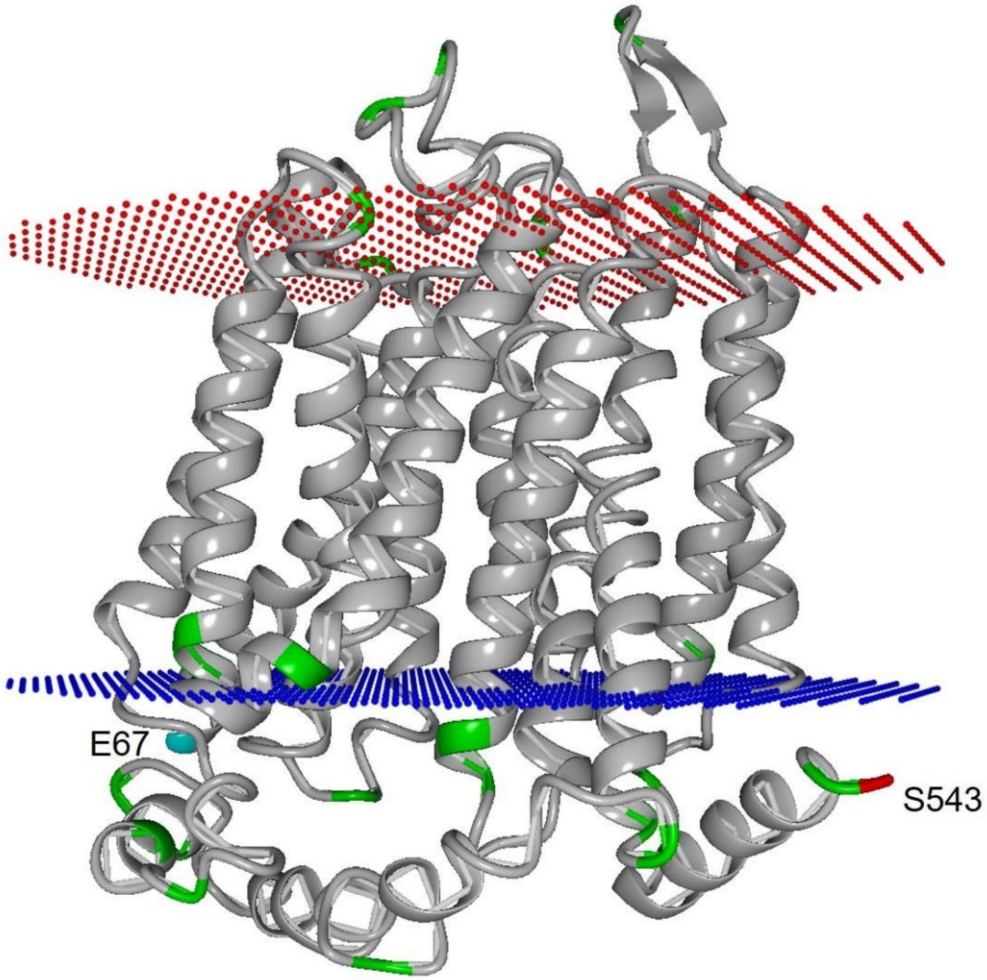

Supplementary Figure S5 | Localization of lysine residues in the Gal2 homology model. The Gal2 homology model (Thomik et al. 2017), shown in ribbon presentation, was used for topology prediction using the PPM server (Lomize et al. 2012). The extracellular and intracellular membrane interfaces are shown as red and blue dots, respectively. The N- and C-terminal tails are not resolved in the model. The first/last resolved N- and C-terminal residues are E67 (cyan) and S543 (red). All lysine residues are shown in green.

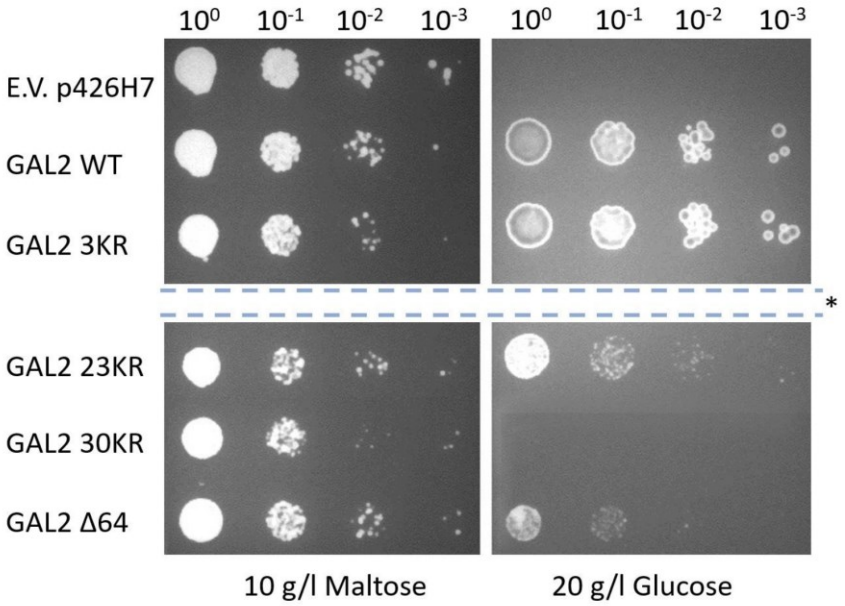

Supplementary Figure S6 | Complementation analysis of the EBY.VW4000 strain with different Gal2-constructs. The strain was transformed with 2µ plasmids expressing the indicated Gal2 variants. The transformants were pre-grown in liquid selective SC medium with maltose as a permissive carbon source. Serial dilutions of washed cells were dropped on solid SC media with the indicated carbon sources. Cells were grown at 30°C for 3 days. **All transformants were cultivated on one agar plate (either maltose or glucose containing). Note that non-relevant transformants were cut from the image for clarity.*

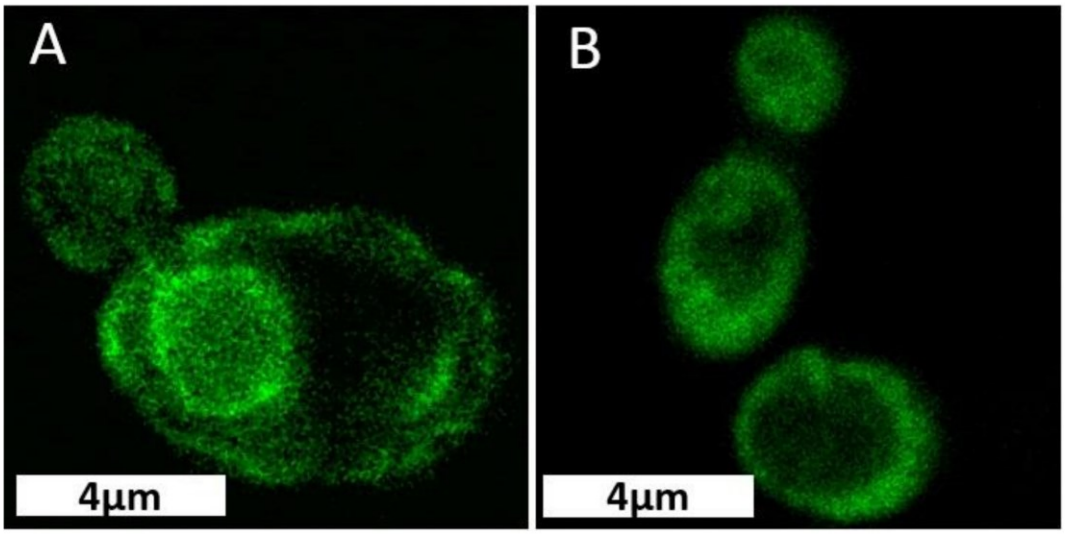

Supplementary Figure S7: Mapping the lysines targeted by ubiquitination. Representative confocal images of CEN.PK2-1C cells expressing GFP-tagged Gal2_Δ523 (A) and Gal2_Δ274-326 (B) from multicopy plasmids. The cells were grown in SC media with 2% galactose. Scale bar represents 4 µm.

Supplementary Information - References

Generoso WC, Gottardi M, Oreb M *et al.* Simplified CRISPR-Cas genome editing for Saccharomyces cerevisiae. *J Microbiol Methods* 2016;**127**:203–5.

Hamacher T, Becker J, Gárdonyi M *et al.* Characterization of the xylose-transporting properties of yeast hexose transporters and their influence on xylose utilization. *Microbiology* 2002;**148**:2783–8.

Lomize MA, Pogozheva ID, Joo H *et al.* OPM database and PPM web server: Resources for positioning of proteins in membranes. *Nucleic Acids Res* 2012;**40**:370–6.

Reynolds SM, Käll L, Riffle ME *et al.* Transmembrane topology and signal peptide prediction using dynamic Bayesian networks. *PLoS Comput Biol* 2008;**4**, DOI: 10.1371/journal.pcbi.1000213.

Thomik T, Wittig I, Choe J *et al.* An artificial transport metabolon facilitates improved substrate utilization in yeast. *Nat Chem Biol* 2017;**13**, DOI: 10.1038/nchembio.2457.

6.2 Identification of a glucose-insensitive variant of Gal2 from *Saccharomyces cerevisiae* exhibiting a high pentose transport capacity

Declaration of author contributions to the publication:
Identification of a glucose-insensitive variant of Gal2 from *Saccharomyces cerevisiae* exhibiting a high pentose transport capacity

Status: Published, December 2021
Journal: Scientific Reports
Type of publication: research article
Contributing authors: Sebastian A. Tamayo Rojas (SR), Virginia Schadeweg (VS), Ferdinand Kirchner (FK), Eckhard Boles (EB), Mislav Oreb (MO)

Contributions of doctoral candidate and co-authors
(1) Concept and design
Doctoral candidate SR: 55%
Co-authors VS, EB, MO: 5%, 20%, 20%
(2) Conducting tests and experiments
Doctoral candidate SR: 75%, yeast molecular biology, fluorescence microscopy, growth-based assays, and fermentations
Co-authors VS, FK: 15%, 10% fermentation and radiolabeled sugar uptake assay
(3) Compilation of data sets and figures
Doctoral candidate SR: 75%, microscopy micrographs, metabolite titers and growth-based assays
Co-authors VS, FK: 15%, 10% metabolite titers, kinetics
(4) Analysis and interpretation of data
Doctoral candidate SR: 70%, microscopy micrographs, metabolite titers and growth-based analysis
EB, MO: 10 %, 20%, supervision and advice
(5) Drafting of manuscript
Doctoral candidate SR: 50%
Co-authors EB, MO: 5%, 45%

www.nature.com/scientificreports

scientific reports

Check for updates

OPEN

Identification of a glucose-insensitive variant of Gal2 from *Saccharomyces cerevisiae* exhibiting a high pentose transport capacity

Sebastian A. Tamayo Rojas, Virginia Schadeweg, Ferdinand Kirchner, Eckhard Boles & Mislav Oreb

As abundant carbohydrates in renewable feedstocks, such as pectin-rich and lignocellulosic hydrolysates, the pentoses arabinose and xylose are regarded as important substrates for production of biofuels and chemicals by engineered microbial hosts. Their efficient transport across the cellular membrane is a prerequisite for economically viable fermentation processes. Thus, there is a need for transporter variants exhibiting a high transport rate of pentoses, especially in the presence of glucose, another major constituent of biomass-based feedstocks. Here, we describe a variant of the galactose permease Gal2 from *Saccharomyces cerevisiae* (Gal2$^{N376Y/M435I}$), which is fully insensitive to competitive inhibition by glucose, but, at the same time, exhibits an improved transport capacity for xylose compared to the wildtype protein. Due to this unique property, it significantly reduces the fermentation time of a diploid industrial yeast strain engineered for efficient xylose consumption in mixed glucose/xylose media. When the N376Y/M435I mutations are introduced into a Gal2 variant resistant to glucose-induced degradation, the time necessary for the complete consumption of xylose is reduced by approximately 40%. Moreover, Gal2$^{N376Y/M435I}$ confers improved growth of engineered yeast on arabinose. Therefore, it is a valuable addition to the toolbox necessary for valorization of complex carbohydrate mixtures.

Economic viability of the fermentative production of biofuels and other valuable chemicals from plant biomass, such as lignocellulosic[1] and pectin-rich[2] residual material, is dependent on the ability of engineered microbial cell factories to efficiently utilize all carbohydrates present in it. Besides glucose, these feedstocks contain large fractions of the pentoses xylose and/or arabinose in varying proportions depending on the biomass type. *Saccharomyces cerevisiae*, one of the most popular organisms in industrial biotechnology, is a very efficient glucose consumer, but does not have the ability to metabolize xylose and arabinose naturally. Therefore, extensive research has been devoted to expand its substrate portfolio accordingly. Overexpression of heterologous xylose isomerases (XI) proved as the most direct way to funnel xylose into the endogenous metabolism. XI converts xylose to xylulose, which can be phosphorylated by the endogenous xylulokinase, Xks1, to yield xylulose-5-P (Xu5P), an intermediate of the non-oxidative branch of the pentose phosphate pathway (noxPPP). For the conversion of arabinose to Xu5P, three bacterial enzymes must be expressed, namely L-arabinose isomerase, L-ribulokinase and L-ribulose-5-P 4-epimerase[3–5]. To improve the subsequent metabolism of Xu5P, overexpression of the noxPPP enzymes (ribose-5-phosphate ketol-isomerase, Rki; D-ribulose-5-phosphate 3-epimerase, Rpe; transketolase, Tkl; transaldolase, Tal) is necessary[6]. A combination of rational metabolic engineering and adaptive laboratory evolution approaches have resulted in great progresses in the last decade, bringing the pentose fermentation technology to the industrial scale[7,8].

Despite these advances, the simultaneous fermentation of pentoses and glucose is still regarded as one of the major limitations of the fermentation performance[9]. Especially the ability of sugar transporters to take up pentoses in the presence of glucose is an important prerequisite for complete and time-efficient valorization of mixed-sugar substrates[9,10]. Although many endogenous[11,12] and heterologously expressed[13] transporters are able

Institute of Molecular Biosciences, Faculty of Biological Sciences, Goethe University, Max-von-Laue Straße 9, 60438 Frankfurt, Germany. email: e.boles@bio.uni-frankfurt.de; m.oreb@bio.uni-frankfurt.de

Strain name	Relevant genotype	References
CEN.PK2-1C	*leu2-3,112 ura3-52 trp1-289 his3Δ1 MAL2-8c SUC2*	Euroscarf
EBY.VW4000	**CEN.PK2-1C** *Δhxt1-17 gal2Δ::loxP stl1Δ::loxP agt1Δ::loxP mph2Δ::loxP mph3Δ::loxP*	Ref.[16]
AFY10	**EBY.VW4000** *glk1Δ::loxP hxk1Δ::loxP hxk2Δ::loxP ylr446wΔ::loxP* [*pyk2Δ::PGK1p-opt.XKS1-PGK1t TPI1p-TAL1-TAL1t TDH3p-TKL1-TKL1t PFK1p-RPE1-RPE1t FBAp-RKI1-RKI1t kanMX*]	Ref.[17]
AFY10X	**AFY10** with YEp181-kanR_optXI plasmid	Ref.[17]
SRY027	**Ethanol Red** (diploid) *MATα/MATa*; 2 × [*pyk2Δ::PGI1p-araA-PGI1t, PYK1p-araD-PYK1t, PGM2p-araB-PGM2t, PFK2p-ARAT-PFK2t, PMA1p-NQM1-ZWF1t, ADH1p-TKL2-PDC1t, loxP, GPM1p-HXT7-HXT7t, FBA1p-RKI1-RKI1t, PFK1p-RPE1-RPE1t, TDH3p-TKL1-TKL1t, TPI1p-TAL1-TAL1t, PGK1p-XKS1-PGK1t, HXT7p$^{1-392}$-xylA-CYC1t*]; 2 × [*HXT7p$^{1-392}$-xylA-CYC1t, PGM2p-araB-PGM2t, PYK1p-araD-PYK1t, PGI1p-araA-PGI1t, GAL2p::FBA1p-GAL2$^{\Delta 70-1655}$-GAL2t*]; 2 × [*HXT7p$^{1-392}$-xylA-CYC1t, PYK1p-HXT9-HXT9t, PGI1p-araA-PGI1t, HXT2p::pENO2-HXT2*]	This study

Table 1. Strains used in this study. The genotypes are annotated according to the standard nomenclature. Promoters and terminators are denoted by suffixes "p" and "t", respectively. Overexpressed ORFs resulting in functional proteins are underlined. The integrated genetic cassettes are shown in brackets. The occurrence of two identical alleles in a diploid genome is indicated by "2×". Gene deletions are indicated by a "Δ", followed by the range of deleted amino acids, where appropriate. Parental strains are indicated in bold under "relevant genotype".

to take up pentoses in *S. cerevisiae*, all of them are naturally sensitive to competitive inhibition by glucose[14]. For instance, the endogenous galactose permease Gal2, which is particularly attractive due to its ability to transport both arabinose[3] and xylose[11], is strongly inhibited in the presence of glucose[15]. To solve this problem, several groups have successfully employed different strategies. In our previous work, we designed a screening system, based on the hexose transporter deficient strain EBY.VW4000[16], in which all genes encoding enzymes with hexokinase (Hxk) activity have additionally been deleted. Furthermore, in this strain background, *XKS1*, the noxPPP genes *RKI1*, *RPE1*, *TAL1* and *TKL1* and a heterologous XI have been overexpressed to enable the utilization of xylose[17]. The resulting strain (AFY10X) was suitable for screening of mutant transporter variants able to transport xylose in the presence of glucose. Thereby, a single mutation of a conserved asparagine residue located in the transmembrane domain 8 (TM8) of Hxt5, Hxt7 and Gal2 was found to be crucial to alleviate the binding of glucose as a competitor[17]. Similar observations regarding the role of the conserved asparagine have also been made in further studies[18–22] with different transporters and several mutant glucose-insensitive transporters are now available. As a rule, however, this beneficial property came at the expense of a reduced transport capacity (reflected by the kinetic parameter called maximal velocity, v_{max}). The corresponding values are systematically compared in a recent review article[10]. For instance, the v_{max} for xylose transport of glucose-insensitive Gal2 variants N376F and N376V described in our previous study[17] was approximately threefold reduced compared to the wildtype protein. In fermentations, this causes a lower net xylose consumption rate and, consequently, prolonged fermentation times. Therefore, in this study, we used the AFY10X screening platform and performed additional rounds of random mutagenesis by error-prone PCR to select novel Gal2 variants that combine glucose-insensitivity with an improved transport capacity.

Materials and methods

Construction and cultivation of yeast strains. The construction of the strains EBY.VW4000[16] and AFY10[17] was previously reported. The strain SRY027 is a derivative of the previously described HDY.GUF12[23,24]. In brief, HDY.GUF12 contains genetic cassettes for overexpression of heterologous genes necessary for the utilization of xylose (codon-optimized gene for xylose isomerase XylA from *Clostridium phytofermentans*) and arabinose (codon-optimized genes for the arabinose transporter AraT from *Scheffersomyces stipitis*, arabinose isomerase AraA from *Bacillus licheniformis*, ribulokinase AraB and ribulose-5-P 4-epimerase AraD, both from *Escherichia coli*). In addition to these heterologous genes, the open reading frames (ORFs) encoding the endogenous xylulokinase Xks1, transaldolases Tal1 and Nqm1, transketolases Tkl1 and Tkl2, Ribose-5-phosphate ketol-isomerase Rki1, D-ribulose-5-phosphate 3-epimerase Rpe1 and the sugar transporters Gal2, Hxt2, Hxt7 and Hxt9 were placed under the control of strong constitutive promoters. To construct SRY027 as a fast pentose utilizing strain for testing engineered transporters without the interference with genomic copies of Gal2, all *GAL2* alleles in HDY.GUF12 were deleted using the CRISPR technology[25]. The genotypes of all strains are listed in Table1.

For the preparation of competent cells, plasmid-free cells were grown in standard YEP-media (1% (w/v) yeast extract, 2% (w/v) peptone) supplemented with 1% (w/v) maltose (M) for EBY.VW4000, 2% (v/v) ethanol (E) for AFY10 and 2% (w/v) of glucose (D) for SRY027. Frozen competent cells were prepared and transformed according to the established protocol[26]. The transformants of auxotrophic strains were initially plated on solid, selective synthetic complete (SC) medium with 1% (w/v) maltose (EBY.VW4000) or 2% (v/v) ethanol (AFY10), in which uracil (-Ura), leucine (-Leu), histidine (-His) and tryptophan (-Trp) were omitted as required depending on the plasmid selection markers. Amino acids were added as previously described[27]. SRY027 was plated on YEPD medium supplemented with 100 µg mL^{-1} ClonNAT (Nourseothricin) or 200 µg mL^{-1} G418 (Geneticin) for the selection of the *natNT2* and *kanMX* markers, respectively.

Plasmid name	Relevant properties	References
YEp181-kanR_optXI	2µ, *LEU2*, codon-optimized xylose isomerase gene *xylA* of *C. phytofermentans* under control of *HXT7p*$^{1\text{-}392}$ and *CYC1t*, Ampicillin marker	Ref.[15]
p426H7	2µ, *URA3*, *HXT7p*$^{1\text{-}392}$, *CYC1t*, Ampicillin marker, pBR322-origin	Ref.[11]
p426H7_GAL2_WT	ORF of GAL2 in p426H7	Ref.[17]
p426H7_GAL2_ep3.1	ORF of GAL2-M107K/V239L/N376Y/M435I/L558S in p426H7	This study
p426H7_GAL2-N376Y	ORF of GAL2-N376Y in p426H7	Ref.[17]
p426H7_GAL2-N376Y/M107K	ORF of GAL2-N376Y/M107K in p426H7	This study
p426H7_GAL2-N376Y/V239L	ORF of GAL2-N376Y/V239L in p426H7	This study
p426H7_GAL2-N376Y/M435I	ORF of GAL2-N376Y/M435I in p426H7	This study
p426H7_GAL2-N376Y/M558S	ORF of GAL2-N376Y/M558S in p426H7	This study
p426H7_GAL2-M435I	ORF of GAL2-M435I in p426H7	This study
p426H7_GAL2-N376F	ORF of GAL2-N376F in p426H7	Ref.[17]
p426H7_GAL2-N376F/M435I	ORF of GAL2-N376F/M435I in p426H7	This study
pRS62N	2µ, *natNT2*; *HXT7p*$^{1\text{-}392}$, *CYC1t*, Ampicillin marker, pBR322-origin	Ref.[17]
pRS62N_Gal2_WT	ORF of GAL2 in pRS62N	Ref.[17]
pRS62N_Gal2_N376F	ORF of GAL2-N376F in pRS62N	Ref.[17]
pRS62N_Gal2_N376F/M435I	ORF of GAL2-N376F/M435I in pRS62N	This study
pRS62N_Gal2_N376Y/M435I	ORF of GAL2-N376Y/M435I in pRS62N	This study
pRS62N_Gal2_6SA/N376Y/M435I	ORF of Gal2_6SA/N376Y/M435I in pRS62N	This study
pRS62N_Gal2_6SA	ORF of Gal2_6SA in pRS62N	This study
pRCC-K	2µ, *kanMX4* marker, employed for the CRISPR/Cas9 deletions; *ROX3p*-cas9-*CYC1t*; *SNR52p-gRNA-SUP4t*	Ref.[25]
pRCC-K_GAL2	pRCC-K with a protospacer targeting *GAL2*	This study
YEparaAsynth	2µ, *HIS3*, codon-optimized *araA* gene from*Bacillus licheniformis*, expressed under control of *HXT7p*$^{1\text{—}392}$ and CYC1t, Ampicillin marker, pBR322-origin	Ref.[5]
YEparaBsynth	2µ, *TRP1*, codon-optimized *E. coli* araB, expressed under control of *HXT7p*$^{1\text{-}392}$ and *CYC1t*, Ampicillin marker, pBR322-origin	Ref.[5]
YEparaDsynth	2µ, *LEU2*, codon-optimized *E. coli araD*, expressed under control of *HXT7p*$^{1\text{-}392}$ and *CYC1t*, Ampicillin marker, pBR322-origin	Ref.[5]
pUCP1	*CEN6/ARS4*, *URA3*, Ampicillin marker, *HXT7p*$^{1\text{-}392}$, *CYC1t*	Ref.[28]
pUCP1 GAL2$^{N376Y/M435I}$-GFP	pUCP1 *GAL2*^{N376}*Y/M435I-GFP* under control of *HXT7p*$^{1\text{-}392}$ and *CYC1t*	This study
pUCP1 GAL2$^{6SA/N376Y/M435I}$-GFP	pUCP1 *GAL2*$^{6SA/N376Y/M435I}$*-GFP* under control of *HXT7p*$^{1\text{-}392}$ and *CYC1t*	This study

Table 2. Plasmids used in this study. Under "relevant properties", promoters and terminators are denoted by suffixes "p" and "t", respectively; ORF, open reading frame.

Plasmid construction and mutagenesis approaches. The DNA sequence of the *GAL2* ORF that was used for plasmid construction and mutagenesis approaches corresponds to CEN.PK2-1C variant. For error-prone PCR (epPCR), the GeneMorph II Random Mutagenesis Kit (Agilent Technologies) was used as previously described[17]. Briefly, the mutagenesis reaction was performed with the primer pair Amp_GAL2_F/R using the p426H7_GAL2 plasmid as template. The epPCR fragments were purified by extraction from agarose gels (NucleoSpin Extract II; Macherey–Nagel) and subjected to a non-mutagenic second round of PCR using the Phusion polymerase (New England Biolabs GmbH) with the primer pair Clon_GAL2_F/R to add overhangs for homologous recombination with the p426H7 vector. AFY10X was transformed with the linearized p426H7 vector and the epPCR products and plated onto selective SCE plates. After colonies appeared, they were replica-plated to plates with various xylose–glucose concentrations (2 + 10, 2 + 20, 10 + 30, and 10 + 50 g L^{-1}) and screened for the fastest growing clones. Site directed mutagenesis was performed using mutagenic primers listed in Supplementary Table 1 and the Phusion polymerase. Green fluorescent protein (GFP) was fused to the C-terminus of Gal2 variants as described previously[28]. Plasmids were isolated from yeast by the standard alkaline lysis protocol and electroporated into *E. coli* strain DH10B for amplification. Plasmid isolation from overnight *E. coli* cultures was carried out using a GeneJET Plasmid Miniprep Kit (Thermo Scientific) according to the manufacturer's instructions and sequenced. The plasmids used in this study are listed in Table 2.

Fermentation experiments and HPLC analysis. Cells were inoculated into selective media as indicated in the Results. Fermentations were performed in 300 mL shake flasks containing 50 mL of the culture medium. The cultures were cultivated at 30 °C with agitation at 180 rpm. For HPLC analysis, 450 µL of the culture supernatant were mixed with 50 µL 50% (w/v) 5-sulfosalicylic acid and centrifuged (16,000 g, 5 min, 4 °C). From this supernatant, 10 µL were subjected to high performance liquid chromatography (Dionex Ultimate 3000, Thermo Scientific) equipped with the ion exchange column HyperREZ XP Carbohydrate H^+ (7.7 × 300 mm; Thermo Scientific) and a refractive index detector. The liquid phase was 5 mM sulfuric acid, run at 0.6 ml min^{-1} and 65 °C. The Chromeleon 6.8 software was employed for quantifications and Prism 9 (GraphPad) for statistical analysis and presentation of the results.

Radiolabeled xylose uptake assay. The uptake assay with radiolabeled xylose was performed according to the published protocol[29]. In brief, EBY.VW4000 yeast cells expressing the indicated Gal2 variants were grown overnight at 30 °C and 180 rpm in SCM-Ura medium. The next day, cells were harvested by centrifugation (4000 g, 5 min, 20 °C). The pellets were washed twice in ice-cold 0.1 M potassium phosphate buffer (pH 6.5), weighed, and resuspended in 0.1 M potassium phosphate buffer to a wet-weight concentration of 60 mg ml^{-1}. Aliquots of 110 µl were prepared and cooled on ice. The residual cell suspension was centrifuged (4,000 g, 5 min, 4 °C) and the pellet was stored at − 80 °C before it was freeze-dried for cell dry weight determination. D-[1-^{14}C] xylose (55 mCi $mmol^{-1}$) was obtained from American Radiolabeled Chemicals Inc. (St. Louis, MO) and diluted with unlabeled sugar to approximately 8 nCi $mmol^{-1}$ and a total xylose concentration of 1500 mM (3 × concentration of that needed in the final uptake mixture). The cell suspension aliquots and the sugar solution were pre-warmed at 30 °C for 5 min. The uptake reaction was started by mixing 100 µl of the cell suspension and 50 µl of the 3 × sugar solution (yielding 500 mM total xylose in the uptake assay). The mixture was incubated for 20 s at 30 °C. The uptake was terminated by pipetting 100 µl of the assay mixture into 10 ml of ice-cold uptake buffer containing 500 mM xylose (quenching buffer). The suspension was filtered through a PVDF membrane filter, 0.22 µM pore size, 47 mm diameter (Durapore, Merck), which was subsequently washed two times with 10 ml of ice-cold quenching buffer. The amount of the radiolabeled sugar was measured in a 10 min window using the Wallac 1409 Liquid Scintillation Counter (Perkin Elmer). The proportion of the intracellular sugar was calculated as a ratio of the counts on the filter (corrected for background binding) to total counts in the uptake mixture. The transport rate (nmol min^{-1}) was calculated and normalized to the dry cell weight.

Fluorescence microscopy. For fluorescence microscopy, CEN.PK2–1C cells expressing the GFP-tagged constructs were cultivated overnight in 50 mL filter-sterilized, low fluorescent SC medium with 3% (w/v) glucose and 1% (w/v) xylose lacking uracil (lf-SC-Ura), containing 6.9 g/L yeast nitrogen base with ammonium sulfate, without amino acids, without folic acid and without riboflavin (MP Biomedicals, Santa Ana, CA). Subsequently, the cells were washed twice with sterile water and re-suspended in 50 mL of fresh medium to an OD_{600} between 1.5 and 3. From these cultures, after 4 h of cultivation at 30 °C with shaking (180 rpm), an aliquot of each one was mixed separately with 500 µL of medium containing 1.2% (w/v) low melting agarose (Roth) to reach a final suspension of 0.6% (w/v) low melting agarose for immobilization of cells. The final cell density in the suspension was $OD_{600} \approx 2$. A total of 6 µL of it were applied to an object plate and sealed with a cover slip. GFP fluorescence was detected with the Confocal Laser Scanning Microscope Zeiss LSM 780 (Jena, Germany).

Homology modeling. The model of Gal2 was created with SWISS-MODEL (https://swissmodel.expasy.org)[30] using the crystal structure of XylE (PDB ID: 4GBZ)[31] as a template. The localization of glucose in the substrate binding pocket of Gal2 was inferred by superimposing the model with the glucose-bound XylE structure. The amino acid replacement and visualization were performed with YASARA View[32], version 17.4.17.

Results

Identification of improved Gal2 mutants. To identify Gal2 variants with improved xylose transport properties in the presence of glucose, the *GAL2* wildtype open reading frame was subjected to error-prone PCR (epPCR) as described in "Materials and methods". The obtained PCR products were co-transformed with the linearized p426H7 plasmids into the strain AFY10X to allow for in vivo plasmid assembly and the transformants were initially plated on the permissive, ethanol-containing (SCE-Ura) agar plates. The resulting colonies were subsequently replica-plated on media containing glucose/xylose mixtures and screened for fastest growth based on the colony size. One of fastest growing clones (designated ep3.1) was selected for further characterization. The *GAL2*-plasmid was isolated and sequenced, revealing five distinct mutations causing amino acid exchanges, namely M107K, V239L, N376Y, M435I and L558S. The substitution N376Y was already described in our previous publication to enable glucose-insensitive xylose transport, but its transport activity for the pentose was rather low[17]. We therefore concluded that at least one of the additional mutations is responsible for the improved phenotype of the ep3.1 mutant. To test this assumption, we combined each of the four mutations individually with N376Y and tested the growth conferred by the resulting plasmids on different carbon sources. For growth tests on hexoses (glucose and galactose) the strain EBY.VW4000, which is deficient for all transporters capable of hexose transport in *S. cerevisiae*[16] was used, whereas the growth on pentoses was assayed in the screening strain AFY10X. In accordance with our previous observations[17], the constructs containing the N376Y mutations were not able to confer growth on glucose (Supplementary Fig. S1). On xylose or xylose/glucose mixtures, the superior properties of the ep3.1 variant compared to the N376Y single mutant could be clearly attributed to the M435I mutation (Supplementary Fig. S2). The N376Y/M435I variant was the only double mutant that conferred strong growth on pure xylose and glucose/xylose mixture.

To see more subtle differences between the different variants than is possible on agar plates, we grew liquid cultures and measured the consumption of xylose in AFY10X cells transformed with the wildtype, ep3.1 and the N376Y/M435I variants (Fig. 1). The media contained 0.5% (w/v) xylose with or without glucose addition (2% w/v). Comparing the growth and xylose consumption rates, the N376Y/M435I variant performed even better than the ep3.1 construct, suggesting that at least one of the remaining ep3.1 mutations (M107K, V239L and L558S) has a negative impact on the xylose transport activity.

Interestingly, the M435I mutation alone appears to have a negative influence on the transport of both glucose and xylose (Supplementary Fig. S3), which implies that there is a synergistic effect of the N376Y and M435I mutations in improving the uptake of xylose. We therefore also combined M435I with N376F, which has a lower v_{max} for xylose compared to wildtype Gal2[17]. In growth tests on agar plates containing pure xylose or a mixture

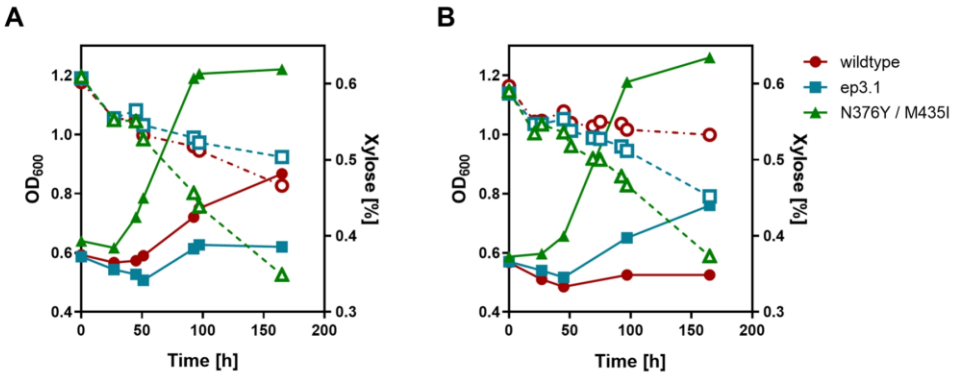

Figure 1. Fermentation of the screening strain AFY10X transformed with different Gal2 variants. The Gal2 constructs (wildtype, the selected mutant ep3.1 and the N376Y/M435I double mutant) were expressed from multicopy plasmids in the hxt^0/hxk^0 strain AFY10X. The consumption of xylose (0.5% w/v; open symbols, dashed lines) in the absence (**A**) or presence (**B**) of glucose (2% w/v) and growth curves (OD_{600}; closed symbols, full lines) are shown. The mean values of three independent cultures are shown. The error bars are omitted for clarity.

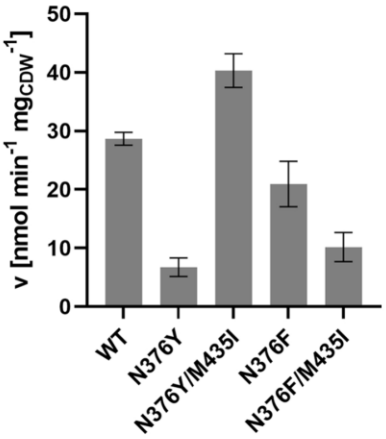

Figure 2. Uptake of ^{14}C-labelled xylose by selected Gal2 variants. Gal2 wildtype (WT) and indicated mutants were expressed in the hxt^0 strain EBY.VW4000 and the uptake velocity was measured at 500 mM total xylose. The uptake velocity is shown as nmol xylose taken up per minute per mg cell dry weight (nmol min^{-1} mg_{CDW}^{-1}). Mean values and standard deviation of triplicate measurements are shown.

of xylose and glucose, the N376F/M435I variant performed comparably to the N376F single mutant, but slightly worse than the N376Y/M435I double mutant (Supplementary Fig. S4).

Xylose uptake capacity of mutant Gal2 variants. To better understand the results described above and to analyze the transport activity of the Gal2 variants independently of cell growth, which is influenced by multiple factors, we performed sugar uptake assays with radiolabeled (^{14}C) xylose (Fig. 2). To estimate the transport capacity (defined by the maximum velocity, v_{max}), the assays were performed at nearly saturating xylose concentrations (500 mM). Strikingly, the measured transport velocities mirror the growth behavior of the transformants described above. Whereas the N376Y mutation alone negatively affects xylose transport[17] (see also Supplementary Fig. S2), this defect is more than compensated by the additional M435I mutation. The lower transport rate by the N376F and N376F/M435I variants is consistent with the results shown in Supplementary Fig. S4.

Taken together, the results show that the M435I substitution increases the transport capacity in combination with tyrosine (but not phenylalanine) at position 376 in a synergistic manner.

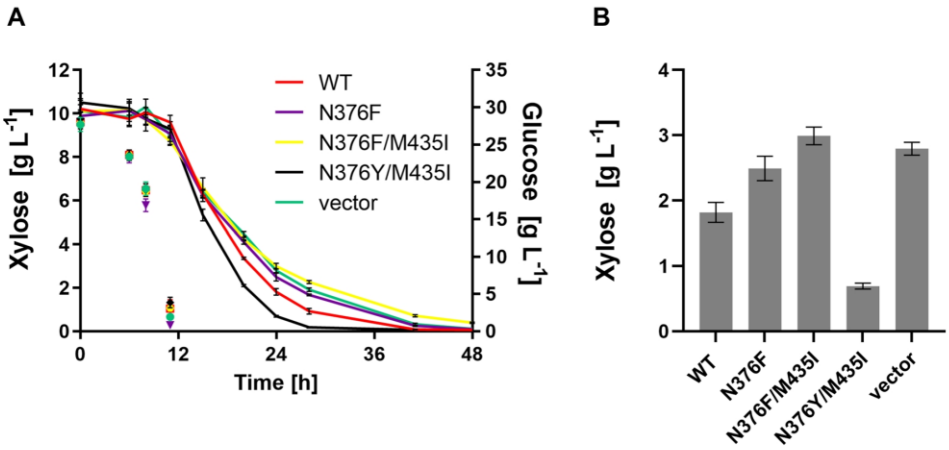

Figure 3. Fermentation of the industrial strain SRY027 expressing different Gal2 variants. The Gal2 constructs (wildtype—WT or the indicated mutants) were expressed from multicopy plasmids in the strain SRY027. (**A**) The consumption of xylose (starting concentration 10 g L^{-1}, solid lines; plotted on the left Y-axis) and glucose (starting concentration 30 g L^{-1}; symbols only, plotted on the right Y-axis) was measured via HPLC analysis. The mean values and standard deviation of three independent cultures are shown. The error bars may be smaller than the symbols. (**B**) Residual xylose concentration measured after 24 h of fermentation is shown. All values differ significantly from the wildtype (Tukey's multiple comparisons test, $P < 0.01$).

Fermentation performance of engineered strains expressing mutant Gal2 variants. After having demonstrated the superior properties of the N376Y/M435I mutant in the screening strain AFY10X, which consumes xylose very slowly (see Fig. 1), we reasoned that the "true" utility of the new transporter variant for mixed-sugar fermentations could be best challenged in a system highly optimized for pentose fermentation. We selected the strain SRY027 (see "Materials and methods" and Table 1 for details), derived from the robust, diploid industrial strain HDY.GUF12 (Ethanol Red background), which was genetically modified by integrating overexpression cassettes necessary for xylose and arabinose utilization, and further optimized to consume xylose through adaptive laboratory evolution[23,24]. In SRY027, the genomic *GAL2* alleles were deleted to avoid any interferences with the engineered *GAL2* constructs. In this background, we overexpressed different Gal2 variants from a multicopy (2µ) plasmid and performed fermentations in glucose/xylose mixtures (30 g L^{-1} and 10 g L^{-1}, respectively). All transformants consumed the sugars sequentially, with a fast glucose consumption phase (up to 12 h), followed by a slower, albeit considerably efficient xylose utilization, where the pentose sugar was consumed within approximately 36 h. Despite the presence of glucose-insensitive transporter variants (all mutants in which N376 was substituted by either Y or F), none of the transformants was able to significantly co-consume both sugars. Nevertheless, they did differ in the rate of xylose consumption (Fig. 3) in a manner that mirrors the xylose uptake capacities shown in Fig. 2, i.e. the N376Y/M435I exhibiting the highest and N376F/M435I the lowest velocity.

One possible explanation for the inability of the cells to co-consume glucose and xylose could be the glucose-induced internalization and degradation of Gal2 in the vacuole[33]. This process is induced by phosphorylation and ubiquitination of the N-terminal cytoplasmic tail and can be abolished by mutating six serine residues at positions 32, 35, 39, 48, 53 and 55 to alanine. The resulting $Gal2^{6SA}$ is stable at the plasma membrane even in the presence of glucose[28]. Therefore, we combined the 6SA N-terminal tail with the N376Y/M435I double mutation. To investigate if the 6SA tail is stabilizing the N376Y/M435I mutant, we also generated green florescent protein (GFP) fusion constructs as previously described[28]. As shown by fluorescence microscopy, the N376Y/M435I variant is internalized in glucose/xylose mixtures, whereas the 6SA/N376Y/M435I is nearly exclusively localized at the plasma membrane (Fig. 4A), as expected. Therefore, we transformed the stabilized constructs (without fused GFP) into the SRY027 strain, and performed a fermentation experiment in mixed-sugar medium. Again, the N376Y/M435I variant enabled faster xylose consumption compared to the control (Fig. 4B,C), reducing the overall duration of total xylose consumption by approximately 20 h (corresponding to 40% of the total fermentation time). Still, the consumption of glucose and xylose was largely sequential. This suggests that the reason for the inability of the strain for the simultaneous fermentation of both sugars does not primarily lie at the level of transport but might be rather due to metabolic constraints (see "Discussion").

The N376Y/M435I variant confers improved growth on arabinose as well. Besides xylose, arabinose is a relevant constituent of plant biomass. Since Gal2 is well-known to transport arabinose, we wanted to test if the N376Y/M435I double mutation is beneficial for the utilization of this pentose as well. AFY10 was enabled to metabolize arabinose by transforming it with plasmids encoding L-arabinose isomerase (*araA*), L-ribulokinase (*araB*), L-ribulose-5-P 4-epimerase (*araD*) and different Gal2 variants (wildtype, N376F, N376F/

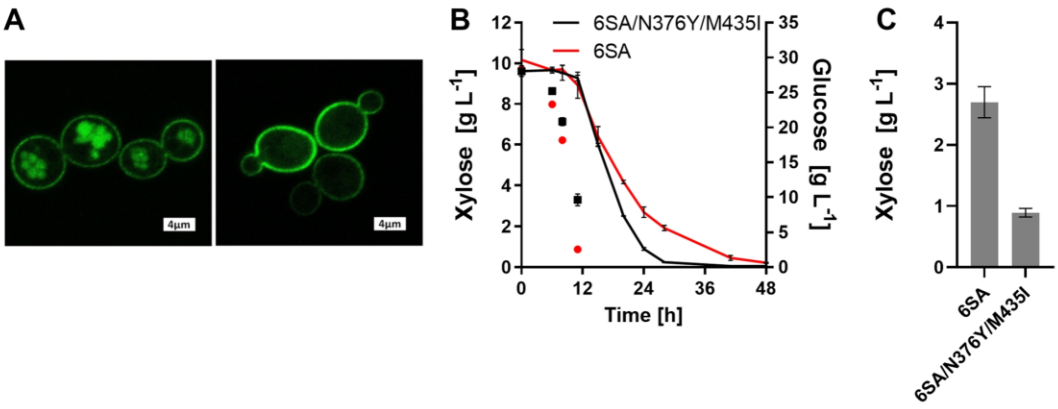

Figure 4. Stabilization of Gal2 variants by the 6SA N-terminal tail. The sextuple mutation within the N-terminal tail (6SA) conferring resistance to glucose-induced internalization was combined with the indicated Gal2 variants. (**A**) N376Y/M435I (left) and 6SA/N376Y/M435I (right) Gal2 variants were expressed as GFP fusions from single copy plasmids in CEN.PK2-1C and the localization of the transporters was analyzed by fluorescence microscopy. (**B**) The consumption of xylose (starting concentration 10 g L^{-1}, solid lines; plotted on the left Y axis) and glucose (starting concentration 30 g L^{-1}; symbols only, plotted on the right Y axis) was measured via HPLC analysis. The mean values and standard deviation of three independent cultures are shown. The error bars may be smaller than the symbols. (**C**) Residual xylose concentration measured after 24 h of fermentation is shown. The values differ significantly (unpaired two-tailed *t* test, $P < 0.01$). The fermentation experiments in (**B**) and (**C**) were performed with the strain SRY027, in which the Gal2 constructs were expressed from multicopy plasmids.

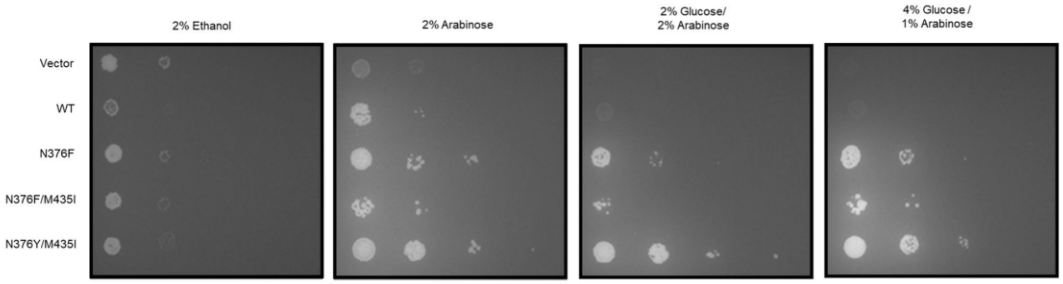

Figure 5. Growth conferred by different Gal2 variants on arabinose-containing media. The strain AFY10 was transformed with 2µ plasmids expressing the indicated Gal2 variants in combination with three additional 2µ plasmid expressing araA, araB and araD. The transformants were pre-grown in liquid selective SC medium with ethanol as a permissive carbon source and spotted onto selective SC solid medium containing the indicated carbon sources. Cells were grown at 30 °C for 6 days.

M435I and N376Y/M435I). Growth tests were performed on solid media containing arabinose or arabinose/glucose mixtures with these transformants. Expectedly, all N376 mutants conferred glucose-resistant growth on arabinose. Moreover, on all media, the N376Y/M435I variant conferred the strongest growth (Fig. 5), similar to what was observed with xylose (see Supplementary Fig. S4). This demonstrates that the $Gal2^{N376Y/M435I}$ could also be used to improve the fermentation of hydrolysates that are rich in arabinose and glucose, such as pectin-rich biomass hydrolysates.

Discussion

Here, we isolated an improved variant of Gal2 (N376Y/M435I), which combines two properties highly desirable for fermentations of lignocellulosic or pectin-rich hydrolysates – the ability to transport pentoses in the presence of glucose (Figs., 1B, 5) and an improved capacity for xylose (Figs. 1A, 2, 3, 4) and arabinose (Fig. 5) transport. Interestingly, both N376Y[17] (Fig. 2) and M435I (Supplementary Fig. 3) mutations individually have a negative impact on xylose transport, which is more than compensated when they are combined (Fig. 2). Strikingly, another substitution at position 435 was identified among multiple mutations in a Gal2 variant that had been generated by error prone PCR and selected for growth on low xylose concentration[34]. The authors did not analyze the individual contributions of the four mutations (L301R, K310R, N314D, M435T), but considering our results it

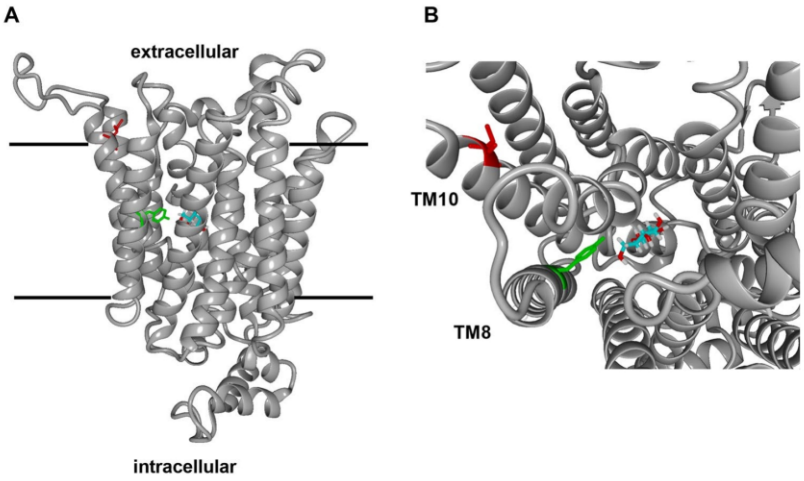

Figure 6. Homology model of the Gal2$^{N376Y/M435I}$ mutant. The model of membrane-inserted Gal2$^{N376Y/M435I}$ is shown as ribbon diagram in (**A**) with bound glucose (cyan backbone) and side chains of Y376 (green) and I435 (red). The view from the extracellular side (**B**) shows the positioning of TM8 and TM10, which could be affected by both mutations. The model was generated using SWISS-MODEL based on the crystal structure of XylE (PDB ID: 4GBZ) and visualized with YASARA View.

is likely that M435T is at least partly responsible for the observed phenotype, possibly in a synergistic manner, as described here. In a screen aiming to identify hexose transporter variants with increased specificity towards xylose, Zhao and coworkers[35] isolated a double mutant of Hxt2 (T339P/M420I, where M420 corresponds to M435 of Gal2). Although this variant was not glucose-insensitive, its specificity (calculated as a ratio of the K_M values for the respective sugar) was shifted from glucose to xylose compared to the wildtype and the mutations acted in a synergistic manner. These reports demonstrate the importance of the conserved methionine residue corresponding to M435 of Gal2 in a different experimental context.

Since no crystal structure of Gal2 is available, it is only possible to speculate about the underlying mechanism on the basis of homology models. The residue 435 is located at the periphery of the transmembrane helix 10 (TM10), at the interface of the lipid bilayer and the extracellular space. Hence, it is distant from the residue 376 that is located close to the sugar binding pocket and decisive for discrimination between pentoses and hexoses (Fig. 6A). The introduction of tyrosine, a large hydrophobic residue at the position 376 instead of asparagine in TM8 could cause clashes and affect the positioning of the proximal TM10. In turn, substituting methionine at the position 435 by the more hydrophobic isoleucine could positively influence the mobility of TM10 within the lipid bilayer at the extracellular membrane interface and thereby alleviate the possible steric constraints introduced by N376Y (Fig. 6B).

It was previously postulated that the sequential consumption of glucose and xylose is mainly due to the competition of both sugars at the level of sugar transporters, which have a much higher affinity for the hexose[15]. Our results show that the expression of glucose-insensitive transporters (Fig. 3), even in an internalization-resistant form (Fig. 4) is not sufficient to enable simultaneous consumption of both sugars. This is consistent with more recent work showing that the interferences of glucose and xylose are more complex and also involve their metabolism as well as glucose repression mechanisms. For instance, laboratory evolution for forced glucose-xylose co-consumption revealed mutations affecting the activity of the hexokinase Hxk2, the Gal83 subunit of the Snf1 kinase complex and of the E3-ubiquitin ligase Rsp5[36]. In another study, it was demonstrated that reducing the hexokinase activity is crucial for achieving simultaneous consumption of glucose and xylose[37]. Interestingly, a reduction in the xylose consumption rate was also observed during the co-consumption of maltose[15], a disaccharide that does not interfere with xylose transport, but is intracellularly cleaved into two glucose moieties, which are subsequently phosphorylated by hexokinases and thereby enter glycolysis. These observations collectively suggest that a fast glucose metabolism (and related signaling) impede the simultaneous consumption of pentoses, but the details of the underlying mechanism are still not well understood. It is conceivable that a buildup of the noxPPP intermediates derived from the fast glucose metabolism prevent the entrance of xylose (via Xu5P) into the equilibrium-driven "scrambling" reactions of this pathway. However, many other metabolic and signaling interferences are possible and further research is necessary to disentangle the individual contributing components.

In conclusion, although Gal2$^{N376Y/M435I}$ alone does not facilitate co-fermentation of glucose and pentoses, it does significantly reduce the overall fermentation time and therefore should prove valuable for valorization of substrates, which contain mixtures of glucose, xylose and/or arabinose, such as lignocellulosic or pectin-rich biomass.

Received: 8 September 2021; Accepted: 6 December 2021
Published online: 22 December 2021

References

1. Lynd, L. R. *et al.* Cellulosic ethanol: Status and innovation. *Curr. Opin. Biotechnol.* **45**, 202–211. https://doi.org/10.1016/j.copbio.2017.03.008 (2017).
2. Schmitz, K., Protzko, R., Zhang, L. & Benz, J. P. Spotlight on fungal pectin utilization-from phytopathogenicity to molecular recognition and industrial applications. *Appl. Microbiol. Biotechnol.* **103**, 2507–2524. https://doi.org/10.1007/s00253-019-09622-4 (2019).
3. Becker, J. & Boles, E. A modified *Saccharomyces cerevisiae* strain that consumes L-arabinose and produces ethanol. *Appl. Environ. Microbiol.* **69**, 4144–4150. https://doi.org/10.1128/AEM.69.7.4144-4150.2003 (2003).
4. Wisselink, H. W. *et al.* Engineering of *Saccharomyces cerevisiae* for efficient anaerobic alcoholic fermentation of L-arabinose. *Appl. Environ. Microbiol.* **73**, 4881–4891. https://doi.org/10.1128/AEM.00177-07 (2007).
5. Wiedemann, B. & Boles, E. Codon-optimized bacterial genes improve L-arabinose fermentation in recombinant *Saccharomyces cerevisiae*. *Appl. Environ. Microbiol.* **74**, 2043–2050. https://doi.org/10.1128/AEM.02395-07 (2008).
6. Kuyper, M. *et al.* Metabolic engineering of a xylose-isomerase-expressing *Saccharomyces cerevisiae* strain for rapid anaerobic xylose fermentation. *FEMS Yeast Res.* **5**, 399–409. https://doi.org/10.1016/j.femsyr.2004.09.010 (2005).
7. Jansen, M. L. A. *et al. Saccharomyces cerevisiae* strains for second-generation ethanol production. From academic exploration to industrial implementation. *FEMS Yeast Res.* **17**, fox044. https://doi.org/10.1093/femsyr/fox044 (2017).
8. Jacobus, A. P., Gross, J., Evans, J. H., Ceccato-Antonini, S. R. & Gombert, A. K. *Saccharomyces cerevisiae* strains used industrially for bioethanol production. *Essays Biochem.* **65**, 147–161. https://doi.org/10.1042/EBC20200160 (2021).
9. Kim, S. R., Ha, S.-J., Wei, N., Oh, E. J. & Jin, Y.-S. Simultaneous co-fermentation of mixed sugars: A promising strategy for producing cellulosic ethanol. *Trends Biotechnol.* **30**, 274–282. https://doi.org/10.1016/j.tibtech.2012.01.005 (2012).
10. Nijland, J. G. & Driessen, A. J. M. Engineering of pentose transport in *Saccharomyces cerevisiae* for biotechnological applications. *Front. Bioeng. Biotechnol.* **7**, 464. https://doi.org/10.3389/fbioe.2019.00464 (2020).
11. Hamacher, T., Becker, J., Gardonyi, M., Hahn-Hagerdal, B. & Boles, E. Characterization of the xylose-transporting properties of yeast hexose transporters and their influence on xylose utilization. *Microbiology* **148**, 2783–2788 (2002).
12. Sedlak, M. & Ho, N. W. Characterization of the effectiveness of hexose transporters for transporting xylose during glucose and xylose co-fermentation by a recombinant Saccharomyces yeast. *Yeast* **21**, 671–684. https://doi.org/10.1002/yea.1060 (2004).
13. Young, E., Poucher, A., Comer, A., Bailey, A. & Alper, H. Functional survey for heterologous sugar transport proteins, using *Saccharomyces cerevisiae* as a host. *Appl. Environ. Microbiol.* **77**, 3311–3319. https://doi.org/10.1128/AEM.02651-10 (2011).
14. Young, E. M., Tong, A., Bui, H., Spofford, C. & Alper, H. S. Rewiring yeast sugar transporter preference through modifying a conserved protein motif. *Proc. Natl. Acad. Sci. USA* **111**, 131–136. https://doi.org/10.1073/pnas.1311970111 (2014).
15. Subtil, T. & Boles, E. Competition between pentoses and glucose during uptake and catabolism in recombinant *Saccharomyces cerevisiae*. *Biotechnol. Biofuels* **5**, 14. https://doi.org/10.1186/1754-6834-5-14 (2012).
16. Wieczorke, R. *et al.* Concurrent knock-out of at least 20 transporter genes is required to block uptake of hexoses in *Saccharomyces cerevisiae*. *FEBS Lett.* **464**, 123–128. https://doi.org/10.1016/S0014-5793(99)01698-1 (1999).
17. Farwick, A., Bruder, S., Schadeweg, V., Oreb, M. & Boles, E. Engineering of yeast hexose transporters to transport D-xylose without inhibition by D-glucose. *Proc. Natl. Acad. Sci. USA* **111**, 5159–5164. https://doi.org/10.1073/pnas.1323464111 (2014).
18. Nijland, J. G. *et al.* Engineering of an endogenous hexose transporter into a specific D-xylose transporter facilitates glucose-xylose co-consumption in *Saccharomyces cerevisiae*. *Biotechnol. Biofuels* **7**, 168. https://doi.org/10.1186/s13068-014-0168-9 (2014).
19. Shin, H. Y. *et al.* An engineered cryptic Hxt11 sugar transporter facilitates glucose-xylose co-consumption in *Saccharomyces cerevisiae*. *Biotechnol. Biofuels*. https://doi.org/10.1186/s13068-015-0360-6 (2015).
20. Li, H., Schmitz, O. & Alper, H. S. Enabling glucose/xylose co-transport in yeast through the directed evolution of a sugar transporter. *Appl. Microbiol. Biotechnol.* **100**, 10215–10223. https://doi.org/10.1007/s00253-016-7879-8 (2016).
21. Reider Apel, A., Ouellet, M., Szmidt-Middleton, H., Keasling, J. D. & Mukhopadhyay, A. Evolved hexose transporter enhances xylose uptake and glucose/xylose co-utilization in *Saccharomyces cerevisiae*. *Sci. Rep.* **6**, 19512. https://doi.org/10.1038/srep19512 (2016).
22. Verhoeven, M. D. *et al.* Laboratory evolution of a glucose-phosphorylation-deficient, arabinose-fermenting *S. cerevisiae* strain reveals mutations in GAL2 that enable glucose-insensitive l-arabinose uptake. *FEMS Yeast Res.* **18**, foy062. https://doi.org/10.1093/femsyr/foy062 (2018).
23. Demeke, M. M. *et al.* Development of a D-xylose fermenting and inhibitor tolerant industrial *Saccharomyces cerevisiae* strain with high performance in lignocellulose hydrolysates using metabolic and evolutionary engineering. *Biotechnol Biofuels.* **6**, 89. https://doi.org/10.1186/1754-6834-6-89 (2013).
24. Generoso, W. C., Brinek, M., Dietz, H., Oreb, M. & Boles, E. Secretion of 2,3-dihydroxyisovalerate as a limiting factor for isobutanol production in *Saccharomyces cerevisiae*. *FEMS Yeast Res.* **17**, fox029. https://doi.org/10.1093/femsyr/fox029 (2017).
25. Generoso, W. C., Gottardi, M., Oreb, M. & Boles, E. Simplified CRISPR-Cas genome editing for *Saccharomyces cerevisiae*. *J. Microbiol. Meth.* **127**, 203–205. https://doi.org/10.1016/j.mimet.2016.06.020 (2016).
26. Gietz, R. D. & Schiestl, R. H. Frozen competent yeast cells that can be transformed with high efficiency using the LiAc/SS carrier DNA/PEG method. *Nat. Protoc.* **2**, 1–4. https://doi.org/10.1038/nprot.2007.17 (2007).
27. Bruder, S., Reifenrath, M., Thomik, T., Boles, E. & Herzog, K. Parallelised online biomass monitoring in shake flasks enables efficient strain and carbon source dependent growth characterisation of *Saccharomyces cerevisiae*. *Microb. Cell Fact.* **15**, 127. https://doi.org/10.1186/s12934-016-0526-3 (2016).
28. Tamayo Rojas, S. A., Schmidl, S., Boles, E. & Oreb, M. Glucose-induced internalization of the *S. cerevisiae* galactose permease Gal2 is dependent on phosphorylation and ubiquitination of its aminoterminal cytoplasmic tail. *FEMS Yeast Res.* **21**, foab019. https://doi.org/10.1093/femsyr/foab019 (2021).
29. Boles, E. & Oreb, M. A growth-based screening system for hexose transporters in yeast. *Methods Mol. Biol.* **1713**, 123–135. https://doi.org/10.1007/978-1-4939-7507-5_10 (2018).
30. Waterhouse, A. *et al.* SWISS-MODEL. Homology modelling of protein structures and complexes. *Nucleic Acids Res.* **46**, W296–W303. https://doi.org/10.1093/nar/gky427 (2018).
31. Sun, L. *et al.* Crystal structure of a bacterial homologue of glucose transporters GLUT1–4. *Nature* **490**, 361–366. https://doi.org/10.1038/nature11524 (2012).
32. Krieger, E. & Vriend, G. YASARA view—molecular graphics for all devices—from smartphones to workstations. *Bioinformatics* **30**, 2981–2982. https://doi.org/10.1093/bioinformatics/btu426 (2014).
33. Horak, J. & Wolf, D. H. Catabolite inactivation of the galactose transporter in the yeast *Saccharomyces cerevisiae*. Ubiquitination, endocytosis, and degradation in the vacuole. *J. Bacteriol.* **179**, 1541–1549. https://doi.org/10.1128/jb.179.5.1541-1549.1997 (1997).
34. Reznicek, O. *et al.* Improved xylose uptake in *Saccharomyces cerevisiae* due to directed evolution of galactose permease Gal2 for sugar co-consumption. *J. Appl. Microbiol.* **119**, 99–111. https://doi.org/10.1111/jam.12825 (2015).
35. Wang, M., Yu, C. & Zhao, H. Identification of an important motif that controls the activity and specificity of sugar transporters. *Biotechnol. Bioeng.* **113**, 1460–1467. https://doi.org/10.1002/bit.25926 (2016).

36. Papapetridis, I. *et al.* Laboratory evolution for forced glucose-xylose co-consumption enables identification of mutations that improve mixed-sugar fermentation by xylose-fermenting *Saccharomyces cerevisiae*. *FEMS Yeast Res.* **18**, foy056. https://doi.org/10.1093/femsyr/foy056 (2018).
37. Lane, S. *et al.* Glucose repression can be alleviated by reducing glucose phosphorylation rate in *Saccharomyces cerevisiae*. *Sci. Rep.* **8**, 2613. https://doi.org/10.1038/s41598-018-20804-4 (2018).

Acknowledgements
We thank Alexander Farwick for isolating the ep3.1 clone, Nils Peiter for the help during the construction of the SRY027 strain and Kilan Schäfer for proof-editing the manuscript.

Author contributions
S.T.R., E.B. and M.O. designed research. S.T.R., V.S. and F.K. performed experiments. All authors analyzed the data. E.B. and M.O. guided the project. S.T.R. and M.O. wrote the manuscript. All authors read and approved the final manuscript.

Funding
Open Access funding enabled and organized by Projekt DEAL. This work was supported by DAAD/BECAS Chile, 2016, grant number 57221134 (to STR) and by the German Federal Ministry of Education and Research, grant number 031B0342B (to MO).

Competing interests
VS, FK, EB and MO are co-inventors of the patent Nr. WO002016062821A1.

Additional information
Supplementary Information The online version contains supplementary material available at https://doi.org/10.1038/s41598-021-03822-7.

Correspondence and requests for materials should be addressed to E.B. or M.O.

Reprints and permissions information is available at www.nature.com/reprints.

Publisher's note Springer Nature remains neutral with regard to jurisdictional claims in published maps and institutional affiliations.

Open Access This article is licensed under a Creative Commons Attribution 4.0 International License, which permits use, sharing, adaptation, distribution and reproduction in any medium or format, as long as you give appropriate credit to the original author(s) and the source, provide a link to the Creative Commons licence, and indicate if changes were made. The images or other third party material in this article are included in the article's Creative Commons licence, unless indicated otherwise in a credit line to the material. If material is not included in the article's Creative Commons licence and your intended use is not permitted by statutory regulation or exceeds the permitted use, you will need to obtain permission directly from the copyright holder. To view a copy of this licence, visit http://creativecommons.org/licenses/by/4.0/.

© The Author(s) 2021

Supplementary Information

Identification of a glucose-insensitive variant of Gal2 from *Saccharomyces cerevisiae* exhibiting a high pentose transport capacity

Sebastian A. Tamayo Rojas, Virginia Schadeweg, Ferdinand Kirchner, Eckhard Boles* and Mislav Oreb*

Institute of Molecular Biosciences, Faculty of Biological Sciences, Goethe University Frankfurt, Frankfurt am Main, Germany

*Corresponding authors

Eckhard Boles

Goethe University Frankfurt

Institute of Molecular Biosciences

Max-von-Laue Straße 9

60438 Frankfurt

Germany

Telephone +49 (0)69 798 29513

Telefax +49 (0)69 798 29527

E-Mail e.boles@bio.uni-frankfurt.de

Mislav Oreb

Goethe University Frankfurt

Institute of Molecular Biosciences

Max-von-Laue Straße 9

60438 Frankfurt

Germany

Telephone +49 (0)69 798 29331

Telefax +49 (0)69 798 29527

E-Mail m.oreb@bio.uni-frankfurt.de

Supplementary Table S1 | Primers used in this study.

Primer name	Application	Sequence 5'-3'
Amp_GAL2_F	Forward primer for GAL2 amplification	ATGGCAGTTGAGGAGAAC
Amp_GAL2_R	Reverse primer for GAL2 amplification	TTATTCTAGCATGGCCTTG
Clon_GAL2_F	Forward primer for GAL2 cloning	AACACAAAAACAAAAAGTTTTTTTAATTTTAATCAAAAAATGGCAGTTGAGGAGAACAA
Clon_GAL2_R	Reverse primer for GAL2 cloning	GAATGTAAGCGTGACATAACTAATTACATGACTCGAGTTATTCTAGCATGGCCTTGTACC
SRp001	Forward primer for cloning GFP, with overhangs for fusing it to Gal2	GGTACAAGGCCATGCTAGAAATGAGTAAAGGAGAAGAACTTTTCAC
SRp002	Forward primer for cloning GFP, with overhangs for CYC1t	AACTAATTACATGACTCGAGTTATTTGTATAGTTCATCCATGCCATG
SRp014	Reverse primer for cloning GAL2, with overhangs for fusing it to GFP	AGTTCTTCTCCTTTACTCATTTCTAGCATGGCCTTGTACC
VSP66	Forward primer for mutagenesis of M435 to I in GAL2	GGTGCCGGTAACTGTATCATTGTCTTTACCTG
VSP67	Reverse primer for mutagenesis of M435 to I in GAL2	ACAGGTAAAGACAATGATACAGTTACCGGCACC
VSP31	Forward primer for mutagenesis of N376 to Y in GAL2	GTCATTGGTGTAGTCTACTTTGCCTCCACTTTCTTTAG
VSP32	Reverse primer for mutagenesis of N376 to Y in GAL2	GAAAGTGGAGGCAAAGTAGACTACACCAATGACAATGG
VSP62	Forward primer for mutagenesis of M107 to K in GAL2	TTGAGAAGGTTTGGTAAGAAACATAAGGATGGTACC
VSP63	Reverse primer for mutagenesis of M107 to K in GAL2	ACCATCCTTATGTTTCTTACCAAACCTTCTCAAAAAGTCTG
VSP64	Forward primer for mutagenesis of V239 to L in GAL2	AGCTATTCGAACTCACTTCAATGGAGAGTTCCATTAGG
VSP65	Reverse primer for mutagenesis of V239 to L in GAL2	TGGAACTCTCCATTGAAGTGAGTTCGAATAGCTCTTTG
VSP68	Forward primer for mutagenesis of L558 to S in GAL2	GGTAATAATTACGATTCAGAGGATTTACAACATGACG
VSP69	Reverse primer for mutagenesis of L558 to S in GAL2	ATGTTGTAAATCCTCTGAATCGTAATTATTACCTCTTC
SRp0171	Forward primer for deletion of GAL2 with CRISPR Cas9 (gRNA)	GCCGGTGAGTCAGGGCCTGAGTTTTAGAGCTAGAAATAGCAAGTTAAAATAAGG
SRp0172	Reverse primer for deletion of GAL2 with CRISPR Cas9 (gRNA)	CTCAGGCCCTGACTCACCGGCGATCATTTATCTTTCACTGCGGAG
SRp0157	Donor DNA for repairing GAL2 locus (forward strand)	ATGGCAGTTGAGGAGAACAATATGCCTGTTGTTTCACAGCAACCCCAAGCTGGTGAAGACGTGATCTCTTAGGTAATAATTACGATTTAGAGGATTTACAACATGACGACAAACCGTGGTACAAGGCCATGCTAGAATAA
SRp0158	Donor DNA for repairing GAL2 locus (reverse strand)	TTATTCTAGCATGGCCTTGTACCACGGTTTGTCGTCATGTTGTAAATCCTCTAAATCGTAATTATTACCTAAGAGATCACGTCTTCACCAGCTTGGGGTTGCTGTGAAACAACAGGCATATTGTTCTCCTCAACTGCCAT
SRp0201	Forward primer for verification of GAL2 deletion	ATGGCAGTTGAGGAGAACAATATG
SRp0202	Reverse primer for verification of GAL2 deletion	TTATTCTAGCATGGCCTTGTACCAC

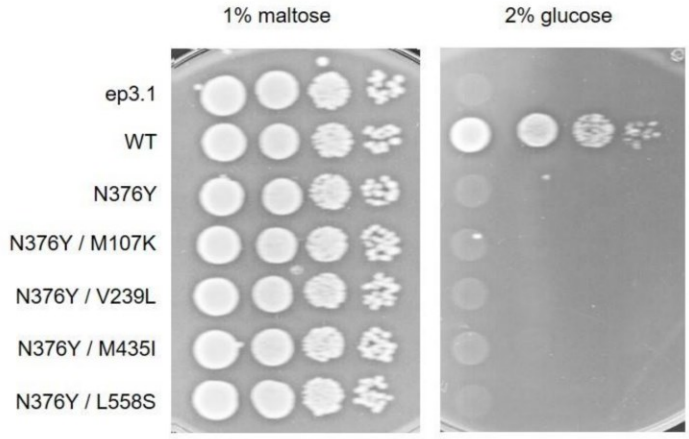

Supplementary Figure S1 | Effect of the mutations in the Gal2 clone ep3.1 on glucose transport. The hxt^0 strain EBY.VW4000 was transformed with plasmids encoding the ep3.1, wildtype (WT) or indicated variants of Gal2 generated by site directed mutagenesis. Dilution series of cell suspensions were spotted onto agar plates containing the indicated sugars (concentrations are given as % w/v) and the growth was analyzed after three days of incubation at 30°C. Maltose as a permissive carbon source for the hxt^0 strain was used to control the viability of the transformants.

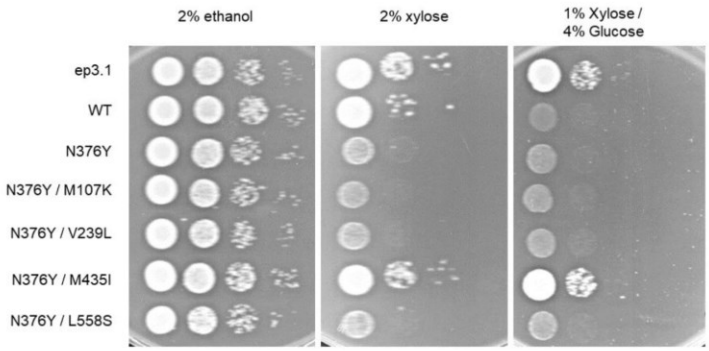

Supplementary Figure S2 | Effect of the mutations in the Gal2 clone ep3.1 on xylose transport. The hxt^0/hxk^0 strain AFY10X was transformed with plasmids encoding the ep3.1, wildtype (WT) or indicated variants of Gal2 generated by site directed mutagenesis. Dilution series of cell suspensions were spotted onto agar plates containing the indicated sugars (concentrations are given as % w/v) and the growth was analyzed after five days of incubation at 30°C. Ethanol as a permissive carbon source for the hxt^0/hxk^0 strain was used to control the viability of the transformants.

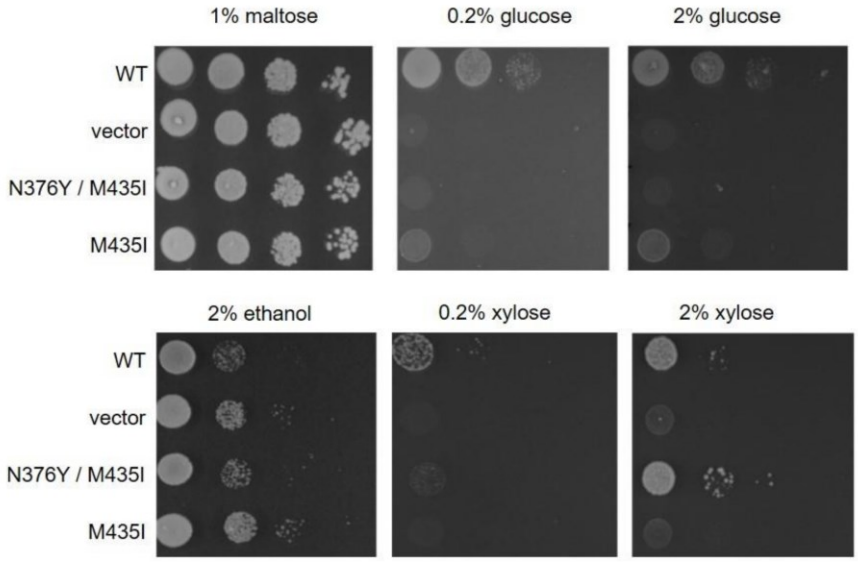

Supplementary Figure S3 | Effect of the M435I mutation alone on xylose and glucose transport. The hxt^0 strain EBY.VW4000 (top) and the hxt^0/hxk^0 strain AFY10 were transformed with plasmids encoding the indicated variants of Gal2 or the empty vector as a negative control. Dilution series of cell suspensions were spotted onto agar plates containing the indicated sugars (concentrations are given as % w/v) and the growth was analyzed after three (hxt^0 strain) or five (hxt^0/hxk^0 strain) days of incubation at 30°C. Maltose as a permissive carbon source for the hxt^0 strain and ethanol for the hxt^0/hxk^0 strain were used to control the viability of the transformants.

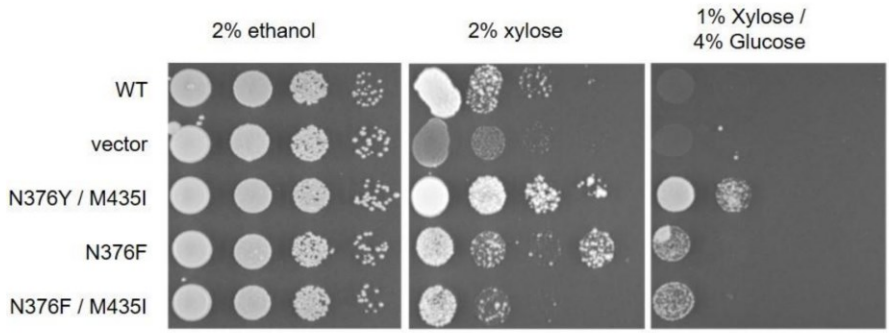

Supplementary Figure S4 | Combination of the N376F with the M435I mutation. The hxt^0/hxk^0 strain AFY10 were transformed with plasmids encoding the indicated variants of Gal2 or the empty vector as a negative control. Dilution series of cell suspensions were spotted onto agar plates containing the indicated sugars (concentrations are given as % w/v) and the growth was analyzed after five days of incubation at 30°C. Ethanol as a permissive carbon source for the hxt^0/hxk^0 strain was used to control the viability of the transformants.

6.3 A yeast-based *in vivo* assay system for analyzing efflux of sugars mediated by glucose and xylose transporters

Declaration of author contributions to the publication:
A yeast-based *in vivo* assay system for analyzing efflux of sugars mediated by glucose and xylose transporters

Status: Published, September 2022
Journal: FEMS Yeast Research
Type of manuscript: research article
Contributing authors: Sebastian A. Tamayo Rojas (SR), Eckhard Boles (EB), and Mislav Oreb (MO)

Contributions of doctoral candidate and co-authors
(1) Concept and design
Doctoral candidate SR: 60%
Co-authors EB, MO: 20%, 20%
(2) Conducting tests and experiments
Doctoral candidate SR: 100%, yeast molecular biology, growth-based assays, and fermentations
(3) Compilation of data sets and figures
Doctoral candidate SR: 100%, schemes, metabolite titers and growth-based assays
(4) Analysis and interpretation of data
Doctoral candidate SR: 65%, metabolite titers and growth-based assays
Co-authors EB, MO: 5 %, 30%, supervision and advice
(5) Drafting of manuscript
Doctoral candidate SR: 55%
Co-authors EB, MO: 5%, 40%

Copyright information:

The following article is reprinted with permission from Oxford University Press

The article is available online:
https://doi.org/10.1093/femsyr/foac038

FEMS Yeast Research, 2022, 21, 1–7
DOI: 10.1093/femsyr/foac038
Advance access publication date: 2 August 2022
Research Article

A yeast-based *in vivo* assay system for analyzing efflux of sugars mediated by glucose and xylose transporters

Sebastian A. Tamayo Rojas, Eckhard Boles, Mislav Oreb*

Goethe University Frankfurt, Faculty of Biological Sciences, Institute of Molecular Biosciences, Max-von-Laue Straße 9, 60438 Frankfurt am Main, Germany
*Corresponding author: Institute of Molecular Biosciences, Faculty of Biological Sciences, Goethe University Frankfurt, Max-von-Laue Straße 9, 60438 Frankfurt am Main, Germany. Tel: +49 (0)69 798 29331. Fax: +49 (0)69 798 29527; E-mail: m.oreb@bio.uni-frankfurt.de
One sentence summary: Screening and characterization of transporters mediating sugar efflux is established in a hexose transporter-free *Saccharomyces cerevisiae* strain.
Editor: John Morrissey.

Abstract

Sugar transporter research focuses on the sugar uptake into cells. Under certain physiological conditions, however, the intracellular accumulation and secretion of carbohydrates (efflux) are relevant processes in many cell types. Currently, no cell-based system is available for specifically investigating glucose efflux. Therefore, we designed a system based on a hexose transporter-deficient *Saccharomyces cerevisiae* strain, in which the disaccharide maltose is provided as a donor of intracellular glucose. By deleting the hexokinase genes, we prevented the metabolization of glucose, and thereby achieved the accumulation of growth-inhibitory glucose levels inside the cells. When a permease mediating glucose efflux is expressed in this system, the inhibitory effect is relieved proportionally to the capacity of the introduced transporter. The assay is thereby suitable for screening of transporters and quantitative analyses of their glucose efflux capacities. Moreover, by simultaneous provision of intracellular glucose and extracellular xylose, we investigated how each sugar influences the transport of the other one from the opposite side of the membrane. Thereby, we could show that the xylose transporter variant Gal2^{N376F} is insensitive not only to extracellular but also to intracellular glucose. Considering the importance of sugar transporters in biotechnology, the assay could facilitate new developments in a variety of applications.

Keywords: xylose transport, sugar efflux, competitive inhibition of xylose transport by glucose, *hxt*^{0} strain, glucose secretion, screening system

Introduction

In all kingdoms of life, sugar efflux from cells is a relevant phenomenon, involved in crucial physiological processes. For instance, in humans, glucose influx and efflux are required to transfer glucose from the lumen of the intestine to the bloodstream through a layer of epithelial cells. During this so-called transepithelial transport, glucose is taken up from the intestinal lumen at the apical membrane of the epithelial cells by sodium–glucose symporters (SGLT1) that act against the concentration gradient, and the sugar is subsequently released at the basolateral membrane by facilitative transporters (e.g. GLUT2) into the extracellular fluid (Thorens 1996). In plants, sugar efflux is known to play a crucial role in processes such as embryo development, nectar production, and plant–pathogen interactions (Sonnewald 2011); the recently discovered SWEET transporter family is responsible for such functions (Chen et al. 2010). Even in unicellular organisms such as *Escherichia coli*, specialized sugar efflux systems were described, e.g. the SET family transporters (Liu et al. 1999), which likely play roles in carbohydrate metabolism or metabolic stress response (Sun and Vanderpool 2011). These examples illustrate the physiological importance of sugar efflux and the need for suitable functional testing platforms, in which libraries of candidate genes could be screened for their efflux function. Although some efflux transporters can be identified based on their ability to mediate sugar influx as well (Chen et al. 2010), this property may not be generalizable. Even for transporters that are functional in both directions, the kinetics of influx and efflux are likely to differ. For instance, it has been reported that the pathologically relevant T295M mutation in human GLUT1 affects sugar efflux and influx in an asymmetrical manner (Wang et al. 2008). Furthermore, the availability of a specific efflux assay would open the possibility to assess the effect of effector molecules on the transporters in a topologically specific manner.

In this study, we developed a yeast-based assay system for glucose efflux, which is derived from the hexose transporter-free (*hxt*^{0}) *Saccharomyces cerevisiae* strain EBY.VW4000 (Wieczorke et al. 1999). Due to its simple handling and amenability to growth-based assays of sugar influx, the *hxt*^{0} strain had been used to screen and characterize a plethora of hexose and pentose transporters from various organisms (Boles and Oreb 2018). We reasoned that it can also be used for background-free assays of hexose efflux. Our approach is based on the observation that, as a consequence of excessive feeding with the disaccharide maltose, intracellular accumulation of glucose is growth-inhibitory to the cell, likely due to osmotic mechanisms (Postma et al. 1990), and that facilitative hexose transporters could relieve this effect by mediating glucose efflux (Jansen et al. 2002). Maltose is taken up by specific maltose transporters of the Malx1 family (Cheng and Michels 1991) into EBY.VW4000 cells and intracellularly hydrolyzed by maltases into two glucose moieties. To prevent the further conversion of (maltose derived) glucose, e.g. via glycolysis, we used the EBY.VW4000 derivative AFY10, in which the genes encoding the known

Received: June 13, 2022. Revised: July 14, 2022. Accepted: July 29, 2022
© The Author(s) 2022. Published by Oxford University Press on behalf of FEMS. All rights reserved. For permissions, please e-mail: journals.permissions@oup.com

Downloaded from https://academic.oup.com/femsyr/article/21/1/foac038/6653521 by Frankfurt University Library user on 26 September 2022

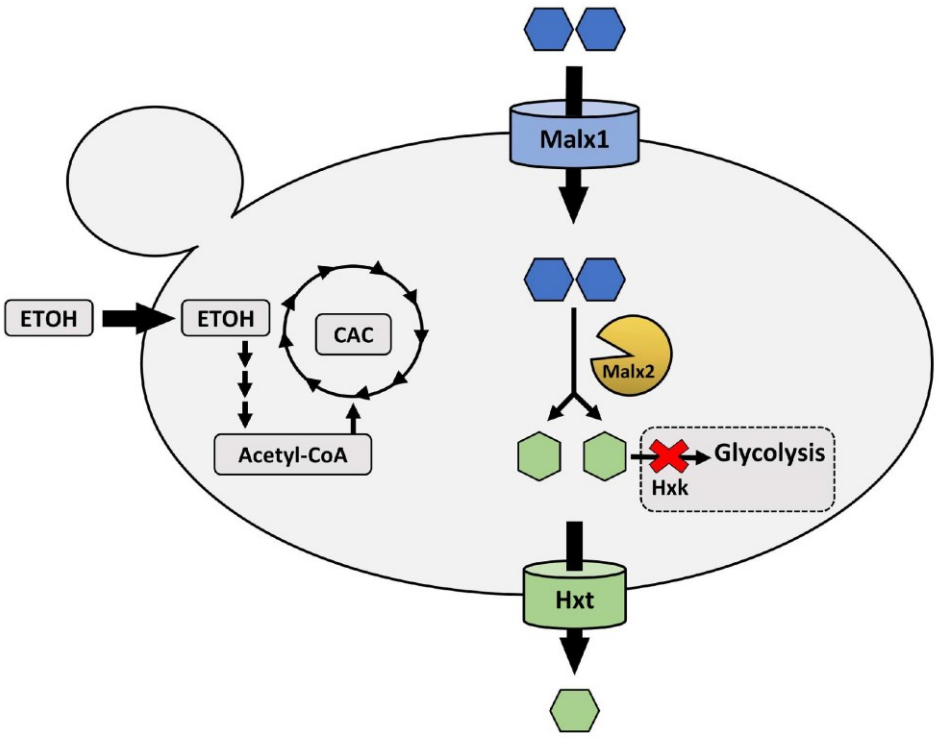

Figure 1. Design of the glucose efflux test system. The disaccharide maltose (blue) is taken up by specialized maltose/proton symporters Malx1 and intracellularly cleaved into two glucose molecules (green) by a maltase (Malx2). The metabolism of glucose is prevented by deleting the hexokinase (Hxk) genes. Individual hexose transporters (Hxt) are expressed from plasmids and mediate glucose efflux to relieve the osmotic pressure caused by accumulating glucose. Ethanol (ETOH) is provided as a carbon and energy source to the cells. Through multiple enzymatic steps, ethanol is converted to acetyl-CoA, which is subsequently metabolized through the citric acid cycle (CAC).

enzymes with glucose kinase activity, i.e. *HXK1*, *HXK2*, *GLK1*, and the putative hexokinase *YLR446W* have been deleted (*hxk*^{0}; Farwick et al. 2014). Due to its *hxt*^{0} *hxk*^{0} genotype, ethanol must be supplemented as a carbon and energy source to AFY10. The design of the test system is summarized in Fig. 1.

Materials and methods

Strains and media

The construction of the screening strain AFY10 (Farwick et al. 2014) was previously described. The auxotrophic wildtype strain CEN.PK2-1C was used solely for plasmid assembly. The genotypes are listed in Table 1.

For the preparation of competent cells, plasmid-free cells were grown in standard YEP-media [1% (w/v) yeast extract, 2% (w/v) peptone] supplemented with 2% (v/v) of ethanol (for AFY10) or 2% (w/v) of glucose (for CEN.PK2-1C). Frozen competent cells were prepared and transformed according to the established protocol (Gietz and Schiestl 2007). AFY10 transformants were plated on solid, selective synthetic complete (SC) medium with 2% (v/v) of ethanol, where only uracil or uracil and leucine were absent (-URA or -URA-LEU) to maintain the selection pressure. Amino acids were added as previously described (Bruder et al. 2016).

Plasmid construction

Most of the plasmids used in this study were previously described as listed in Table 2. For the construction of the plasmid LAC12-p426H7, the ORF of the *LAC12* gene (GenBank accession: X06997.1) was PCR-amplified from the genomic DNA isolated from the *Kluyveromyces lactis* strain CBS 2359 using primers LAC12-HXT7.fw (CACAAAAACAAAAAGTTTTTTTAATTTTAA TCAAAAAATGGCAGATCATTCGAGCAGC) and LAC12-CYC1.rv (GTGAATGTAAGCGTGACATAACTAATTACATGACTCGAGTTAAA CAGATTCTGCCTCTGAAAGCT). The resulting PCR product was co-transformed with the XhoI/BamHI linearized multicopy (2μ) p426H7 vector in CEN.PK2-1C frozen competent cells to allow for plasmid assembly via homologous recombination (Oldenburg et al. 1997). Cells were plated on SC-URA agar plates containing 2% glucose (w/v) and incubated for 3 days at 30°C. Single colonies from these plates were picked, subcultivated and plasmids were recovered by the standard alkaline lysis protocol. For propagation and amplification, plasmids were transformed via electroporation into *E. coli* strain DH10B, which was grown on LB medium

Downloaded from https://academic.oup.com/femsyr/article/21/1/foaa038/6653521 by Frankfurt University Library user on 26 September 2022

Table 1. Strains used in this study.

Strain	Genotype	Reference
CEN.PK2-1C	*leu2-3,112 ura3-52 trp1-289 his3Δ1 MAL2-8c SUC2*	Euroscarf
AFY10	*leu2-3,112 ura3-52 trp1-289 his3Δ1 MAL2-8c SUC2 Δhxt1-17 gal2Δ::loxP stl1Δ::loxP agt1Δ::loxP mph2Δ::loxP mph3Δ::loxP glk1Δ::loxP hxk1Δ::loxP hxk2Δ::loxP ylr446wΔ::loxP pyk2Δ::[PGK1p-opt.XKS1-PGK1t TPI1p-TAL1-TAL1t TDH3p-TKL1-TKL1t PFK1p-RPE1-RPE1t FBAp-RKI1-RKI1t kanMX]*	Farwick et al. (2014)

The genotype is annotated according to the standard nomenclature. Promoters and terminators are denoted by suffixes "p" and "t", respectively. Overexpressed ORFs are underlined. The genetic cassette integrated into the *PYK2* locus is shown in brackets. Gene deletions are indicated by a "Δ."

Table 2. Plasmids used in this study.

Plasmid name	Relevant properties	Reference
YEp181_pHXT7-optXI_Clos	2μ, *LEU2*, codon-optimized xylose isomerase gene *xylA* of *C. phytofermentans* under control of $HXT7p^{-1-392}$ and *CYC1t*, *E. coli* Ampicillin-marker.	Subtil and Boles (2012)
p425H7	2μ, *LEU2* marker, $HXT7p^{-1-392}$, *CYC1t*, *E. coli* Ampicillin-marker and pBR322-origin	Becker and Boles (2003)
p426H7	2μ, *URA3* marker, $HXT7p^{-1-392}$, *CYC1t*, *E. coli* Ampicillin-marker and pBR322-origin	Becker and Boles (2003)
GAL2-p426H7	ORF of *GAL2* in p426H7	Farwick et al. (2014)
$GAL2^{3KR}$-p426H7	ORF of $GAL2^{K27R/K37R/K44R}$ in p426H7	Tamayo Rojas et al. (2021b)
$GAL2^{N376F}$-p426H7	ORF of $GAL2^{N376F}$ in p426H7	Farwick et al. (2014)
HXT1-p426H7	ORF of *HXT1* in p426H7	Schmidl et al. (2021)
HXT5-p426H7	ORF of *HXT5* in p426H7	Schmidl et al. (2021)
HXT7-p426H7	ORF of *HXT7* in p426H7	Schmidl et al. (2021)
LAC12-p426H7	Lactose permease LAC12 of *K. lactis* in p426H7	This study

Under "relevant properties," promoters and terminators are denoted by suffixes "p" and "t," respectively; ORF, open reading frame.

with Ampicillin as a selective marker. Plasmid isolation from overnight *E. coli* cultures was carried out using a GeneJET Plasmid Miniprep Kit (Thermo Scientific) according to the manufacturer's instructions.

Growth-based analysis

Growth tests were performed on solid minimal SC (-URA or -URA-LEU) medium with 1.9% (w/v) agarose containing the indicated carbon sources. Precultures were grown overnight in 50 ml SC (-URA or -URA-LEU) medium with 2% (v/v) of ethanol at 30°C and 180 rpm. Cells were harvested by centrifugation (3000 *g*, 2 min, 20°C) and washed twice with sterile water. Cells were resuspended in sterile water at $OD_{600} = 1$. Dilutions of OD_{600} of 0.1, 0.01, and 0.001 were prepared and 5 μl of each dilution were dropped onto the agar plates containing the respective carbon source(s). Plates were incubated at 30°C for 6–8 days.

Bioconversion experiments and HPLC analysis

For bioconversions in liquid medium, precultures of cells expressing the transporters in high copy vectors were grown over 4 days in 900 ml SC (-URA or -URA-LEU), 2% (v/v) ethanol medium at 30°C with agitation at 180 rpm. Cells were harvested by centrifugation (3000 *g*, 3 min, 20°C) and washed twice with double-distilled sterile water. Washed cells were used to inoculate 20 ml SC (-URA or -URA-LEU) medium with the respective carbon source(s) to an OD_{600} of ≈ 8 in 300 ml shake flasks.

For HPLC analysis, 450 μl of the culture supernatants were mixed with 50 μl 50% (w/v) 5-sulfosalicylic acid and centrifuged (16,000 *g*, 5 min, 4°C). A volume of 470 μl of the supernatants were transferred into HPLC vials. A volume of 10 μl of each sample were subjected to high performance liquid chromatography (Dionex Ultimate 3000, Thermo Scientific) equipped with the ion exchange column HyperREZ XP Carbohydrate H^+ (7,7 × 300 mm; Thermo Scientific) and a refractive index detector. The liquid phase was 5 mM sulfuric acid, run at 0.6 ml min^{-1} and 65°C. The Chromeleon 6.8 software was employed for quantifications and Prism 5 (GraphPad) for statistical analysis and presentation of the results.

Results and discussion

Proof of concept for the growth-based glucose efflux assay

Glucose secretion by *S. cerevisiae* upon excessive maltose feeding was shown to be dependent on one or multiple hexose transporters (Jansen et al. 2002), but their individual capability to facilitate this process was not investigated. For the proof of concept, we therefore, selected the following *S. cerevisiae* hexose permeases exhibiting different properties: Hxt1, Hxt5, and Hxt7, representing low, medium and high affinity transporters, respectively (Leandro et al. 2009, Schmidl et al. 2021); Gal2, an *S. cerevisiae* galactose permease , which is also able to transport glucose and xylose; its mutant variant $Gal2^{N376F}$, which is able to transport xylose even in the presence of glucose (Farwick et al. 2014); and $Gal2^{3KR}$, a variant which is resistant to ubiquitination-mediated degradation and, due to the higher protein abundance, shows a higher transport capacity compared to wildtype Gal2 (Tamayo Rojas et al. 2021b). All transporters were expressed from p426H7 multicopy plasmids under the control of a strong promoter. As negative controls, we used the empty vector (E.V.) and a plasmid encoding the lactose/proton symporter Lac12 from *K. lactis*. Lac12 has been chosen since it is active in *S. cerevisiae* (Rubio-Texeira et al. 2000) and has not been reported to transport glucose. The functionality of Lac12 expressed from our construct was demonstrated by its ability to confer growth of CEN.PK2-1C and

Downloaded from https://academic.oup.com/femsyr/article/21/1/foaa038/6053521 by Frankfurt University Library user on 26 September 2022

EBY.VW4000 cells on lactose, when expressed together with the β-galactosidase Lac4 from *K. lactis* (data not shown).

A growth test of the transformants was performed on solid media containing 2% (v/v) of ethanol and varying maltose concentrations (Fig. 2). All transformants grew comparably on ethanol, while maltose exerted a growth-inhibitory effect in a concentration-dependent manner, as expected. Whereas no growth was observed for the negative controls, all permeases facilitating glucose transport (Hxt1, Hxt5, Hxt7, Gal2, and Gal2^{3KR}) alleviated the growth defect to different extents. With the mutant Gal2^{N376F}, weak growth was observed only at the lowest maltose concentration, which is explained by its almost complete loss of the glucose transport capability (Farwick et al. 2014). Among the wildtype transporters, Hxt7 conferred the weakest growth, consistent with its low glucose transport capacity (Reifenberger et al. 1997). Thus, this experiment demonstrates the feasibility of the approach for functional screening of glucose efflux-mediating transporters.

Quantification of hexose transporter-mediated glucose efflux

To quantitatively validate the assay system, we cultivated selected transformants (E.V., Gal2, Gal2^{N376F}, Gal2^{3KR}, and Hxt1) in liquid media and measured the sugar concentrations over time (Fig. 3).

The cells were inoculated at a high cell density (starting $OD_{600} \approx 8$) and only a small increase of the biomass was observed over the course of the experiment (Fig. 3A). All transformants comparably consumed ethanol (Fig. 3B), which confirmed their viability and metabolic activity. Remarkable differences in the maltose consumption (Fig. 3C) and glucose efflux (Fig. 3D) kinetics were observed between the transformants that are in agreement with the known properties of individual glucose transporters (as measured with external glucose in previously published work; Reifenberger et al. 1997, Farwick et al. 2014). The E.V. control shows only a minor consumption of maltose stopping after 12 h of cultivation, which could be explained by an inhibitory effect of intracellular glucose on maltose transporters and/or on the maltase activity. In contrast, the strain expressing the main hexose permease of *S. cerevisiae* Hxt1 (Ozcan and Johnston 1999) completely converts maltose to extracellular glucose within 24 h. The bioconversion is much slower with Gal2, which is consistent with its lower glucose transport capacity (Reifenberger et al. 1997, Farwick et al. 2014). Strikingly, the Gal2^{3KR} mutant exports more glucose in the course of the bioconversion, which is consistent with its higher stability at the plasma membrane in comparison with the wildtype protein (Tamayo Rojas et al. 2021b). The Gal2^{N376F} mutant expectedly mediates only a very low glucose efflux, only slightly higher than the E.V. control, demonstrating that not only glucose uptake but also glucose efflux is affected by the N376F mutation.

Overall, this experiment confirms the correlation between glucose influx and efflux kinetics of yeast HXTs, which is expected based on their passive transport mechanism (Maier et al. 2002) and demonstrates the applicability of the system for quantitative comparisons between individual efflux transporters.

Inhibition of glucose efflux by xylose

We next investigated if the assay system can be used to assess the effect of molecules added *in trans*, at the extracellular side of the membrane, on the efflux of intracellular glucose. As an effector, we have chosen xylose, which is known to be a substrate for wildtype Gal2 and Gal2^{N376F} (Farwick et al. 2014) and can, therefore, be assumed to act in a competitive manner. Since AFY10 cannot consume xylose unless a heterologous xylose isomerase is overexpressed, this pentose is expected to act solely as an effector of the introduced hexose transporters, not further interfering with the cellular metabolism. Due to the facilitative transport mechanism of Gal2, it is reasonable to assume that xylose can enter the cells until a concentration equilibrium across the membrane is reached. Thereby, the pentose likely can exert an inhibitory effect on glucose efflux on both sides of the membrane. We performed a bioconversion experiment in the presence of ethanol and maltose as described above, where xylose was added or omitted from the mixture. As expected, xylose was not consumed by the cells (Fig. 4A). The consumption of maltose (Fig. 4B) correlated with the different abilities of the two Gal2 variants to export glucose (Fig. 4C), which was clearly reduced in the presence of xylose, consistent with its character as a competitive inhibitor.

Determining the inhibition of Gal2 variants by intracellular glucose

The competitive inhibition of xylose uptake by glucose was assumed for long time to be the main obstacle for the efficient cofermentation of these two sugars in strains engineered to produce ethanol from carbohydrate mixtures such as lignocellulosic biomass hydrolysates (Subtil and Boles 2012, Kim et al. 2012). In our previous work, we unexpectedly observed that the Gal2 variants with the mutated N376 residue, although they are insensitive to the competitive inhibition by glucose (Farwick et al. 2014), do not confer the ability for simultaneous consumption of glucose and xylose to the engineered *S. cerevisiae* cells (Tamayo Rojas et al. 2021a). One possible explanation could be that the engineered Gal2 variants, which were isolated based on their insensitivity to extracellular glucose, might still be inhibited by glucose at the intracellular side of the membrane. Our assay system offered an excellent opportunity to test this hypothesis. In the AFY10 strain, the xylulokinase Xks1 and all enzymes of the nonoxidative pentose phosphate pathway (ribose-5-phosphate ketol-isomerase, Rki1; D-ribulose-5-phosphate 3-epimerase, Rpe1; transketolase, Tkl1; and transaldolase, Tal1) are overexpressed from strong constitutive promoters (Farwick et al. 2014; see Table 1) as a prerequisite for the utilization of xylose as a carbon source (Kuyper et al. 2005). Therefore, only a multicopy plasmid encoding the xylose isomerase from *Clostridium phytofermentans* (Brat et al. 2009) needed to be additionally introduced.

To quantify the xylose uptake capability of Gal2 and Gal2^{N376F} in the presence of intracellular glucose, we cultivated the transformants in liquid xylose media with or without maltose addition (again starting at $OD_{600} \approx 8$). In the presence of xylose as a carbon end energy source, the supplementation of ethanol was not necessary. Although the N376F mutation reduces the xylose transport velocity per se (Tamayo Rojas et al. 2021a), both variants showed comparable xylose consumption rates in media containing only the pentose sugar (Fig. 5A). This suggests that, in the AFY10 strain background, the utilization of xylose is limited rather by metabolic constraints than the sugar uptake. In the presence of maltose, the velocity of xylose consumption mediated by wildtype Gal2 was clearly reduced, whereas no inhibitory effect on Gal2^{N376F} was observed (Fig. 5B). Intriguingly, the addition of maltose apparently increased the xylose consumption rate in the cells expressing Gal2^{N376F}. It has been reported that xylose, even at high concentrations, elicits a signaling response similar to low carbon availability (similar to low concentration of glucose), which could be one of the reasons for low xylose consumption rates in engineered *S. cerevisiae* strains (Brink et al. 2021). Therefore, it is

Downloaded from https://academic.oup.com/femsyr/article/21/1/foaa038/6653521 by Frankfurt University Library user on 26 September 2022

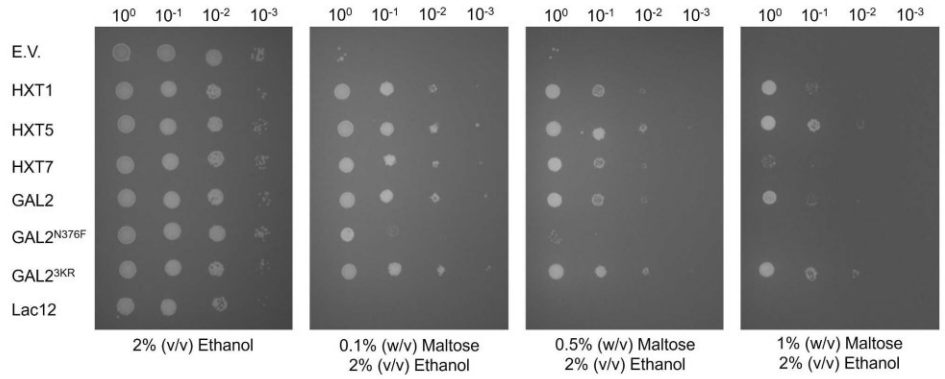

Figure 2. Growth-based analysis of the glucose efflux capacity. The yeast strain AFY10 was transformed with 2μ plasmids expressing the indicated hexose transporters and their variants. The E.V. and the lactose/proton symporter Lac12 were included as negative controls. The transformants were pregrown in liquid selective SC medium with ethanol as a permissive carbon source and spotted onto selective SC solid medium containing the indicated carbon sources. Cells were grown at 30°C for 6 days.

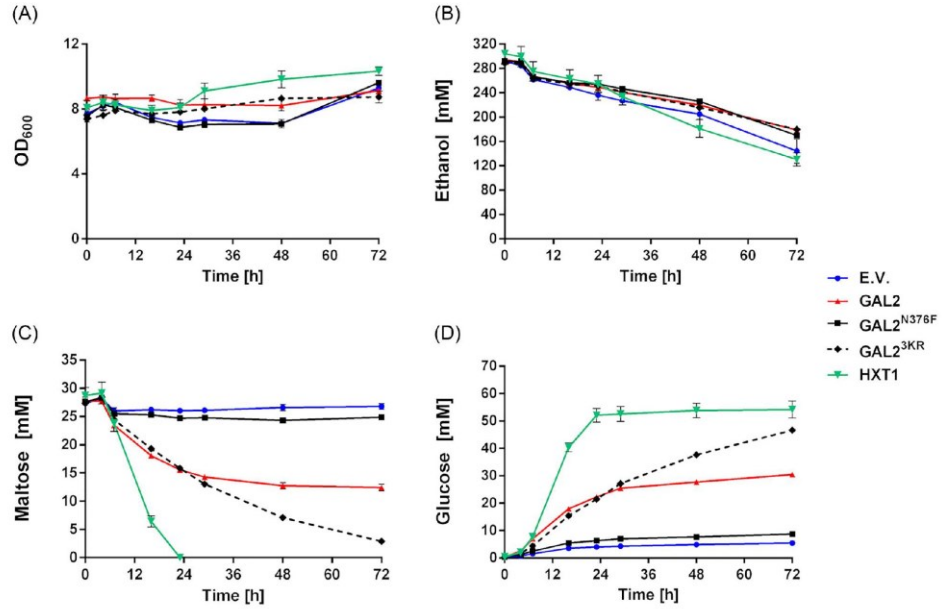

Figure 3. Measurement of glucose efflux mediated by hexose transporters. AFY10 cells expressing indicated hexose transporters (or mutant variants) were cultivated at high cell density (starting $OD_{600} \approx 8$) in liquid SC medium with 2% (v/v) of ethanol and 1% (w/v) of maltose. The E.V. instead of a transporter plasmid was used as a negative control. OD_{600} was recorded over the course of the cultivation (A). The concentrations (shown in mM) of ethanol (B), maltose (C), and glucose (D) in culture supernatants were measured by HPLC. Error bars indicate the standard deviation of three replicates. Error bars may be smaller than the symbols.

possible that the presence of maltose and/or glucose derived from it, stimulates the metabolism of xylose by inducing a metabolic response to high carbon availability. The comparison of E.V. controls between both conditions reveals another effect that may be attributed to signaling. In pure xylose medium, there is a basal level of xylose consumption (about 25 mM after 96 h), which is not seen in the presence of maltose. In our previous work (Tamayo Rojas et al. 2021a), we similarly observed a basal growth of AFY10

Downloaded from https://academic.oup.com/femsyr/article/21/1/foac038/6653521 by Frankfurt University Library user on 26 September 2022

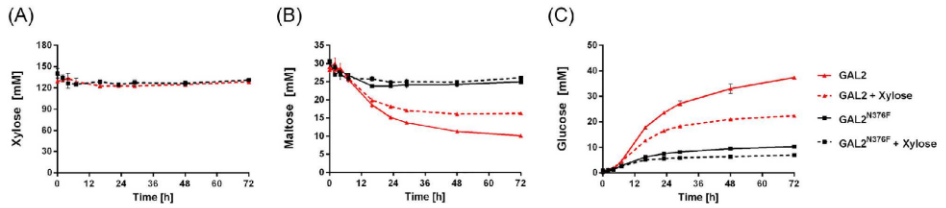

Figure 4. Influence of extracellularly added xylose on glucose efflux. The AFY10 cells were grown in SC medium with 2% (v/v) of ethanol as a carbon source, 1% (w/v) of maltose as a donor of intracellular glucose, and 2% (w/v) of xylose as a competitive inhibitor. Concentrations (shown in mM) of xylose (A), maltose (B), and glucose (C) were measured by HPLC. Error bars indicate the standard deviation of three replicates. Error bars may be smaller than the symbols.

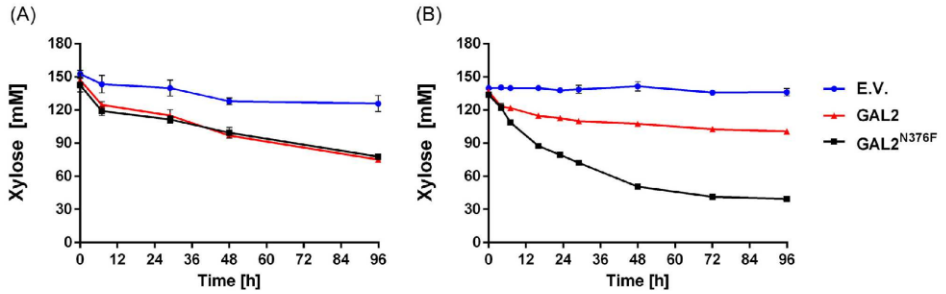

Figure 5. Effect of intracellular glucose on xylose transport by Gal2 variants. The AFY10 cells were grown in SC medium with 2% (w/v) of xylose as a carbon source. In (A), maltose was omitted, whereas in (B) 1% (w/v) of maltose was added as a donor of intracellular glucose. The transformants expressed a xylose isomerase and the indicated hexose transporter variants from a multicopy plasmid. The E.V. instead of a transporter plasmid was used as a negative control. Concentrations (shown in mM) of xylose in the supernatants were measured by HPLC. Error bars indicate the standard deviation of three replicates. Error bars may be smaller than the symbols.

transformed with the E.V. on agar plates containing xylose, but not on glucose/xylose mixtures. This may be explained by the presence of an uncharacterized sugar transporter, which is able to transport xylose, but is repressed by glucose. Consistent with this notion, the deletion of the glucose sensor gene *SNF3* partially restores the ability of the *hxt*^{0} strain to grow on glucose (Wieczorke et al. 1999). These interesting observations are certainly worthy of further investigation, which, however, would go beyond the scope of this study. Despite the obviously complex interplay between sugars, the experiment shown in Fig. 5 clearly shows that the N376F mutation confers insensitivity to inhibition by glucose not only from the extracellular, but also from the intracellular side of the membrane. For biotechnological purposes, this is an important observation as during glucose/xylose cofermentations intracellular glucose levels might increase due to inhibition of hexo- and glucokinases by xylose (Fernández et al. 1985).

Conclusion

In this work, we developed an assay platform that allows for qualitative and quantitative assessment of the glucose efflux mediated by facilitative hexose and pentose transporters. Thereby, we demonstrated the correlation of their capability to export glucose with their catalytic properties previously determined for glucose influx. By supplying intracellular glucose and extracellular xylose simultaneously, we demonstrated that each sugar inhibits the transport of the other one from the opposite side of the membrane. Moreover, the assay enabled us to show clearly that the xylose uptake by the engineered Gal2^{N376F} variant in comparison to the wildtype transporter is less sensitive to the competitive inhibition by glucose not only at the extracellular but also at the intracellular side of the plasma membrane. These results exemplarily show how the effect of compounds affecting the transport can be investigated in a topologically specific manner. Thus, we anticipate that this experimental system will expand the possibilities for investigating the sugar transporter properties and enable the screening and characterization of putative efflux-mediating permeases.

Authors' contributions

S.T.R., E.B., and M.O. contributed to the design of the study. S.T.R. and M.O. analyzed that data and wrote the manuscript. All authors read and approved the final manuscript.

Acknowledgments

We thank Bernhard Valldorf for constructing the LAC12 plasmid. We are grateful to Professor Bruno André (Brussels) for stimulating discussions.

Downloaded from https://academic.oup.com/femsyr/article/21/1/foaa038/6653521 by Frankfurt University Library user on 26 September 2022

Conflict of interest. The authors declare no conflict of interest.

Funding

This work was supported by DAAD/BECAS Chile, 2016, grant number 57221134 (to S.T.R.).

Data availability

All data shown in the manuscript are available from the corresponding author upon request.

References

Becker J, Boles E. A modified *Saccharomyces cerevisiae* strain that consumes L-arabinose and produces ethano. *Appl Environ Microbiol* 2003;**69**:4144–50.

Boles E, Oreb M. A growth-based screening system for hexose transporters in yeast. *Methods Mol Biol* 2018;**1713**:123–35.

Brat D, Boles E, Wiedemann B. Functional expression of a bacterial xylose isomerase in *Saccharomyces cerevisiae*. *Appl Environ Microbiol* 2009;**75**:2304–11.

Brink DP, Borgstrom C, Persson VC *et al.* D-xylose sensing in *Saccharomyces cerevisiae*: insights from D-glucose signaling and native D-xylose utilizers. *Int J Mol Sci* 2021;**22**:12410

Bruder S, Reifenrath M, Thomik T *et al.* Parallelised online biomass monitoring in shake flasks enables efficient strain and carbon source dependent growth characterisation of *Saccharomyces cerevisiae*. *Microb Cell Fact* 2016;**15**:1–14.

Chen L-Q, Hou B-H, Lalonde S *et al.* Sugar transporters for intercellular exchange and nutrition of pathogens. *Nature* 2010;**468**:527–32.

Cheng Q, Michels CA. MAL11 and MAL61 encode the inducible high-affinity maltose transporter of *Saccharomyces cerevisiae*. *J Bacteriol* 1991;**173**:1817–20.

Farwick A, Bruder S, Schadeweg V *et al.* Engineering of yeast hexose transporters to transport D-xylose without inhibition by D-glucose. *Proc Natl Acad Sci USA* 2014;**111**:5159–64.

Fernández R, Herrero P, Moreno F. Inhibition and inactivation of glucose-phosphorylating enzymes from *Saccharomyces cerevisiae* by D-xylose. *J Gen Microbiol* 1985;**131**:2705–9.

Gietz RD, Schiestl RH. Frozen competent yeast cells that can be transformed with high efficiency using the LiAc/SS carrier DNA/PEG method. *Nat Protoc* 2007;**2**:1–4.

Jansen MLA, de Winde JH, Pronk JT. Hxt-carrier-mediated glucose efflux upon exposure of *Saccharomyces cerevisiae* to excess maltose. *Appl Environ Microbiol* 2002;**68**:4259–65.

Kim SR, Ha S-J, Wei N *et al.* Simultaneous co-fermentation of mixed sugars: a promising strategy for producing cellulosic ethanol. *Trends Biotechnol* 2012;**30**:274–82.

Kuyper M, Hartog MM, Toirkens MJ *et al.* Metabolic engineering of a xylose-isomerase-expressing *Saccharomyces cerevisiae* strain for rapid anaerobic xylose fermentation. *FEMS Yeast Res* 2005;**5**:399–409.

Leandro MJ, Fonseca C, Goncalves P. Hexose and pentose transport in ascomycetous yeasts: an overview. *FEMS Yeast Res* 2009;**9**:511–25.

Liu JY, Miller PF, Gosink M *et al.* The identification of a new family of sugar efflux pumps in *Escherichia coli*. *Mol Microbiol* 1999;**31**:1845–51.

Maier A, Völker B, Boles E *et al.* Characterisation of glucose transport in *Saccharomyces cerevisiae* with plasma membrane vesicles (countertransport) and intact cells (initial uptake) with single Hxt1, Hxt2, Hxt3, Hxt4, Hxt6, Hxt7 or Gal2 transporters. *FEMS Yeast Res* 2002;**2**:539–50.

Oldenburg KR, Vo KT, Michaelis S *et al.* Recombination-mediated PCR-directed plasmid construction in vivo in yeast. *Nucleic Acids Res* 1997;**25**:451–2.

Ozcan S, Johnston M. Function and regulation of yeast hexose transporters. *Microbiol Mol Biol Rev* 1999;**63**:554–69.

Postma E, Verduyn C, Kuiper A *et al.* Substrate-accelerated death of *Saccharomyces cerevisiae* CBS 8066 under maltose stress. *Yeast* 1990;**6**:149–58.

Reifenberger E, Boles E, Ciriacy M. Kinetic characterization of individual hexose transporters of *Saccharomyces cerevisiae* and their relation to the triggering mechanisms of glucose repression. *Eur J Biochem* 1997;**245**:324–33.

Rubio-Texeira M, Arévalo-Rodrı´guez M, Luis Lequerica J *et al.* Lactose utilization by *Saccharomyces cerevisiae* strains expressing *Kluyveromyces lactis* LAC genes. *J Biotechnol* 2000;**84**:97–106. DOI: 10.1016/S0168-1656(00)00350-3.

Schmidl S, Iancu CV, Reifenrath M *et al.* A label-free real-time method for measuring glucose uptake kinetics in yeast. *FEMS Yeast Res* 2021;**21**:foaa069.

Sonnewald U. Sweets - the missing sugar efflux carriers. *Front Plant Sci* 2011;**2**:7.

Subtil T, Boles E. Competition between pentoses and glucose during uptake and catabolism in recombinant *Saccharomyces cerevisiae*. *Biotechnol Biofuels* 2012;**5**:14.

Sun Y, Vanderpool CK. Regulation and function of *Escherichia coli* sugar efflux transporter A (SetA) during glucose-phosphate stress. *J Bacteriol* 2011;**193**:143–53.

Tamayo Rojas SA, Schadeweg V, Kirchner F *et al.* Identification of a glucose-insensitive variant of Gal2 from *Saccharomyces cerevisiae* exhibiting a high pentose transport capacity. *Sci Rep* 2021a;**11**:24404.

Tamayo Rojas SA, Schmidl S, Boles E *et al.* Glucose-induced internalization of the *S. cerevisiae* galactose permease Gal2 is dependent on phosphorylation and ubiquitination of its aminoterminal cytoplasmic tail. *FEMS Yeast Res* 2021b;**21**:foab019. 10.1093/femsyr/foab019

Thorens B. Glucose transporters in the regulation of intestinal, renal, and liver glucose fluxes. *Am J Physiol* 1996;**70**:G541–53.

Wang D, Yang H, Shi L *et al.* Functional studies of the T295M mutation causing Glut1 deficiency: glucose efflux preferentially affected by T295M. *Pediatr Res* 2008;**64**:538–43.

Wieczorke R, Krampe S, Weierstall T *et al.* Concurrent knock-out of at least 20 transporter genes is required to block uptake of hexoses in *Saccharomyces cerevisiae*. *FEBS Lett* 1999;**464**:123–8.

Downloaded from https://academic.oup.com/femsyr/article/21/1/foac038/6653521 by Frankfurt University Library user on 26 September 2022

7 Deutsche Zusammenfassung

Heutzutage besteht eine große Abhängigkeit von fossilen Brennstoffen wie Erdöl, Kohle und Erdgas. Diese spielen sowohl im Energiesektor als auch bei der Synthese von Massen- und Feinchemikalien eine entscheidende Rolle. Die Verfügbarkeit fossiler Brennstoffe ist jedoch auf einige wenige Vorkommen weltweit beschränkt, sodass eine Nutzung durch die Erschöpfung der Vorkommen sowie aus wirtschaftlichen und geopolitischen Gründen begrenzt ist. Außerdem trägt die Nutzung fossiler Brennstoffe aufgrund der hohen Treibhausgasemissionen, die bei der Verarbeitung oder Verbrennung in die Atmosphäre gelangen, zum Klimawandel bei.

Eine vielversprechende Strategie zur Verringerung der Abhängigkeit von fossilen Brennstoffen ist die Verwendung der Hefe *Saccharomyces cerevisiae* zur Biokonvertierung erneuerbarer Non-Food-Rohstoffe oder Abfallströme, wie beispielsweise lignozellulosehaltiger Biomasse, in Bioethanol und andere wertvolle Moleküle. Lignozellulosehaltige Rohstoffe bestehen aus Glukose und – je nach Biomasseart in unterschiedlichen Anteilen – den Pentosen Xylose und Arabinose. *S. cerevisiae* ist ein effizienter Glukoseverbraucher, kann aber Xylose und Arabinose nicht auf natürliche Weise verstoffwechseln.

Daher wurden umfangreiche Forschungsarbeiten mit Hilfe rekombinanter DNA-Techniken durchgeführt, um die biochemischen Stoffwechselwege, die für die Nutzung dieser nichtphysiologischen Substrate erforderlich sind, in *S. cerevisiae* einzubringen und zu verbessern. Jeder funktionelle Stoffwechselweg, der D-Xylose und L-Arabinose in *S. cerevisiae* verwerten kann, erfordert jedoch den Transport dieser Zucker durch die Zellmembran. Das endogene Zuckertransportsystem von *S. cerevisiae* kann D-Xylose und L-Arabinose nur in begrenztem Umfang aufnehmen; diese Aufnahme ermöglicht nur ein basales Wachstum, sofern die enzymatischen Stoffwechselwege zur Verfügung stehen. Aus diesem Grund wurde die Aufnahme von D-Xylose und L-Arabinose als limitierender Schritt für die effiziente Nutzung dieser nicht-physiologischen Substrate, insbesondere bei niedrigen Konzentrationen, erkannt.

In *S. cerevisiae* wird die Aufnahme von Zuckern durch die Plasmamembran von der Familie der „Sugar Porter“ (SP) vermittelt, die zur „Major Facilitator Superfamily“ (MFS) gehört, der größten und vielfältigsten Superfamilie sekundärer Carrier, die in allen Reichen des Lebens zu finden ist. Die SP-Familie besteht aus einer Vielzahl von Membrantransportproteinen, die je nach Substrat oder Bandbreite der transportierten Substrate in verschiedene phylogenetische Cluster zusammengefasst werden können.

Hefe-Hexosetransporter haben, wie viele Mitglieder der MFS, 12 mutmaßliche Transmembrandomänen (TM), die in zwei Bündeln von 6 TM organisiert sind. Die beiden Bündel sind durch eine lange und flexible intrazelluläre Schleife verbunden, die strukturelle Elemente enthalten kann. Jedes Bündel von 6 TM besteht aus einem Paar invertierter 3 TM, was nahelegt, dass drei TM-Wiederholungen eine grundlegende Struktureinheit für MFS-Proteine bilden.

In *S. cerevisiae* gibt es 17 funktionelle Hexose-Transporter, die von den Genen *HXT1* bis *HXT17* und *GAL2* kodiert werden (abgesehen von *HXT12*, einem Pseudogen). Die große Anzahl von Hexose-Transportern in *S. cerevisiae* ermöglicht die Anpassung an eine Umgebung mit schwankenden Zuckerkonzentrationen, wie sie während einer Fermentation üblicherweise auftreten. Unter physiologischen Bedingungen scheinen die wichtigsten Hexose-Transporter Hxt1 bis Hxt4, Hxt6 und Hxt7 zu sein. Die Expression des *GAL2*-Gens erfolgt nur in Galaktose-limitierten Kulturen. Gal2 ist jedoch einer der am besten untersuchten Hexose-Transporter in *S. cerevisiae*. Obwohl seine Expression in Gegenwart von Glukose unterdrückt wird, transportiert er diesen Zucker auch bei konstitutiver Expression mit hoher Affinität. Jüngste Versuche Hefestämme für die Verwertung pflanzlicher Biomasse zu entwickeln, haben die Fähigkeit von Gal2 entschlüsselt nicht-physiologische Substrate wie Xylose und Arabinose zu transportieren. Die Verbesserung der kinetischen Eigenschaften und der Substratspezifität von Gal2, insbesondere für Pentosen, ist zu einem wichtigen Ziel bei der Hefe-Stammentwicklung geworden. Das Hauptziel dieser Arbeit bestand darin, die Verwertung von Xylose und Arabinose zu verbessern, indem die Zellpermeabilität für diese nicht-physiologischen Substrate durch die gentechnische Veränderung der Galaktose-Permease Gal2 erhöht wird.

Wie bereits erwähnt, hängt die Expression des *GAL2-Gens* von Galaktose ab, die als Induktor wirkt. Doch selbst in Gegenwart von Galaktose wirkt Glukose als strenger Repressor. Daher wird das *GAL2*-Gen normalerweise von einem konstitutiven Promotor kontrolliert. Die Anwesenheit von Glukose löst allerdings zusätzlich den Abbau von Gal2 aus. Der Abbau von Gal2 wird durch die kovalente Bindung des kleinen 76-Aminosäure-Proteins Ubiquitin (Ub) an den Zieltransporter in einem mehrstufigen Prozess, der Ubiquitinierung genannt wird, vermittelt.

Die Ubiquitinierung von Hexose-Permeasen beinhaltet die Aktivierung des Ub-Moleküls durch das Ub-aktivierende Enzym E1 unter Verbrauchvon ATP. Anschließend wird das aktivierte Ub auf ein spezifisches Ub-konjugierendes Enzym E2 übertragen, das das Ub indirekt über ein spezifisches HECT-E3-Enzym (Rsp5) an ein Lysin des Substrats abgibt,

und zwar mit Hilfe eines Adaptorproteins, das das Ziel erkennt (Rsp5-Adaptor). Ubiquitierte Permeasen werden durch Membraneinstülpung zu frühen Endosomen geschickt, wo sie auf ESCRTs (endosomal sorting complex required for transport) treffen. Die zielgerichteten Permeasen werden in intralumenale Vesikel (ILV) innerhalb des Endosoms sortiert, welches sich nach mehreren Zyklen in einen multivesikulären Körper (MVB) verwandelt, der anschließend mit der Vakuole fusioniert, um den Proteininhalt der ILVs für den Abbau durch lumenale Hydrolasen freizugeben.

Gal2 enthält 30 Lysinreste, die das Ubiquitinmolekül aufnehmen können, das auf den Gal2-Abbau abzielt. Es ist bekannt, dass eine Mono-Ubiquitinierung durch Rsp5 an mehreren Lysinresten notwendig ist, um den Abbau von Gal2 einzuleiten (Horak & Wolf, 2001). Die Autoren konnten jedoch nicht die spezifischen Lysinreste, die an den Ubiquitinierungsprozessen beteiligt sind, identifizieren. In dieser Studie wurden mehrere Gal2-Varianten untersucht, bei denen Lysinreste mutiert oder aus der Proteinsequenz entfernt wurden, um herauszufinden, welche Lysinreste wahrscheinlich an der Ubiquitinierung und dem daraus resultierenden Umsatz des Transporters beteiligt sind. Die Ergebnisse des Screenings zeigten, dass die Mutation der N-terminalen Lysinreste 27, 37 und 44 zu Arginin ($Gal2_{3KR}$) zu einem funktionalen Transporter führte, der, wenn er mit GFP ($Gal2_{3KR\_GFP}$) fusioniert wurde, eine ausschließliche Lokalisierung an der Plasmamembran in Zellen zeigte, die mit Galaktose oder Glukose als einziger Kohlenstoffquelle wachsen (Tamayo Rojas et al., 2021b).

In dieser Studie wurden auch die durch Phosphorylierung verursachten Signale, die die Ubiquitinierung und die daraus resultierende Umwandlung des Zielproteins auslösen, untersucht. Mit ähnlichen Screening-Ansätzen zur Bewertung der Stabilisierung von Gal2 durch Modifikationen von Lysinen konnte festgestellt werden, dass die N-terminalen Serine 32, 35, 39, 48, 53 und 55 an der Internalisierung von Gal2 beteiligt sind. Dies konnte mit einem Gal2-Konstrukt, bei dem alle diese Serine zu Alanin mutiert sind und mit GFP markiert waren ($Gal2_{6SA\_GFP}$) in Zellen, die mit Galaktose oder Glukose als einziger Kohlenstoffquelle wachsen, gezeigt werden. Hierbei wurde eine praktisch vollständige Lokalisierung an der Plasmamembran beobachtet (Tamayo Rojas et al. , 2021b). Das Ziel zukünftiger Studien besteht jedoch darin, die Kinase(n) zu identifizieren, die für die Phosphorylierung der Serinreste am N-Terminus von Gal2 verantwortlich sind.

Die Konstrukte $Gal2_{3KR}$ und $Gal2_{6SA}$ zeigten eine vergleichbare Stabilität an der Plasmamembran. Die Aufnahmerate des Konstrukts $Gal2_{6SA}$ war jedoch höher als die von $Gal2_{3KR}$ (V_{max} 0,8330 bzw. 0,6698 nmol min^{-1} mg_{CDW}^{-1}). Außerdem war das Wachstum, das durch die Expression von $Gal2_{6SA}$ in dem Hexose-Transporter-freien (*hxt*^{0})

Saccharomyces cerevisiae-Stamm EBY.VW4000 (Wieczorke et al., 1999) erzielt wurde, besser als die Expression von $Gal2_{3KR}$ in demselben Stamm, wenn die Zellen in SC-Medium mit 2 % (w/v) Glucose wuchsen (Tamayo Rojas et al., 2021b).

Unsere Hypothese zu diesen Unterschieden zwischen $Gal2_{3KR}$ und $Gal2_{6SA}$ basiert auf der Annahme, dass die Phosphorylierung der Ubiquitinierung vorausgeht; daher könnte der arrestin-Rsp5-Komplex $Gal2_{3KR}$ immer noch binden, da alle Phosphorylierungsstellen in diesem Konstrukt vorhanden sind. Die Bindung des arrestin-Rsp5-Komplexes an die Permease könnte die Transportrate von $Gal2_{3KR}$ teilweise beeinträchtigen, wobei der arrestin-Rsp5-Komplex als nicht-kompetitiver Inhibitor wirken könnte, eine Art der Inhibition, die zur Verringerung der V_{max}-Werte führt.

Ein weiteres Ziel dieser Arbeit war es, Rsp5-Adaptoren zu identifizieren, die an der Erkennung der Gal2-Permease beteiligt sind. Unsere Ergebnisse zeigten, dass die Rsp5-Adaptoren Bul1 und Rod1 vermutlich an der Ubiquitinierung von Gal2 beteiligt sind, da ihre individuelle Deletion zu einer Stabilisierung von Gal2 an der Plasmamembran in Zellen, die mit Glukose als einziger Kohlenstoffquelle wuchsen, führte. Die Stabilisierung war jedoch weniger stark als bei den Varianten $Gal2_{3KR}$ oder $Gal2_{6SA}$. Aus diesem Grund wurde vermutet, dass mehrere Rsp5-Adaptoren an der Internalisierung von Gal2 beteiligt sein könnten (Tamayo Rojas et al., 2021b).

Die Beeinträchtigung der Aufnahme von Xylose oder Arabinose durch sterische Hemmung von Glukose führt zu einer verringerten Aufnahme dieser Pentosen in Co-Fermentationen dieser Zucker. In dieser Studie wurde eine fehleranfällige PCR-Technik in Verbindung mit einem Screening-Stamm von *S. cerevisiae* verwendet, dem alle Hexose-Transporter (hxt^0) sowie alle Glukose-Hexokinasen (hxk^0) fehlen und der über einen Xylose-Verwertungsweg verfügt (Farwick et al., 2014). Wir konnten zwei Mutationen in Gal2 (N376Y/M435I) finden, die zusammen zwei wünschenswerte Eigenschaften für die Fermentation von Lignozellulosehydrolysaten beinhalten: die Fähigkeit, Pentosen ohne die sterische Hemmung von Glukose zu transportieren, und eine verbesserte Kapazität für den Transport von Xylose und Arabinose (Tamayo Rojas et al., 2021a). Durch das Einfügen von Serin-zu-Alanin-Mutationen an den Resten 32, 35, 39, 48, 53 und 55 wurde ein Transporter ($Gal2_{6SA\_N376Y\_M435I}$) mit den oben genannten Eigenschaften und einer erhöhten Stabilität an der Plasmamembran entwickelt, der zu den fortschrittlichsten Pentose-Transportern gehört. Die Überexpression dieses Transporters in einem rekombinanten diploiden Industriestamm, der in der Lage ist, Xylose zu verstoffwechseln, verringerte die Fermentationszeit des gesamten Xyloseverbrauchs um etwa 20 Stunden, was 40 % des gesamten Fermentationsverlaufs einer Glukose/Xylose-Misch-

Fermentation entspricht. Der Stamm war jedoch nur in der Lage, Glukose und Xylose nacheinander zu verbrauchen, was beweist, dass die Xyloseaufnahme nicht der einzige Faktor für die gleichzeitige Verstoffwechslung beider Zucker ist (Tamayo Rojas et al., 2021a).

Die Substitution von Gal2-Asparagin 376 durch Tyrosin ($Gal2_{N376Y}$) oder Phenylalanin ($Gal2_{N376F}$) führte zu einer Transportervariante, die die Aufnahme von Glukose im Vergleich zum Wildtyp vollständig aufhob (Farwick et al., 2014). Daher wird bei diesen beiden Varianten die Aufnahme von Xylose während der Co-Fermentation nicht kompetitiv durch Glukose gehemmt. Es ist jedoch unbekannt ob diese Gal2-Varianten immer noch durch intrazelluläre Glukose gehemmt werden und ob die Abnahme der Glukoseaffinität symmetrisch oder asymmetrisch in Bezug auf die Richtung des Glukoseflusses ist. Zur Beantwortung dieser Frage wurde eine Assay-Plattform entwickelt, die eine qualitative und quantitative Bewertung des durch Hexose- und Pentose-Transpoter vermittelten Glukose-Effluxes ermöglicht. Für den Assay wird der bereits erwähnte Stamm AFY10 verwendet. Wenn dieser Stamm mit dem Disaccharid Maltose, das intern durch Maltasen in zwei Glukoseteile hydrolysiert wird, gefüttert wird, erreicht die Glukose wachstumshemmende Werte innerhalb der Zellen, da sie nicht weiter verstoffwechselt werden kann. Wenn in diesem System eine Permease exprimiert wird, die den Glukose-Efflux vermittelt, wird die hemmende Wirkung proportional zur Kapazität des eingeführten Transporters gemindert (Tamayo Rojas et al., 2022). Durch Fütterung des Systems mit Maltose und Xylose bei gleichzeitiger Expression der $Gal2_{N376F}$-Variante und Xylose-Isomerase (XylA von *Clostridium phytofermentans*) konnte gezeigt werden, dass intrazelluläre Glukose die Aufnahme von Xylose nicht hemmt. Damit konnte nachgewiesen werden, dass diese Gal2-Variante eine Unempfindlichkeit gegenüber Glukose von beiden Seiten der Plasmamembran aufweist. Dies steht im Gegensetz zum Wildtyp, der intern und extern durch Glukose gehemmt wird (Tamayo Rojas et al., 2022).

Obwohl der in-vivo-Screening-Assay mit dem Ziel entwickelt wurde, die Dynamik der intrazellulären Hemmung, die der Glukose-Efflux auf die Xylose-Aufnahme hat, zu verstehen, zeigte das Screening-System Anwendbarkeit über das vorgegebene Thema hinaus. Dieses in-vivo-Screening, mit dem die Glukose-Efflux-Kapazität gemessen werden kann, wird zur Charakterisierung endogener und heterologer Transporter in *S. cerevisiae* beitragen.